Article

Cell Host & Microbe

Highly potent quinoxalinediones inhibit α-hemolysin and ameliorate *Staphylococcus aureus* lung infections

Graphical abstract

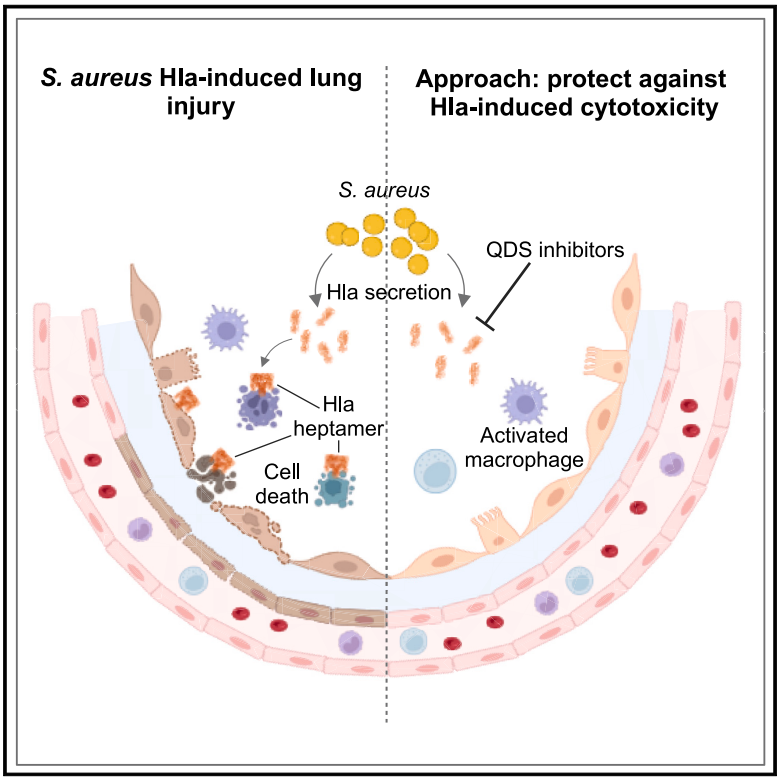

Authors

Aditya Shekhar, Raffaella Di Lucrezia, Karoline Jerye, ..., Ursula Bilitewski, Klaus Dinkel, Mark Brönstrup

Correspondence

mark.broenstrup@helmholtz-hzi.de

In brief

Treatment failures for *Staphylococcus aureus* pneumonia are high despite antibiotic therapy. Shekhar et al. identified quinoxalinediones as small molecules that protect host cells by neutralizing the *S. aureus* toxin α-hemolysin. Quinoxalinediones demonstrate how a large toxin can be inhibited by a small molecule with potency *in vitro* and *in vivo*.

Highlights

- A cellular screen identified QDS, small molecule inhibitors of *S. aureus* α-hemolysin
- QDS revert the hallmarks of α-hemolysin pathogenicity
- QDS prevent the formation of functional pores by interacting with α-hemolysin
- The QDS analog H052 is active *in vivo* when given prophylactically or therapeutically

Shekhar et al., 2025, Cell Host & Microbe *33*, 560–572
April 9, 2025 © 2025 The Author(s). Published by Elsevier Inc.
https://doi.org/10.1016/j.chom.2025.03.006

CellPress

CellPress
OPEN ACCESS

Cell Host & Microbe

Article

Highly potent quinoxalinediones inhibit α-hemolysin and ameliorate *Staphylococcus aureus* lung infections

Aditya Shekhar,[1,19] Raffaella Di Lucrezia,[2,19] Karoline Jerye,[3] Vadim S. Korotkov,[3] Kirsten Harmrolfs,[3] Katharina Rox,[3,4] Herbert A. Weich,[3] Ishan Ghai,[5] Florent Delhommel,[6,7] Isabelle Becher,[8] Carsten Degenhart,[2] Eyad Fansa,[2] Anke Unger,[2] Peter Habenberger,[2] Bert Klebl,[2] Peer Lukat,[9] Stefan Schmelz,[9] Steffi Henke,[9] Sebastian Borgert,[9] Julia C. Lang,[10] Florenz Sasse,[3] Randi Diestel,[3] Clémentine Richter,[11,12] Nicole Schneider-Daum,[11] Bettina Hinkelmann,[3] Jana Niemz,[13] Claus-Michael Lehr,[11,12] Lothar Jänsch,[14] Jochen Huehn,[13,15] Richard Alm,[16] Mikhail Savitski,[8] Tobias Welte,[17] Thomas Hesterkamp,[4] Michael Sattler,[6,7] Mathias Winterhalter,[5] Wulf Blankenfeldt,[9] Eva Medina,[10] Ursula Bilitewski,[1] Klaus Dinkel,[2] and Mark Brönstrup[3,4,18,20,*]

[1]Compound Profiling and Screening, Helmholtz Centre for Infection Research, Inhoffenstrasse 7, 38124 Braunschweig, Germany
[2]Lead Discovery Center, Otto-Hahn-Str. 15, 44227 Dortmund, Germany
[3]Chemical Biology, Helmholtz Centre for Infection Research, Inhoffenstrasse 7, 38124 Braunschweig, Germany
[4]German Center for Infection Research (DZIF), Site Hannover-Braunschweig, Braunschweig, Germany
[5]Life Sciences and Chemistry, Constructor University, 28759 Bremen, Germany
[6]Technical University of Munich, TUM School of Natural Sciences, Department of Bioscience, Bavarian NMR Center, Lichtenbergstrasse 4, 85747 Garching, Germany
[7]Helmholtz Munich, Molecular Targets and Therapeutics Center, Institute of Structural Biology, Ingolstädter Landstrasse 1, 85764 Neuherberg, Germany
[8]Proteomics Core Facility, European Molecular Biology Laboratory, Meyerhofstrasse 1, 69117 Heidelberg, Germany
[9]Structure and Function of Proteins, Helmholtz Centre for Infection Research, Inhoffenstrasse 7, 38124 Braunschweig, Germany
[10]Infection Immunology, Helmholtz Centre for Infection Research, Inhoffenstrasse 7, 38124 Braunschweig, Germany
[11]Department of Drug Delivery, Helmholtz-Institute for Pharmaceutical Research (HIPS), Campus E8.1, 66123 Saarbrücken, Germany
[12]Department of Pharmacy, Saarland University, 66123 Saarbrücken, Germany
[13]Experimental Immunology, Helmholtz Centre for Infection Research, Inhoffenstrasse 7, 38124 Braunschweig, Germany
[14]Cellular Proteomics, Helmholtz Centre for Infection Research, Inhoffenstrasse 7, 38124 Braunschweig, Germany
[15]Cluster of Excellence Resolving Infection Susceptibility (RESIST; EXC 2155), Hannover Medical School, Carl-Neuberg-Straße 1, 30625 Hannover, Germany
[16]CARB-X, Boston, MA, USA
[17]Department of Respiratory Medicine and Infectious Disease, Hannover Medical School, Carl-Neuberg-Strasse 1, Hannover 30625, Germany
[18]Center of Biomolecular Drug Research (BMWZ), Leibniz Universität, 30167 Hannover, Germany
[19]These authors contributed equally
[20]Lead contact
*Correspondence: mark.broenstrup@helmholtz-hzi.de
https://doi.org/10.1016/j.chom.2025.03.006

SUMMARY

Hospital-acquired pneumonia caused by *Staphylococcus aureus* is associated with patient morbidity and mortality, despite adequate antibiotic therapy. This illustrates the need for treatments beyond antibiotics. The pore-forming heptameric toxin α-hemolysin (Hla) is a major pathogenicity factor of *S. aureus* and a clinically validated target. We identify quinoxalinediones (QDS) as highly potent Hla inhibitors, conferring protection against the hallmarks of Hla-induced pathogenicity such as Ca^{2+} influx, cytotoxicity, hemolysis, and monolayer destruction. The effects were exerted across major Hla subtypes in all relevant cell types. QDS prevented the formation of functional pores by interacting with Hla near the phospholipid-binding site. The QDS analog, H052, was active in mouse models of *S. aureus* lung infections, when administered prophylactically or therapeutically, either as monotherapy or when given in combination with the antibiotic linezolid. The study provides evidence that complex bacterial toxins can be targeted *in vivo* by drug-like small molecules.

INTRODUCTION

Staphylococcus aureus is a gram-positive human pathobiont that can cause severe invasive infections of the skin, soft tissues, and the lung, as well as bloodstream infections and vegetations of heart valves, endocarditis and bone.[1] It is a major contributor to infection-related mortality.[1,2] In particular, nosocomial pneumonia caused by *S. aureus* represents a

 © 2025 The Author(s). Published by Elsevier Inc.
This is an open access article under the CC BY license (http://creativecommons.org/licenses/by/4.0/).

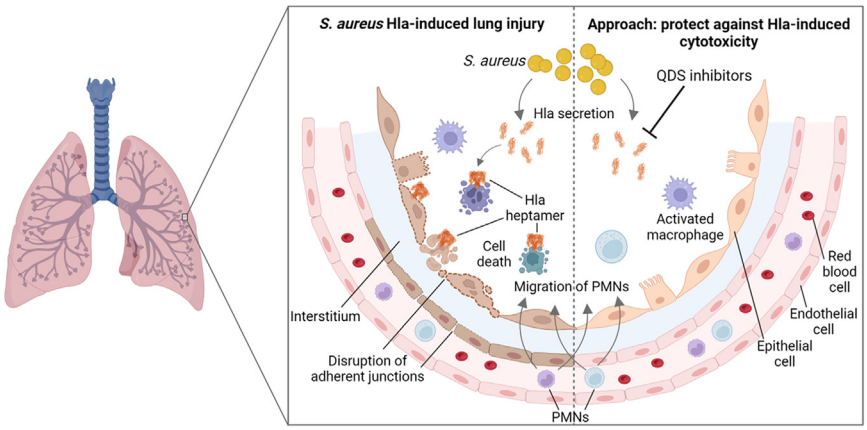

Figure 1. Hallmarks of Hla-induced lung injury following a *S. aureus* infection

Hla is secreted as a monomer and heptamerizes on host cells to form pores. Subsequent cell death as well as the disruption of adherens junctions is prevented by QDS inhibitors. Created with Biorender.com.

serious clinical challenge due to its high prevalence, the absorption of considerable health resources, and its high attributable mortality rate.[3] The global emergence of methicillin-resistant *S. aureus* (MRSA) strains that are resistant to commonly used antibiotics has impaired the successful treatment of these infections.[3] Remarkably, treatment failures remain high in spite of an adequate therapy with antibiotics that reach minimum inhibitory concentrations (MICs) well below the clinical susceptibility breakpoint. This led to the hypothesis that an improvement in clinical outcome cannot be achieved by bacterial killing with antibiotics alone but requires new therapy concepts that ameliorate the disease pathology on the host side. Such a non-traditional "pathoblocker" strategy is believed to reduce resistance formation due to the absence of a direct selection pressure on the bacteria and to leave the commensal microbiota intact.[4–6] A key virulence factor causing host tissue damage is the protein α-hemolysin (Hla) secreted by *S. aureus*.[7–9] Following its receptor-mediated attachment to host cells, the Hla monomer oligomerizes to a 232-kDa heptamer,[10] which forms a membrane pore that causes leakage of cellular constituents and cell lysis (Figure 1).[11] Hla is not only cytotoxic for primary endothelial and epithelial cells and a broad range of immune cells but also exacerbates inflammation at sublytic concentrations and fosters tissue destruction by the impairment of endothelial and epithelial barrier integrity.[12] Hla has also been shown to potentiate co-infections by gram-negative pathogens.[13] Because there is ample evidence from cellular models, animal infection experiments[14] and human studies showing that attenuating Hla functions improves infection outcome, Hla is recognized as an attractive drug target, and nosocomial pneumonia has been selected as the preferred indication for this approach. After achieving clinical proof-of-concept, two human monoclonal antibodies that neutralize Hla, MEDI4893/AR-320 (Suvratoxumab) and AR-301 (Salvecin), have advanced to phase 3 clinical studies.[15,16]

We envisaged that, compared with monoclonal antibodies, a small molecule inhibitor would have advantages in terms of cost-of-goods and with respect to achieving a rapid exposure in the lung. Whereas first tool compounds such as beta-cyclodextrin derivatives[17–19] or flavones[20–26] have been shown to inhibit Hla non-specifically, demonstration that the membrane-interacting virulence factor Hla can be targeted by a drug-like small molecule has not yet been provided. Herein, we report the development of a cascade of cellular models to characterize Hla action and present cellular, structural, biophysical, *in vitro,* and *in vivo* data for quinoxalinediones (QDS) as highly potent small molecule inhibitors of Hla.

RESULTS

Discovery and optimization of Hla inhibitors

Pores of Hla heptamers induce the permeation of extracellular calcium ions across the cell membrane driven by a concentration gradient. We developed a miniaturized assay, amenable to high-throughput screening conditions, that detects the Hla-induced increase of intracellular calcium concentrations. The addition of Hla to the human leukocyte cell line U937 led to a more than 5-fold increase in fluorescence of the Ca^{2+}-sensitive indicator dye Fluo-4, and this effect could be reverted by an anti-Hla antibody. The cellular assay was miniaturized and automated to a 1,536-well plate format in a volume of only 9 μL with a Z′ factor of 0.79 and applied to test more than 182,000 compounds from in-house libraries. After enrichment of the primary screening set, several actives with a QDS moiety caught our attention, *inter alia* compound **1** (Figure 2), which showed a half-maximal effective concentration (EC_{50}) of 0.34 μM. Because the compound was not cytotoxic in an MTT (3-[4,5-dimethylthiazol-2-yl]-2,5 diphenyl tetrazolium bromide) assay, had a good aqueous solubility (150 μM at pH 7.4), and was metabolically stable in plasma and in the presence of liver microsomes, QDS were selected as a hit series for optimization.

Synthesis of a variety of compounds containing carboxamide or sulfonamide groups revealed a general trend toward the sulfonamides being more potent than the carboxamide analogs (**2** vs. **4** and **8** vs. **10**; Figure 2; Table S1). Moreover, shorter alkyl chain sulfonamides showed higher activity than longer ones (**5** vs. **4**). The NH group of the sulfonamide moiety was important because its alkylation as in **6** led to a loss of activity (EC_{50} > 3.5 μM) compared with **12** (EC_{50} = 0.113 μM). Also, reversed sulfonamides such as **3** or **9** showed generally lower inhibitory activity than **4** or **10**, respectively. The introduction of a methyl group at position **7** of the QDS scaffold led to a sharp increase in potency (compare **H831** vs. **S2** in Table S1).

The QDS motif turned out to be the essential pharmacophore: the omission of one or two carbonyl oxygens, as in the quinoxalineones **S11** and **S12** or the quinoxaline **S13**, led to poorly active or inactive compounds (Table S1). Also, the formal expulsion of a carbonyl group, as in the urea derivative **S14** or mono- and

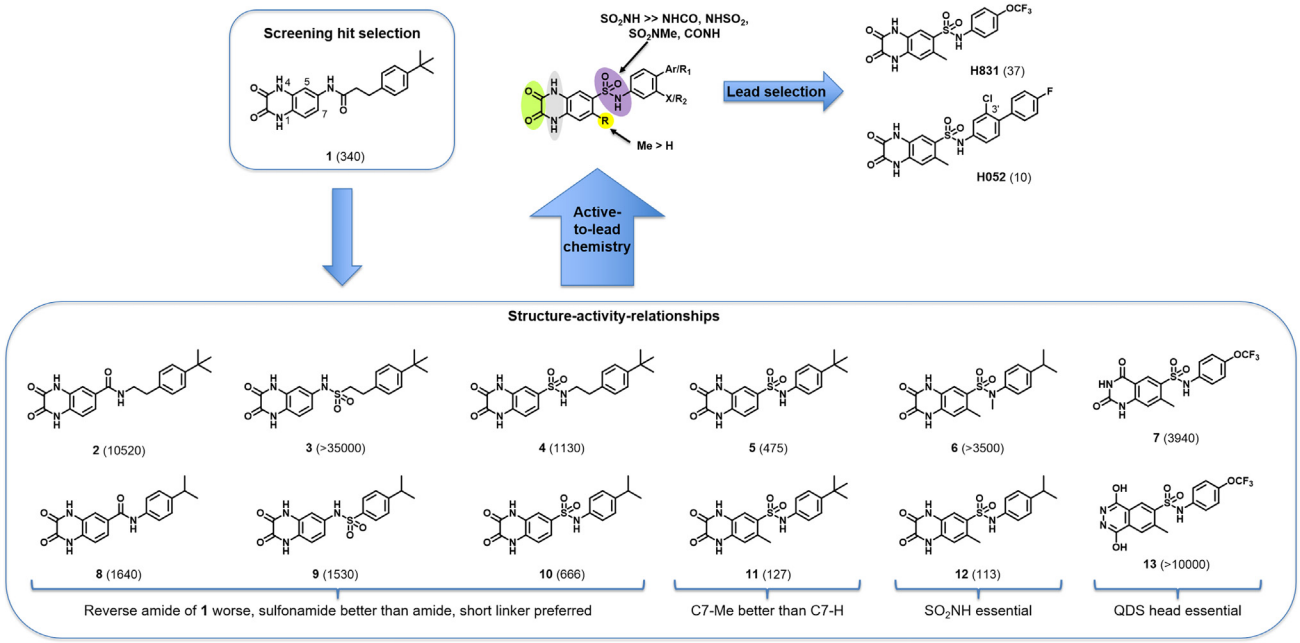

Figure 2. Optimization of QDS inhibitors by medicinal chemistry

Compound IDs are in bold, and EC_{50} values in nM from the Ca^{2+} influx assay are in brackets.
See Table S1.

di-alkylation of the nitrogens as in **S15** and **S16**, respectively, abolished bioactivity. Likewise, attempts to widen the ring to a 1,5-dihydro-2*H*-benzo[*b*][1,4]diazepine-2,4(3*H*)-dione as in **S17** or to swap the carbonyl and NH positions to the quinazoline-2,4(1*H*,3*H*)-dione **7** or the 6-methylisoindoline-1,3-dione **13** led to less-active or inactive compounds (Table S1).

The eastern, aryl-containing part was investigated systematically through >500 analogs that will be reported elsewhere. The monoaryl H831 and the biaryl H052 exhibited particularly favorable cellular efficacies (Figure 3A) and pharmaceutical properties (see below) and were selected as leads for in-depth studies. Both analogs are readily available in a 2-3-step synthesis. In summary, a QDS core, substituted with a methyl group at the 7-position and an arylated sulfonamide at the 6-position, were key structural elements of highly potent Hla inhibitors such as H831 and H052.

QDS restore Hla-induced damage of host cell integrity

The QDS H831 and H052 were further profiled in cellular models of higher translational relevance. As Hla exerts its major damage to lung epithelial cells, microvascular endothelial cells, and immune cells recruited to the lung in response to infection, assays were set up with primary human small airway epithelial cells (HSAEpCs), pulmonary microvascular endothelial cells (HPMECs), and monocytes isolated freshly from human donors. In addition, murine Th1 cells and rabbit erythrocytes were used.

Calcium influx

Hla induced calcium influx in natural killer (NK) cells, monocytes, small airway epithelial cells, and microvascular endothelial cells (Figures 3 and S3). Importantly, the QDS inhibitors H831 and H052 prevented Hla-induced calcium influx in $CD14^+$ monocytes with EC_{50} values of 30 and 90 nM, respectively (Figure 3B). Similar effects were seen in lung endothelial cells at EC_{50} values of 110 and 830 nM (Figure 3C)

Cytotoxicity

We next tested whether QDS could prevent Hla-induced cytotoxicity across a range of diverse cell types. Exposing A549 lung epithelial cells to 0.66 μg/mL Hla led to the release of lactate dehydrogenase (LDH). This effect could be inhibited by H831 and H052 at concentrations of 0.002 and 0.04 μM, respectively (Figure 3D). Secondly, human airway epithelial cells were marked in a live-dead assay with two fluorescent probes for cell viability and for cytotoxicity. Hla (2 μg/mL) increased the number of dead cells and decreased that of living cells. This effect could be suppressed by H831 and H052 with EC_{50}s of 1.6 and 7.3 μM, respectively (Figures 3E and S3). Albeit evident from the above data, we confirmed that H831 and H052 were not cytotoxic in a standard cytotoxicity assay for 72 h at concentrations of up to 100 μM.

In a recent study with murine *in vitro*-generated $CD4^+$ helper T (Th) cell subsets, we demonstrated that Hla induced the death of Th1 cells, whereas cells polarized under Th17 conditions were resistant.[27] Hence, we tested whether QDS exert protective effects on Th1 cells by culturing *ex vivo*-isolated naive $CD4^+$ T cells under Th1-polarizing conditions in the presence of Hla and titrated doses of H831. In line with our previous findings, Hla very efficiently induced death of Th1 cells. This was prevented by H831 in a dose-dependent manner, reaching complete protection from Hla-induced death at a concentration of 10 μM (Figure 3G).

Hemolysis

The ability of Hla to lyse erythrocytes is an important mechanism of collateral damage following *S. aureus* infections. Because rabbit erythrocytes are highly susceptible, they were used to probe

CellPress
OPEN ACCESS

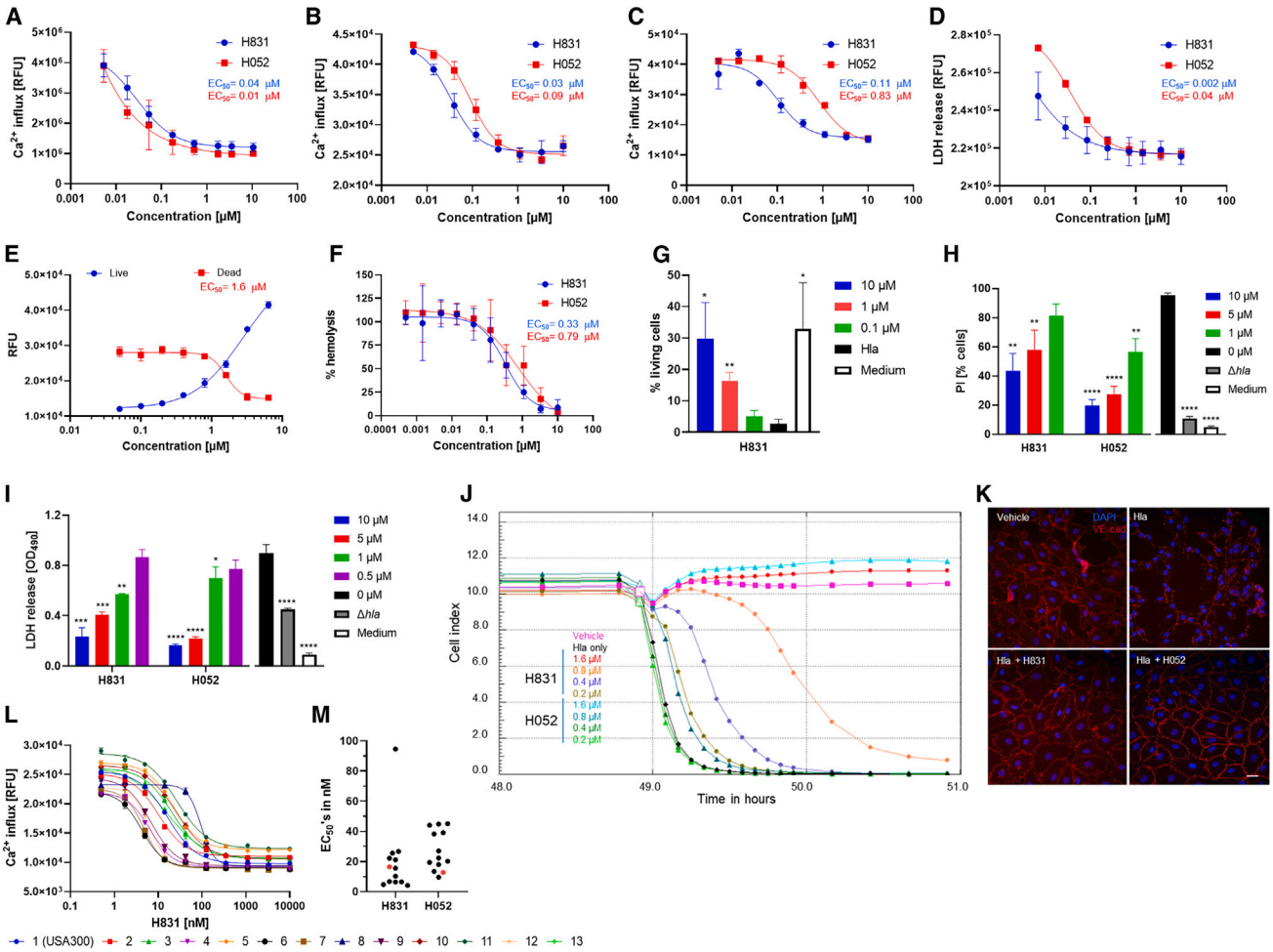

Figure 3. QDS inhibitors protect cells from Hla-induced Ca^{2+} influx and cell death and restore monolayer integrity and adherens junction

(A–C) Prevention of Ca^{2+} influx. U937 cells (A) were treated with 0.43 μg/mL Hla in the presence of increasing amounts of H052 or H831. Data points represent three independent experiments (mean values ± SD). See also Figure S3. (B and C) Human $CD14^+$ monocytes (B) and pulmonary microvascular endothelial cells (C) were treated with 1 μg/mL Hla in the presence of increasing amounts of H831 or H052. Data points represent two independent experiments (mean values ± SD).

(D) Prevention of LDH release from A549 epithelial cells. A549 cells were treated with 0.66 μg/mL Hla in the presence of increasing amounts of H831 or H052. Data points represent three independent experiments (mean values ± SD).

(E) Cytotoxicity assay with primary HSAEpCs. HSAEpC were grown in the presence of increasing amounts of H831 and treated with 2 μg/mL Hla for 20 h. Live cell (505 nm) and dead cell (520 nm) fluorescence was measured. Data points represent three independent experiments (mean values ± SD).

(F) Prevention of hemolysis in rabbit erythrocytes. Cells were treated with 0.8 μg/mL Hla in the presence of increasing amounts of H831 or H052. Data points represent three independent experiments (mean values ± SD).

(G) Murine naive CD4+ T cells were differentiated *in vitro* into Th1 cells in the presence or absence of H831 and Hla. Cells cultured in the absence of Hla served as medium control. On day 4, survival of the cells was analyzed by flow cytometry. Graph depicts frequencies of living cells (mean ± SD). Data were pooled from three independent experiments, each based on 4–6 technical replicates. Statistical significance was determined by unpaired, two-tailed t test compared with the inhibitor-free Hla control, $n = 3$. $^*p < 0.05$, $^{**}p < 0.01$.

(H and I) Co-culture of adherent A549 epithelial cells with *S. aureus* USA300. After incubation of cells with USA300 wild type (WT) for 6 h in the presence of H831 or H052, cells were labeled with the necrosis marker PI and analyzed by flow cytometry (H), and LDH release in the cell culture medium was determined (I). Bars represent three independent experiments (mean values ± SD). Statistical significance was determined by unpaired, two-tailed t test compared with inhibitor-free 0 μM control, $n = 3$. $^{****}p < 0.0001$, $^{***}p < 0.001$, $^{**}p < 0.01$, $^*p < 0.05$. See also Figure S2.

(J) Electrical impedance measurement of human lung cells treated with Hla in the absence and presence of QDS. HPMEC were seeded in E-plates and, at confluence after 48.9 h, cells were treated with 1 μg/mL Hla and H831 or H052. Mean cell impedance as cell index from four single wells in the time period between 48 and 51 h is shown. Measurement time was over 75 h.

(K) QDS prevented Hla-induced degradation of adherens junctions in primary human lung endothelial cells. HPMEC were grown on 8-well coverslips (top left) and incubated with 1 μg/mL Hla for 30 min in the absence (top right) or presence of H831 (1.6 μM, bottom left) or H052 (1.6 μM, bottom right). Cells were fixed in MeOH/acetone (50:50) and immunostained with VE-cadherin antibodies and Alexa647 IgG as secondary antibodies (red). DNA was visualized by DAPI staining (blue). Shown is a representative from three independent experiments with similar results. Scale bar: 20 μm. See also Figure S1.

(L and M) QDS inhibitors exert activity across all major Hla subtypes. (L) Concentration-response curves of H831 on Ca^{2+} influx in U937 cells induced by 13 Hla variants at 1 μg/mL (see Table S2). Data for H052 is shown in Figure S3F. Data points indicate two experiments (mean values ± SD). (M) Distribution of EC_{50} of the two QDS inhibitors H831 and H052. EC_{50} on Hla variant USA300 is highlighted in red. See also Table S3.

the effect of QDS. Hemolysis, induced by 0.8 μg/mL of Hla and tracked by the absorption of heme at 540 nm, was inhibited in the presence of H831 and H052 with EC_{50}s of 0.33 and 0.79 μM, respectively (Figure 3F).

Whole-cell infection model

All experiments mentioned above have been conducted with defined concentrations of pure, recombinant Hla. In order to more closely mimic an infection situation, the effect of Hla secreted *in situ* from *S. aureus* was probed. For this purpose, A549 lung epithelial cells were co-cultured with *S. aureus* USA300 at a multiplicity of infection of 10. The infection led to a pronounced increase in apoptosis and necrosis, as monitored by flow cytometry following annexin V and propidium iodide (PI) staining, respectively (Figure S2). An *hla*-deficient mutant strain of *S. aureus* USA300 was significantly less active, thereby proving that Hla was a major contributor to the phenotype. Apoptosis and necrosis could be prevented in a dose-dependent manner by H831 or H052, with H052 being more potent (Figures 3H and S2D). Similar effects were observed by QDS in preventing LDH release from infected cells (Figure 3I). To assess whether H831 or H052 exerted Hla-independent effects in the co-culture, we repeated the experiment with an *hla*-deficient *S. aureus* strain (USA300 *Δhla*). Neither H831 nor H052 reduced LDH release at concentrations of up to 20 μM (Figure S3D). Thus, we conclude that the neutralizing effect of the QDS was specific to Hla. We also verified that H831 or H052 had no antibiotic effect against the USA 300 strain with MIC of $\geq$50 μM.

Integrity of cellular monolayers and adherens junctions

Further hallmarks of Hla's pathogenicity are the destruction of endothelial and epithelial monolayers and endothelial tight junctions, enabling pathogen dissemination.[28] The monolayer integrity was monitored by single-frequency impedance spectroscopy, a label-free and non-invasive technique, which responds sensitively to changes in the morphology and viability of eukaryotic cells adherent to an electrode surface.[29–31] We grew a confluent monolayer of human microvascular lung endothelial cells on the surface of a gold microelectrode array in a microtiter plate. After 48.9 h, 1 μg/mL Hla was added and induced a rapid collapse of impedance within 30 min (Figure 3J). This collapse was inhibited in a dose-dependent manner by H831 and H052 with EC_{50}s of 0.20 and 0.98 μM, respectively. In addition, the effects on intercellular tight junctions and barrier function of the human bronchial epithelial cell line Calu-3 were monitored by measuring the transepithelial electrical resistance (TEER) in transwells. In the presence of either QDS, the Hla-induced drop of TEER could be prevented in a dose-dependent way, leading to complete protection of the epithelial barrier at 4.0 μM for either drug (Figure S1).

To confirm the protective effects of QDS on confluent cell layers with an orthogonal readout, immunofluorescence microscopy was used to visualize adherens junctions. HPMECs were grown on 8-well coverslips, incubated with 1 μg/mL Hla, fixed, and subsequently immunostained with anti-vascular endothelial (VE)-cadherin antibodies. Although Hla induced the degradation of adherens junctions, this effect was prevented in the presence of 1.6 μM of either H831 or H052 (Figure 3K).

Activity across major clinical Hla subtypes

The Hla sequence is known to be relatively well conserved overall across clinical isolates but variants exist. In order to probe whether QDS are efficacious against all major Hla variants, these were defined by a bioinformatic analysis. Sequences of clinical isolates[32,33] were analyzed and filtered for duplicates, for subtypes differing only in the N-terminal leader peptide that is cleaved off after secretion, and for variants with frameshift or stop codon mutations that would generate non-functional Hla. The selection led to thirteen sequences that cover 79% of the published clinical isolates (Table S2). All variants were produced recombinantly in *E. coli* and purified. The pore-forming activity of all subtypes was verified by Ca^{2+}-influx assays in U937 cells. It was observed that H052 (EC_{50} = 9–45 nM) and H831 (EC_{50} = 4–95 nM) inhibited Ca^{2+} influx in all subtypes (Figures 3L and 3M). This demonstrates that QDS can be applied broadly, effectively covering all prevalent clinical variants of the Hla sequence.

QDS bind to Hla and prevent the formation of functional pores

To decipher the mode of action of QDS, time-of-addition experiments were conducted. We first tested the effect of QDS addition before or after Hla on Ca^{2+} influx in U937 cells. H831 or H052 abrogated Hla-dependent Ca^{2+} influx when added before Hla (Figure 4A). However, the activity of QDS inhibitors was reduced when added after Hla (Figure 4B). Next, we tested the preferential interacting partner of QDS. Herein, adherent A549 cells were preincubated with H831 or H052 for 1 h. Cells were washed to remove unbound compounds, followed by the addition of Hla. No activity of QDS was observed, suggesting that the interaction of QDS with a cellular target is unlikely (Figure 4C). To determine whether QDS act directly on Hla, H831 or H052 were preincubated with Hla for 1 h, followed by removing unbound inhibitors with centrifugal membrane filters (5 kDa cutoff). When the retentates were applied to A549 cells, the viability of cells was preserved in a concentration-dependent manner (Figure 4D). This indicated that QDS exerted their activity by interacting with Hla.

In order to validate that QDS directly interact with Hla, independent from cellular proteins, we conducted single-channel electrophysiology experiments in lipid bilayers of 1,2-diphytanoyl-sn-glycerophosphocholine.[34] The addition of Hla led to a stepwise increase in the ion current,[35,36] in line with the incorporation of functional pores into the lipid bilayer (Figure 4E). The addition of either H831 or H052 at concentrations of 30 μM had no effect on the conductivity of a pre-formed pore (Figure S5). In contrast, a preincubation of H831 or H052 at concentrations of 3 μM with Hla prevented the Hla-induced stepwise increase of ion current (Figure 4F). These experiments demonstrate that QDS did not inhibit pre-existing pores, but they prevented the formation of functional pores by interacting with Hla.

To further pinpoint the molecular interactions of QDS with Hla, we first pursued a chemoproteomic approach with the H831 analog **14**, equipped with a diazirine-based photoaffinity probe and an alkyne handle for purification (Figure 5A). The probe was either incubated with U937 cells or pure Hla, then irradiated at 365 nm to induce a covalent attachment of the probe to its bound target(s). After cell lysis, the probe was derivatized with biotin azide through a copper-catalyzed click reaction, followed by affinity purification with avidin-coated beads. Proteins were eluted, separated by SDS-PAGE, and visualized by stain-free imaging. Whereas the probe did not pull down cellular proteins,

CellPress
OPEN ACCESS

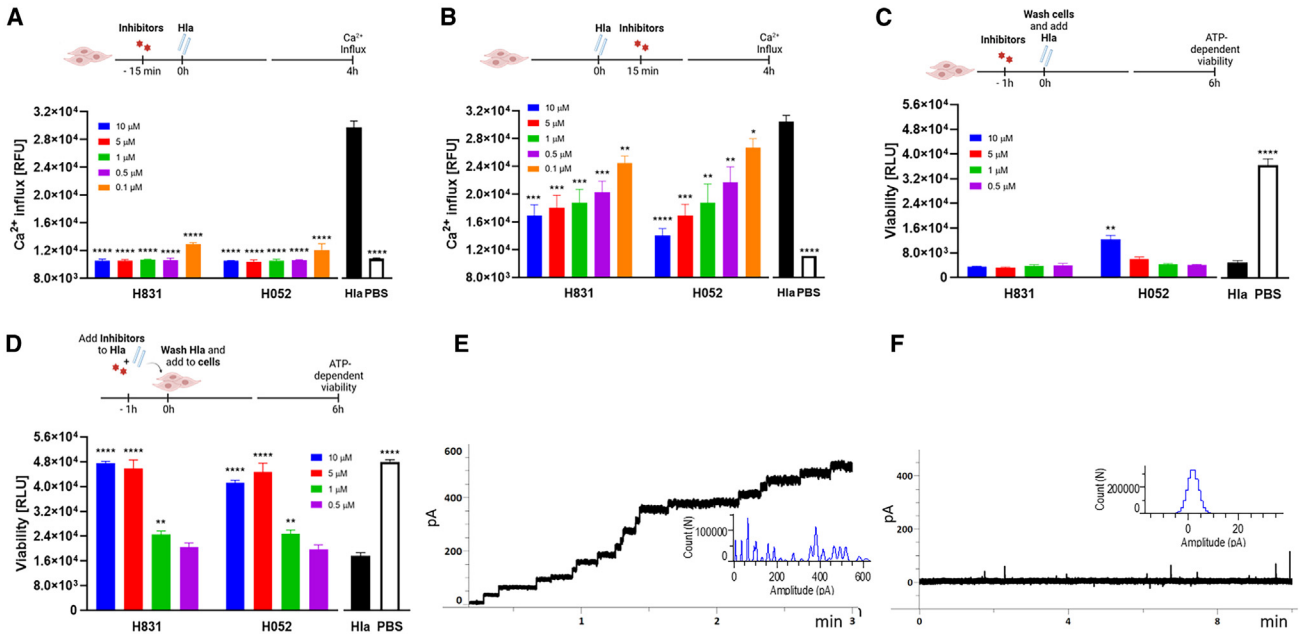

Figure 4. Mode of action of QDS

(A) H831 or H052 were added to U937 cells 15 min before the addition of 1 μg/mL Hla, and Ca^{2+} influx was measured after 4 h.

(B) H831 or H052 were added to U937 cells 15 min after Hla addition (1 μg/mL), and Ca^{2+} influx was measured after 4 h. QDS had reduced activity when added after Hla and did not fully block existing pores.

(C) H831 or H052 were preincubated with adherent A549 cells for 1 h. Thereafter, cells were washed and 1 μg/mL Hla was added. Cell viability was measured after 6 h.

(D) H831 or H052 were preincubated with Hla for 1 h. Thereafter, Hla was washed using centrifugal membrane filters (5 kDa cutoff) and added to cells. Cell viability was measured after 6 h. Viability was restored by QDS upon Hla incubation under (D) but not under (C). Bars represent three experiments with similar results (mean values ± SD). Statistical significance was determined by unpaired, two-tailed t test compared with inhibitor-free Hla control, $n = 3$. $^{****}p < 0.0001$, $^{***}p < 0.001$, $^{**}p < 0.01$, $^{*}p < 0.05$.

(E) Ion current recordings from a lipid bilayer in symmetrical 200 mM (*cis/trans*) NaCl solution at Vm = 50 mV after addition of a <1 μL droplet of Hla at 10 ng/mL at t = 0. Within 3 min, ≃20 Hla pores incorporated into the bilayer. Insert shows the corresponding ion current amplitude histogram at Vm = 50 mV.

(F) Ion current recordings over 10 min under conditions as in (E), but following preincubation of Hla with 3 μM H831. See also Figure S5.

a band for Hla was clearly visible after affinity purification (Figure 5B). Next, the binding site of a photoprobe on Hla was mapped at low resolution by tryptic digestion of Hla, followed by a tandem mass spectrometry analysis for QDS-modified peptides. This experiment was carried out with **15** (EC_{50} = 6.9 nM) and its deuterated version **16**, which were based on the biaryl H052 and equipped with an aryl azide for photoactivation. Tandem mass spectra demonstrated that **15** and **16** mainly labeled the amino acids W286 and Y54 (UniProtKB accession no: P09616) (Figure 5C). Interestingly, the labeled amino acid W286 is located at the brim of the heptameric mushroom-like head, close to the binding site for phospholipid headgroups that trigger heptamerization (Figure 5D).[10] The importance of the W286 position for the cellular interaction of Hla was proven by introducing a W286A mutation into Hla, which led to a complete abrogation of Hla activity in the Ca^{2+} assay (Figure S3G). To validate the chemoproteomics findings with an orthogonal method, we performed nuclear magnetic resonance (NMR) experiments with QDS and recombinant Hla (Figures 5E–5G and S4). First, saturation transfer difference (STD)[37] data with H831 and H052 clearly demonstrated that both compounds were interacting with Hla. In contrast, the inactive QDS analog **17** (EC_{50} > 32 μM) did not show an STD signal. The findings were further supported by ligand epitope mapping with increasing saturation times (Figure S4D). Secondly, ^{19}F-NMR shift experiments with QDS led to line broadening effects and chemical shift changes upon addition of Hla, which also points toward a specific binding event.[38] In contrast, such effects did not occur with the fluorinated, truncated analogs **S18** and **18**, which were devoid of the QDS pharmacophore and therefore functionally inactive (Figures S4E and S4F). A third and strong indication for ligand binding was obtained by chemical shift perturbation via transverse relaxation optimized spectroscopy (TROSY) experiments with a ^{15}N-labeled Hla variant (Figures 5C, 5D, 5G, and S4G). The addition of H831 induced distinct and specific chemical shifts mainly localized in one, contiguous region, close to its known binding site for phospholipid headgroups.[10] Overall, the NMR experiments provide evidence that the QDS mechanism of action starts by binding to monomeric Hla as the initial mechanism of action.

Although this mechanistic picture is plausible and sufficient, we wanted to probe whether secondary mechanisms involving binding to targets on the surface or inside the host cell exist. For example, the inhibition of cellular sphingomyelinase has been reported to counteract Hla effects.[28] However, H831 or H052 were not found to have any effect on sphingomyelinase activity

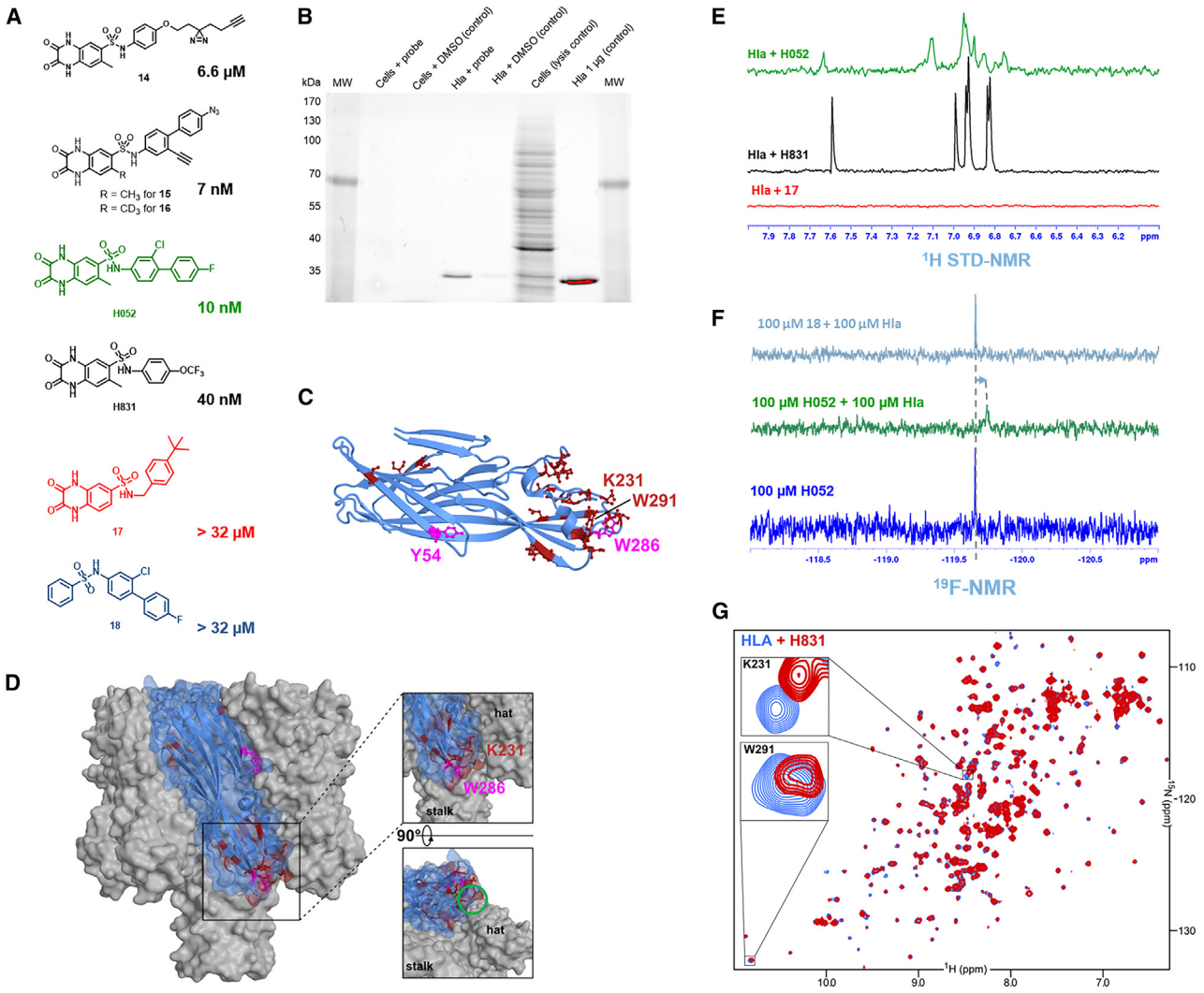

Figure 5. QDS bind to Hla according to chemoproteomics and NMR experiments

(A) Structures and EC_{50} values (Ca-influx assay) of photoaffinity probes and QDS used for NMR experiments (E)–(G).

(B–D) Chemoproteomics experiments. (B) Probe **14** was incubated with cells (lane 1) or pure Hla (lane 3), irradiated at 365 nm for 30 min, clicked with biotin azide, and affinity purified with avidin-coated beads. Proteins were eluted, separated by SDS-PAGE, and visualized in-gel with trichloroethanol. Whereas the probe did not pull down cellular proteins, an affinity purification of Hla was clearly visible. See also Figure S4 and Table S5. (C and D) Peptide residues that were modified by **15** and **16**, according to tandem mass spectrometry of a tryptic digest, were mapped to the structure of the Hla monomer (PDB: 4IDJ) (C) or to the structure of the heptameric pore (D) (PDB: 3ANZ) and are shown in magenta, whereas significant CSPs (CSP > 0.013) from the NMR titration are shown in red. The known binding site for phospholipid headgroups that trigger heptamerization is indicated with a green circle (under the "rim").

(E–G) NMR experiments. (E) Saturation transfer difference NMR (STD-NMR) experiments demonstrate an STD effect of Hla (10 µM) to QDS inhibitors H831 and H052, whereas no effect was visible toward the inactive analog **17**. Experiments were performed in aqueous buffer (TRIS, pH 8.5) with the addition of 10% D_2O, the QDS concentration was 500 µM. (F) ^{19}F NMR experiments with fluorine-containing QDS (100 µM) and Hla (100 µM, buffer conditions: see E). The signal shift and line broadening indicate binding of H052, whereas the effect was not observed for negative control compound **18**. (G) ^{1}H-^{15}N TROSY experiment of ^{15}N-labeled Hla (inactive H61A variant) at 125 µM (blue) with 0.6 equivalents of H831 titrated (red) resulted in distinct and specific signal shifts. Examples of significantly perturbated residues (CSP >0.013) are shown. See also Figure S4.

(Figure S3J). We observed a moderate antagonism of the *N*-methyl-D-aspartate (NMDA) receptor in binding assays (44% @ 10 µM) that, however, could not account for the high nM potency of the QDS. In order to detect potential secondary targets in an unbiased manner, a large-scale thermal proteome profiling (TPP) of A549 cells exposed to H052 in a dilution series was conducted. Among 7,229 proteins detected, only 19 exhibited a dose-dependent thermal shift upon H052 treatment (Table S5). A disintegrin and metalloproteinase (ADAM)10, the host cell receptor for Hla, was detected, but not regulated, by H052. Overall, the number of binders to QDS was small and we did not recognize proteins of potential mechanistic relevance. In sum, experiments using NMR, photoaffinity labeling, TPP, and electrophysiological measurements imply that QDS prevent the formation of functional pores by binding to Hla.

CellPress
OPEN ACCESS

QDS have favorable PK properties and are well tolerated

H052 and H831 were stable in liver microsomes and in plasma (human and mouse) and had solubilities of 202 and 337 μM at pH 7.4, respectively (Table S3). Their permeability in CaCo-2 cells was low as a result of efflux as well as an inherently low passive membrane permeation, as demonstrated by a directional flux analysis and a parallel artificial membrane permeation assay (PAMPA) (Table S3). In pharmacokinetic (PK) studies in CD-1 mice, the half-life in plasma after intravenous (i.v.) dosing of 1 mg/kg was 1.25 h for H831 and 1.67 h for H052, with respective C_0 values of 1.39 and 1.45 μg/mL (Table S3). The volumes of distribution of 1.1–1.2 L/kg for both inhibitors suggest that the compounds were largely confined to the circulating system and extracellular fluids of the body. The metabolic stability *in vitro* was reflected by relatively low clearances of 10.5 and 8.2 mL/kg/min for H831 and H052, respectively. Compound levels in lung tissue and bronchoalveolar lavage fluid (BALF) were assessed after subcutaneous (s.c.) and intraperitoneal (i.p.) administration of 60 mg/kg. Remarkably, H052 showed much higher terminal plasma and tissue levels compared with H831 (Figures 6A and 6C). A single i.p. dose of 60 mg/kg H052 led to terminal concentrations of 0.54 and 0.85 μM after 8 h in lung parenchyma and BALF, respectively (Table S3). To get a better understanding of penetration of H052 and H831 into the lung, we administered both compounds at 20 mg/kg via nebulization (Figures 6B and 6D). Both compounds penetrated rapidly into lung tissue, and their PK behavior in lung tissue was similar to that in the BALF. Compounds then transitioned into plasma, as seen by a slightly later C_{max} in plasma compared with lung tissue.

QDS show efficacy in *S. aureus* lung infection models

The PK data encouraged us to pursue *in vivo* efficacy studies with H052, which was preferred over H831 due to its better exposure in lung tissue and BALF. To assure compound levels above the EC_{50} in the lung over a long time period, an i.p. administration of 60 mg/kg was selected based on the PK data reported above. Adapting an established study design,[39,40] male, immunocompetent C57BL/6 mice were intranasally infected with *S. aureus* USA300 with a dose of 5×10^8 colony-forming units (CFUs)/mouse, which led to rapid lethality within 24 h. However, animals that were treated twice daily (BID) with 60 mg/kg of H052 had a significantly improved survival rate compared with the vehicle control (Figure 6E; Table S4). Moreover, mice with a high disease score after infection completely recovered over time when treated with H052. Next, a lung infection model was set up in order to show compound effects beyond survival (Figures 6G and 6H; Table S4). We observed that a prophylactic treatment with H052 led to a significant reduction of bacterial loads in the lung 24 h post infection, from 9.5 ± 0.11 (vehicle control) to 6.48 ± 0.54 CFU/g. This was accompanied by a reduction of pro-inflammatory interleukin-6 (IL-6) levels in the lung tissue from 4,325 ± 2,876 to 899 ± 990 pg/mL. The protective effects were further confirmed by histopathological data (Figure S6). Finally, H052 was tested in combination with linezolid (LZD), the standard-of-care treatment for MRSA lung infections in the hospital, with a reduced inoculum of 4×10^8 CFU/mouse. In addition, we probed whether the drugs were effective when administered after infection (Figure 6F; Table S4). The administration of 100 mg/kg of LZD, given 1 h post infection, conferred full protection. When the LZD dose was reduced to 2.5 mg/kg, only little, non-significant improvement in survival over the vehicle control (40% vs. 30%) was observed. The survival rate with 60 mg/kg (i.p., twice a day [BID]) of H052 improved from 30% for the vehicle control to 60%. However, a combination of 2.5 mg/kg LZD plus 60 mg/kg H052 restored the survival rate to 90%, and a pre-emptive dose of H052 1 day before infection led to 100% survival. The experiments demonstrate that the inhibition of Hla by QDS can be combined with antibiotic therapy to enhance efficacy in a therapeutic setting.

In summary, although H052 possessed no antibiotic activity, its action as an Hla inhibitor led to a reduction of CFU counts and inflammatory biomarkers and an improvement of survival, even when given as a monotherapy.

DISCUSSION

S. aureus secretes a broad cocktail of toxins.[41] A critical question for target validation is whether the inhibition of a single factor is sufficient, given that the other components remain unaffected. The role of Hla as the major virulence factor in lung infections caused by *S. aureus* is supported by numerous preclinical and human data. A pharmacological treatment, wherein Hla alone was neutralized by selective monoclonal antibodies, showed efficacy in preclinical and clinical settings.[15,16] The prospect to discover first-in-class small molecule inhibitors of a validated target motivated us to find inhibitors of Hla. An assay strategy that sampled effects induced by a single component—pure, recombinant Hla—in a relevant cellular context was pursued. The miniaturization of the cellular assay to a 9-μL scale enabled a high-throughput screen and the discovery of the QDS series. QDS efficacy was confirmed in assays with orthogonal readouts that cover all cell types of relevance for infection. QDS inhibited pore formation, cell death, hemolysis, and the destruction of monolayer integrity, thereby addressing the hallmarks of Hla pathogenicity. The efficacy of QDS differed depending on the readout and cell type; for example, while the EC_{50} of H052 in the Ca^{2+} influx assay was 10 nM in U937 cells, an EC_{50} of 400 nM was observed for human NK cells (Table S3). We hypothesize that this reflects different cellular sensitivities toward the remaining, non-neutralized Hla fraction. Cellular time-of-addition experiments, electrophysiology data from protein-free lipid bilayers, biophysical as well as structural data obtained by NMR, and chemoproteomics imply that QDS interfere directly with Hla. An alternative mechanism of action involving the modulation of intracellular targets was probed by proteome-wide thermal profiling that, however, disclosed a relatively small number of binding partners. Interactions with cellular sphingomyelinase or with ADAM10 would account for Hla inhibition but could be excluded. An intracellular action of QDS is also hampered by their low cellular permeability, as demonstrated by PAMPA and Caco-2 assays. We conclude that the QDS' mechanism of action is the inhibition of functional pore formation by a direct interaction with Hla monomers.[42,43]

The short, non-optimized synthesis of H831 and H052 with 35%–37% overall yield, conducted in a >100 g scale for H052, demonstrates that QDS can be readily produced, also rendering their use affordable in low-cost settings, particularly when compared with monoclonal antibodies. In PK studies with

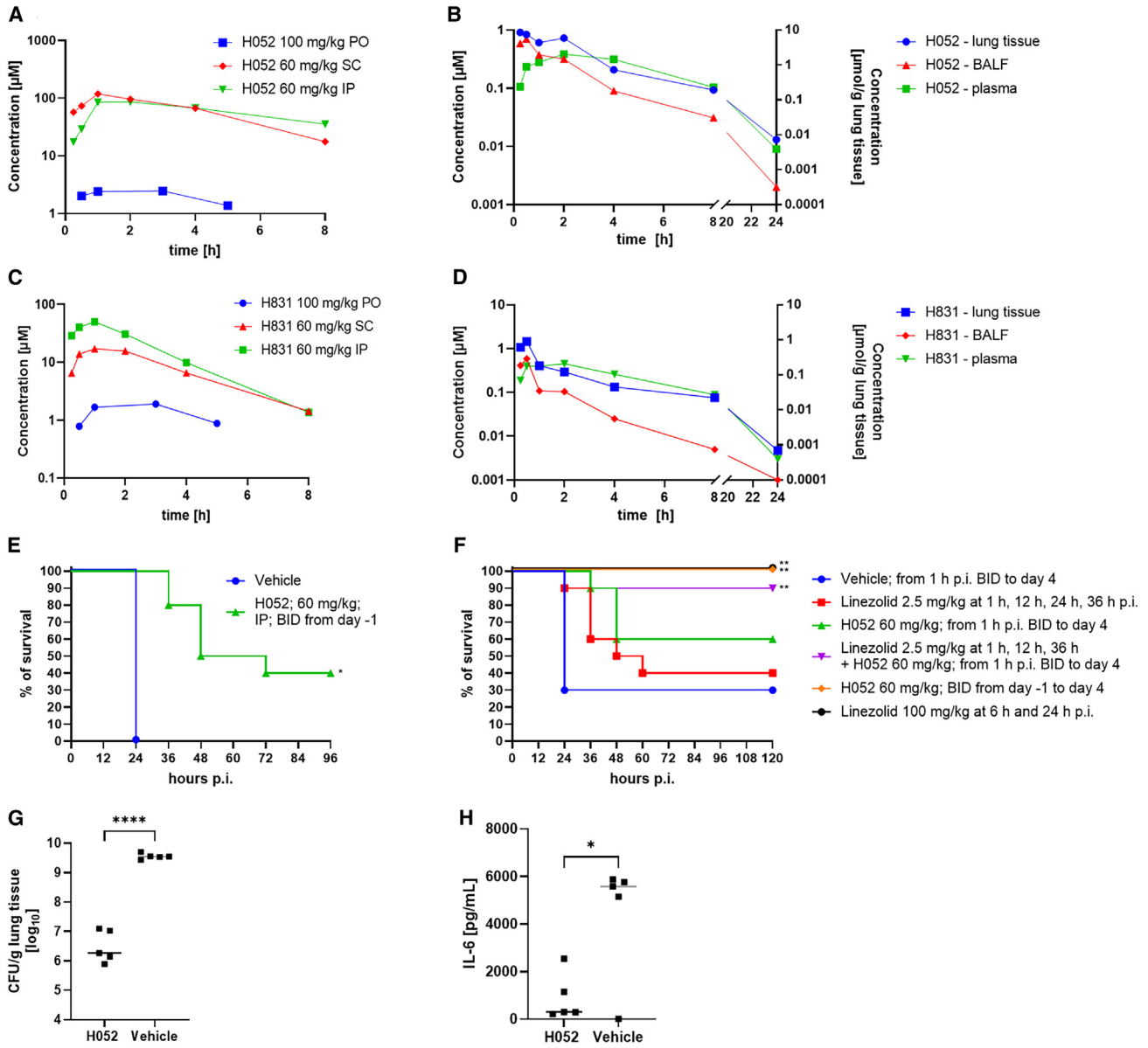

Figure 6. *In vivo* pharmacokinetics and efficacy of QDS

(A–D) PKs of H052 and H831. Plasma concentrations in CD-1 mice after single administration of H052 (A) or H831 (C) via subcutaneous (s.c., red, $n = 3$), intraperitoneal (i.p., green, $n = 3$) or peroral (PO, blue, $n = 2$) routes. Lung tissue (blue, $n = 3$), bronchoalveolar lavage fluid (BALF, red, $n = 3$), and plasma (green, $n = 3$) concentrations in CD-1 mice after single administration of 20 mg/kg H052 (B) or H831 (D) via inhalation. See also Table S3.

(E–H) Efficacy studies performed in C57BL/6 mice after intranasal infection with *S. aureus* USA300. (E) Survival rate plotted vs. hours post infection after H052 treatment (60 mg/kg i.p., BID); $^*p < 0.0001$ vs. vehicle, log rank test (Mantel-Cox), $n = 10$ animals each group. See also Table S4. (F) Survival rate plotted vs. hours post infection of H052 as standalone and in combination with linezolid. $^*p < 0.01$ vs. vehicle, log rank test (Mantel-Cox), $n = 10$ animals each group, apart from the treatment with H052 60 mg/kg from day −1, where one animal was excluded at the start of the experiment due to a technical issue. (G) Bacterial burden in lungs treated either with H052 (60 mg/kg) or with vehicle alone; $^{****}p < 0.0001$. (H) IL-6 concentration in lungs. $^*p < 0.05$. Error bars indicate SD, $n = 5$ animals each group. See also Figure S6 and Table S4.

healthy volunteers, the anti-Hla monoclonal antibody ASN-1 reached its maximum concentration in the epithelial lining fluid (ELF) after 8 days following i.v. administration.[44] Although there are no directly comparable human PK data for H052, concentrations above the EC_{50} were reached at 8 h post administration of a well-tolerated dose in mice. An inhalative administration was also feasible and led to high nM concentrations in BALF. We therefore anticipate that the distribution kinetics of the small QDS helps achieve rapid drug exposure to the ELF, the relevant lung compartment where Hla inhibition is indicated.

QDS inhibitors are classified as non-traditional antibacterial compounds or pathoblockers. Although the advantages of pathoblockers, such as reduced selection pressure or microbiota preservation, have been widely recognized,[6,45] their clinical

translation has been hampered by challenges in demonstrating efficacy in preclinical models, which often require combination with standard antibiotics, and in deriving dose predictions without standard, MIC-based pharmacokinetic/pharmacodynamic (PK/PD) tools.[46] The current study demonstrates that the inhibition of large bacterial toxins can be achieved by a small molecule. A recent paper reported small molecule inhibitors of pneumolysin by *in vitro* and cellular experiments.[47] Notably, QDS inhibitors have shown clear *in vivo* effects already as a monotherapy on endpoints like survival. Moreover, QDS reduced bacterial load *in vivo* and reduced the levels of the inflammation marker IL-6, readouts that facilitate establishing PK/PD relationships. We hypothesize that a reduction of bacterial load in spite of a missing antibiotic effect is a consequence of protecting phagocytic cells in the lungs from the damaging effect of Hla, resulting in maintained eradication of *S. aureus*. QDS prevent the formation of functional pores but do not inhibit existing pores. Accordingly, their efficacy in a prevention mode was higher than in a therapeutic mode (Figure 6D). This suggests that a preferred clinical application lies in the prevention of pneumonia in patient populations at high risk of developing nosocomial pneumonia caused by *S. aureus*. Such a concept would spare antibiotics and contribute to limit the spread of antimicrobial resistance.

RESOURCE AVAILABILITY

Lead contact

Further information and requests for resources and reagents should be directed to, and will be fulfilled by, the lead contact, Mark Brönstrup (mark.broenstrup@helmholtz-hzi.de).

Materials availability

Materials generated in this study are available upon request from the lead contact in accordance with existing guidelines and regulations.

Data and code availability

- All data supporting the findings of this study are available within the article and its supplemental information or have been deposited to the indicated databases.
- Two-dimensional TPP (2D-TPP) mass spectrometry proteomics data have been deposited to the ProteomeXchange Consortium via the PRIDE partner repository (https://www.ebi.ac.uk/pride/). The dataset identifier is PXD046735.
- Photoaffinity labeling for binding site identification mass spectrometry proteomics data have been deposited to the ProteomeXchange Consortium (http://proteomecentral.proteomexchange.org) via the PRIDE partner repository.[48] The dataset identifier is PXD050156.
- This paper does not report original code.
- Any additional information required to reanalyze the data reported in this work paper is available from the lead contact upon request.

ACKNOWLEDGMENTS

The project has received funding from the Helmholtz validation fund (HVF-LDC-003), the HZI pre-4D fund, the German Center for Infection Research (grant no. TTU09.722), and CARB-X (grant no. 4500003713). K.J. received funding via the doctoral program "Drug Discovery and Cheminformatics for New Anti-Infectives" (iCA). The content of this publication is solely the responsibility of the authors and does not necessarily represent the official views of CARB-X or any of its funders. We thank Andrea Ahlers, Friederike Kruse, Brigitte Pawletta, Janine Schreiber, and Rebecka Wünsche for excellent technical assistance. We thank Dr. Lothar Gröbe and Maria Höxter for support with flow cytometry experiments and Alix Grünhagen for assistance with microscopy. We are grateful to Prof. Teresa Carlomagno for her valuable input for NMR studies and Dr. Matthias Köck for initiating the NMR experiments. We thank Anja Meier for MS/MS measurements.

AUTHOR CONTRIBUTIONS

Conceptualization, T.W., T.H., W.B., E.M., U.B., K.D., and M.B.; methodology, A.S., R.D.L., K.J., V.S.K., K.R., H.A.W., C.D., E.F., A.U., B.K., P.L., F.S., C.-M.L., L.J., J.H., R.A., M. Savitski, M. Sattler, and M.W.; investigation, A.S., R.D.L., K.J., V.S.K., K.H., K.R., H.A.W., I.G., F.D., I.B., C.D., P.H., P.L., S.S., S.H., L.J., R.D., C.R., N.S.-D., B.H., and J.N.; writing – original draft, A.S., K.J., V.S.K., and M.B.; writing – review and editing, A.S., R.D.L., K.H., K.R., and M.B.; visualization, A.S., K.J., V.S.K., and M.B.; supervision, K.R., H.A.W., B.K., W.B., E.M., U.B., K.D., and M.B.; and funding acquisition, M.B.

DECLARATION OF INTERESTS

R. Dilucrezia, M. Brönstrup, U. Bilitewski, C. Degenhart, K. Dinkel, K. Jerye, E. Kalawi Fansa, V. Korotkov, E. Medina, K. Rox, A. Shekhar, and H. Weich are inventors on the patent application WO2023280970A1 on QDS inhibitors. M. Brönstrup and R. Di Lucrezia are inventors on the patent application WO2024133220 A1 on QDS inhibitors.

STAR★METHODS

Detailed methods are provided in the online version of this paper and include the following:

- KEY RESOURCES TABLE
- EXPERIMENTAL MODEL AND STUDY PARTICIPANT DETAILS
  - Mammalian primary cells and cell lines
  - S. aureus USA300 and generation of S. aureus USA300 Δhla
  - Animal models
  - Ethics statement
- METHOD DETAILS
  - Cytotoxicity assay and cell viability assays
  - Calcium influx assay
  - Hemolysis assay
  - VE stain
  - Studies on epithelial and microvascular leakage with primary cells
  - NMR experiments
  - Pharmacokinetic (PK) studies
  - MS compound analytics
  - Pneumonia survival model
  - Lung infection model for bacterial load and IL-6
  - Pneumonia survival model for prophylactic and therapeutic monotherapy
  - Assay development and high throughput screening
  - Two-dimensional thermal proteome profiling (2D-TPP)
  - LC-MS measurement and data analysis
  - Lipid bilayer experiments
  - Photoaffinity labelling for target identification
  - Photoaffinity labelling for binding site identification
  - LDH assay
  - MTT assay
  - Whole cell infection model
  - LDH release in the infection model
  - Apoptosis-necrosis staining for the infection model
  - Western blot for Hla
  - Recombinant protein production
  - Differential Scanning Floriometry
  - Sphingomyelinase activity assay
  - In vitro pharmacology
  - Starting Materials for chemical synthesis
  - Accurate Mass method
  - NMR methods
  - Flash Column Chromatography

- High-Performance Liquid Chromatography (HPLC)
- Scale up synthesis for H052
- Chemical synthesis

- QUANTIFICATION AND STATISTICAL ANALYSIS

SUPPLEMENTAL INFORMATION

Supplemental information can be found online at https://doi.org/10.1016/j.chom.2025.03.006.

Received: August 23, 2024
Revised: January 27, 2025
Accepted: March 6, 2025
Published: March 31, 2025

REFERENCES

1. Tong, S.Y.C., Davis, J.S., Eichenberger, E., Holland, T.L., and Fowler, V.G., Jr. (2015). Staphylococcus aureus infections: epidemiology, pathophysiology, clinical manifestations, and management. Clin. Microbiol. Rev. *28*, 603–661. https://doi.org/10.1128/CMR.00134-14.
2. Murray, C.J.L., Ikuta, K.S., Sharara, F., Swetschinski, L., Robles Aguilar, G., Gray, A., Han, C., Bisignano, C., Rao, P., Wool, E., et al. (2022). Global burden of bacterial antimicrobial resistance in 2019: a systematic analysis. Lancet *399*, 629–655. https://doi.org/10.1016/S0140-6736(21)02724-0.
3. Rubinstein, E., Kollef, M.H., and Nathwani, D. (2008). Pneumonia caused by methicillin-resistant Staphylococcus aureus. Clin. Infect. Dis. *46*, S378–S385. https://doi.org/10.1086/533594.
4. Allen, R.C., Popat, R., Diggle, S.P., and Brown, S.P. (2014). Targeting virulence: can we make evolution-proof drugs? Nat. Rev. Microbiol. *12*, 300–308. https://doi.org/10.1038/nrmicro3232.
5. Dickey, S.W., Cheung, G.Y.C., and Otto, M. (2017). Different drugs for bad bugs: antivirulence strategies in the age of antibiotic resistance. Nat. Rev. Drug Discov. *16*, 457–471. https://doi.org/10.1038/nrd.2017.23.
6. Theuretzbacher, U., and Piddock, L.J.V. (2019). Non-traditional Antibacterial Therapeutic Options and Challenges. Cell Host Microbe *26*, 61–72. https://doi.org/10.1016/j.chom.2019.06.004.
7. Los, F.C.O., Randis, T.M., Aroian, R.V., and Ratner, A.J. (2013). Role of pore-forming toxins in bacterial infectious diseases. Microbiol. Mol. Biol. Rev. *77*, 173–207. https://doi.org/10.1128/MMBR.00052-12.
8. Dal Peraro, M.D., and van der Goot, F.G. (2016). Pore-forming toxins: ancient, but never really out of fashion. Nat. Rev. Microbiol. *14*, 77–92. https://doi.org/10.1038/nrmicro.2015.3.
9. Berube, B.J., and Wardenburg, J. (2013). Staphylococcus aureus alpha-toxin: nearly a century of intrigue. Toxins *5*, 1140–1166. https://doi.org/10.3390/toxins5061140.
10. Song, L., Hobaugh, M.R., Shustak, C., Cheley, S., Bayley, H., and Gouaux, J.E. (1996). Structure of staphylococcal alpha-hemolysin, a heptameric transmembrane pore. Science *274*, 1859–1865. https://doi.org/10.1126/science.274.5294.1859.
11. Wilke, G.A., and Wardenburg, J.B. (2010). Role of a disintegrin and metalloprotease 10 in Staphylococcus aureus alpha-hemolysin-mediated cellular injury. Proc. Natl. Acad. Sci. USA *107*, 13473–13478. https://doi.org/10.1073/pnas.1001815107.
12. Kwak, Y.K., Vikström, E., Magnusson, K.E., Vécsey-Semjén, B., Colque-Navarro, P., and Möllby, R. (2012). The Staphylococcus aureus alpha-toxin perturbs the barrier function in Caco-2 epithelial cell monolayers by altering junctional integrity. Infect. Immun. *80*, 1670–1680. https://doi.org/10.1128/IAI.00001-12.
13. Cohen, T.S., Hilliard, J.J., Jones-Nelson, O., Keller, A.E., O'Day, T., Tkaczyk, C., DiGiandomenico, A., Hamilton, M., Pelletier, M., Wang, Q., et al. (2016). Staphylococcus aureus alpha toxin potentiates opportunistic bacterial lung infections. Sci. Transl. Med. *8*, 329ra331. https://doi.org/10.1126/scitranslmed.aad9922.
14. Bubeck Wardenburg, J., Bae, T., Otto, M., Deleo, F.R., and Schneewind, O. (2007). Poring over pores: alpha-hemolysin and Panton-Valentine leukocidin in Staphylococcus aureus pneumonia. Nat. Med. *13*, 1405–1406. https://doi.org/10.1038/nm1207-1405.
15. François, B., Jafri, H.S., Chastre, J., Sánchez-García, M., Eggimann, P., Dequin, P.F., Huberlant, V., Viña Soria, L., Boulain, T., Bretonnière, C., et al. (2021). Efficacy and safety of suvratoxumab for prevention of Staphylococcus aureus ventilator-associated pneumonia (SAATELLITE): a multicentre, randomised, double-blind, placebo-controlled, parallel-group, phase 2 pilot trial. Lancet Infect. Dis. *21*, 1313–1323. https://doi.org/10.1016/S1473-3099(20)30995-6.
16. François, B., Mercier, E., Gonzalez, C., Asehnoune, K., Nseir, S., Fiancette, M., Desachy, A., Plantefève, G., Meziani, F., de Lame, P.A., et al. (2018). Safety and tolerability of a single administration of AR-301, a human monoclonal antibody, in ICU patients with severe pneumonia caused by Staphylococcus aureus: first-in-human trial. Intensive Care Med. *44*, 1787–1796. https://doi.org/10.1007/s00134-018-5229-2.
17. Karginov, V.A., Nestorovich, E.M., Schmidtmann, F., Robinson, T.M., Yohannes, A., Fahmi, N.E., Bezrukov, S.M., and Hecht, S.M. (2007). Inhibition of S. aureus alpha-hemolysin and B. anthracis lethal toxin by beta-cyclodextrin derivatives. Bioorg. Med. Chem. *15*, 5424–5431. https://doi.org/10.1016/j.bmc.2007.05.058.
18. Karginov, V.A., Nestorovich, E.M., Yohannes, A., Robinson, T.M., Fahmi, N.E., Schmidtmann, F., Hecht, S.M., and Bezrukov, S.M. (2006). Search for cyclodextrin-based inhibitors of anthrax toxins: synthesis, structural features, and relative activities. Antimicrob. Agents Chemother. *50*, 3740–3753. https://doi.org/10.1128/AAC.00693-06.
19. Ragle, B.E., Karginov, V.A., and Bubeck Wardenburg, J. (2010). Prevention and treatment of Staphylococcus aureus pneumonia with a beta-cyclodextrin derivative. Antimicrob. Agents Chemother. *54*, 298–304. https://doi.org/10.1128/AAC.00973-09.
20. Qiu, J., Niu, X., Dong, J., Wang, D., Wang, J., Li, H., Luo, M., Li, S., Feng, H., and Deng, X. (2012). Baicalin protects mice from Staphylococcus aureus pneumonia via inhibition of the cytolytic activity of alpha-hemolysin. J. Infect. Dis. *206*, 292–301. https://doi.org/10.1093/infdis/jis336.
21. Dong, J., Qiu, J., Zhang, Y., Lu, C., Dai, X., Wang, J., Li, H., Wang, X., Tan, W., Luo, M., et al. (2013). Oroxylin A inhibits hemolysis via hindering the self-assembly of alpha-hemolysin heptameric transmembrane pore. PLoS Comput. Biol. *9*, e1002869. https://doi.org/10.1371/journal.pcbi.1002869.
22. Qiu, J., Wang, D., Zhang, Y., Dong, J., Wang, J., and Niu, X. (2013). Molecular modeling reveals the novel inhibition mechanism and binding mode of three natural compounds to staphylococcal alpha-hemolysin. PLoS One *8*, e80197. https://doi.org/10.1371/journal.pone.0080197.
23. Dong, J., Qiu, J., Wang, J., Li, H., Dai, X., Zhang, Y., Wang, X., Tan, W., Niu, X., Deng, X., et al. (2013). Apigenin alleviates the symptoms of Staphylococcus aureus pneumonia by inhibiting the production of alpha-hemolysin. FEMS Microbiol. Lett. *338*, 124–131. https://doi.org/10.1111/1574-6968.12040.
24. Feng, J., Sun, D., Wang, L., Li, X., Guan, J., Wei, L., Yue, D., Wang, X., Zhao, Y., Yang, H., et al. (2022). Biochanin A as an α-hemolysin inhibitor for combating methicillin-resistant Staphylococcus aureus infection. World J. Microbiol. Biotechnol. *38*, 6. https://doi.org/10.1007/s11274-021-03182-4.
25. Wang, J., Zhou, X., Liu, S., Li, G., Shi, L., Dong, J., Li, W., Deng, X., and Niu, X. (2015). Morin hydrate attenuates Staphylococcus aureus virulence by inhibiting the self-assembly of alpha-hemolysin. J. Appl. Microbiol. *118*, 753–763. https://doi.org/10.1111/jam.12743.
26. Wang, T., Zhang, P., Lv, H., Deng, X., and Wang, J. (2020). A Natural Dietary Flavone Myricetin as an alpha-Hemolysin Inhibitor for Controlling Staphylococcus aureus Infection. Front. Cell. Infect. Microbiol. *10*, 330. https://doi.org/10.3389/fcimb.2020.00330.
27. Bonifacius, A., Goldmann, O., Floess, S., Holtfreter, S., Robert, P.A., Nordengrün, M., Kruse, F., Lochner, M., Falk, C.S., Schmitz, I., et al. (2020). Staphylococcus aureus Alpha-Toxin Limits Type 1 While

Fostering Type 3 Immune Responses. Front. Immunol. *11*, 1579. https://doi.org/10.3389/fimmu.2020.01579.

28. Becker, K.A., Fahsel, B., Kemper, H., Mayeres, J., Li, C., Wilker, B., Keitsch, S., Soddemann, M., Sehl, C., Kohnen, M., et al. (2018). Staphylococcus aureus Alpha-Toxin Disrupts Endothelial-Cell Tight Junctions via Acid Sphingomyelinase and Ceramide. Infect. Immun. *86*, e00606–e00617. https://doi.org/10.1128/IAI.00606-17.
29. Giaever, I., and Keese, C.R. (1993). A morphological biosensor for mammalian cells. Nature *366*, 591–592. https://doi.org/10.1038/366591a0.
30. Valdés-Varela, L., Alonso-Guervos, M., García-Suárez, O., Gueimonde, M., and Ruas-Madiedo, P. (2016). Screening of Bifidobacteria and Lactobacilli Able to Antagonize the Cytotoxic Effect of Clostridium difficile upon Intestinal Epithelial HT29 Monolayer. Front. Microbiol. *7*, 577. https://doi.org/10.3389/fmicb.2016.00577.
31. Ludwig, A., Sommer, A., and Uhlig, S. (2011). Assessment of endothelial permeability and leukocyte transmigration in human endothelial cell monolayers. Methods Mol. Biol. *763*, 319–332. https://doi.org/10.1007/978-1-61779-191-8_22.
32. Tabor, D.E., Yu, L., Mok, H., Tkaczyk, C., Sellman, B.R., Wu, Y., Oganesyan, V., Slidel, T., Jafri, H., McCarthy, M., et al. (2016). Staphylococcus aureus Alpha-Toxin Is Conserved among Diverse Hospital Respiratory Isolates Collected from a Global Surveillance Study and Is Neutralized by Monoclonal Antibody MEDI4893. Antimicrob. Agents Chemother. *60*, 5312–5321. https://doi.org/10.1128/AAC.00357-16.
33. Tavares, A., Nielsen, J.B., Boye, K., Rohde, S., Paulo, A.C., Westh, H., Schønning, K., de Lencastre, H., and Miragaia, M. (2014). Insights into alpha-hemolysin (Hla) evolution and expression among Staphylococcus aureus clones with hospital and community origin. PLoS One *9*, e98634. https://doi.org/10.1371/journal.pone.0098634.
34. Gutsmann, T., Heimburg, T., Keyser, U., Mahendran, K.R., and Winterhalter, M. (2015). Protein reconstitution into freestanding planar lipid membranes for electrophysiological characterization. Nat. Protoc. *10*, 188–198. https://doi.org/10.1038/nprot.2015.003.
35. Benz, R., Schmid, A., Wagner, W., and Goebel, W. (1989). Pore formation by the Escherichia coli hemolysin: evidence for an association-dissociation equilibrium of the pore-forming aggregates. Infect. Immun. *57*, 887–895. https://doi.org/10.1128/iai.57.3.887-895.1989.
36. Krasilnikov, O.V., Sabirov, R.Z., Ternovsky, V.I., Merzliak, P.G., and Tashmukhamedov, B.A. (1988). The structure of Staphylococcus aureus alpha-toxin-induced ionic channel. Gen. Physiol. Biophys. *7*, 467–473.
37. Angulo, J., and Nieto, P.M. (2011). STD-NMR: application to transient interactions between biomolecules-a quantitative approach. Eur. Biophys. J. *40*, 1357–1369. https://doi.org/10.1007/s00249-011-0749-5.
38. Tengel, T., Fex, T., Emtenäs, H., Almqvist, F., Sethson, I., and Kihlberg, J. (2004). Use of 19F NMR spectroscopy to screen chemical libraries for ligands that bind to proteins. Org. Biomol. Chem. *2*, 725–731. https://doi.org/10.1039/B313166A.
39. Hua, L., Hilliard, J.J., Shi, Y., Tkaczyk, C., Cheng, L.I., Yu, X., Datta, V., Ren, S., Feng, H., Zinsou, R., et al. (2014). Assessment of an anti-alpha-toxin monoclonal antibody for prevention and treatment of Staphylococcus aureus-induced pneumonia. Antimicrob. Agents Chemother. *58*, 1108–1117. https://doi.org/10.1128/AAC.02190-13.
40. Hua, L., Cohen, T.S., Shi, Y., Datta, V., Hilliard, J.J., Tkaczyk, C., Suzich, J., Stover, C.K., and Sellman, B.R. (2015). MEDI4893* Promotes Survival and Extends the Antibiotic Treatment Window in a Staphylococcus aureus Immunocompromised Pneumonia Model. Antimicrob. Agents Chemother. *59*, 4526–4532. https://doi.org/10.1128/AAC.00510-15.
41. Bennett, M.R., and Thomsen, I.P. (2020). Epidemiological and Clinical Evidence for the Role of Toxins in S. aureus Human Disease. Toxins *12*, 408. https://doi.org/10.3390/toxins12060408.
42. Walker, B., Krishnasastry, M., Zorn, L., and Bayley, H. (1992). Assembly of the oligomeric membrane pore formed by Staphylococcal alpha-hemolysin examined by truncation mutagenesis. J. Biol. Chem. *267*, 21782–21786. https://doi.org/10.1016/S0021-9258(19)36680-3.
43. Walker, B., Krishnasastry, M., Zorn, L., Kasianowicz, J., and Bayley, H. (1992). Functional expression of the alpha-hemolysin of Staphylococcus aureus in intact Escherichia coli and in cell lysates. Deletion of five C-terminal amino acids selectively impairs hemolytic activity. J. Biol. Chem. *267*, 10902–10909. https://doi.org/10.1016/S0021-9258(19)50103-X.
44. Magyarics, Z., Leslie, F., Bartko, J., Rouha, H., Luperchio, S., Schörgenhofer, C., Schwameis, M., Derhaschnig, U., Lagler, H., Stiebellehner, L., et al. (2019). Randomized, Double-Blind, Placebo-Controlled, Single-Ascending-Dose Study of the Penetration of a Monoclonal Antibody Combination (ASN100) Targeting Staphylococcus aureus Cytotoxins in the Lung Epithelial Lining Fluid of Healthy Volunteers. Antimicrob. Agents Chemother. *63*, e00350–e00319. https://doi.org/10.1128/AAC.00350-19.
45. Rasko, D.A., and Sperandio, V. (2010). Anti-virulence strategies to combat bacteria-mediated disease. Nat. Rev. Drug Discov. *9*, 117–128. https://doi.org/10.1038/nrd3013.
46. Rex, J.H., Fernandez Lynch, H., Cohen, I.G., Darrow, J.J., and Outterson, K. (2019). Designing development programs for non-traditional antibacterial agents. Nat. Commun. *10*, 3416. https://doi.org/10.1038/s41467-019-11303-9.
47. Aziz, U.B.A., Saoud, A., Bermudez, M., Mieth, M., Atef, A., Rudolf, T., Arkona, C., Trenkner, T., Böttcher, C., Ludwig, K., et al. (2024). Targeted small molecule inhibitors blocking the cytolytic effects of pneumolysin and homologous toxins. Nat. Commun. *15*, 3537. https://doi.org/10.1038/s41467-024-47741-3.
48. Perez-Riverol, Y., Bai, J., Bandla, C., García-Seisdedos, D., Hewapathirana, S., Kamatchinathan, S., Kundu, D.J., Prakash, A., Frericks-Zipper, A., Eisenacher, M., et al. (2022). The PRIDE database resources in 2022: a hub for mass spectrometry-based proteomics evidences. Nucleic Acids Res. *50*, D543–D552. https://doi.org/10.1093/nar/gkab1038.
49. Miyao, T., Floess, S., Setoguchi, R., Luche, H., Fehling, H.J., Waldmann, H., Huehn, J., and Hori, S. (2012). Plasticity of Foxp3(+) T cells reflects promiscuous Foxp3 expression in conventional T cells but not reprogramming of regulatory T cells. Immunity *36*, 262–275. https://doi.org/10.1016/j.immuni.2011.12.012.
50. Horsburgh, M.J., Aish, J.L., White, I.J., Shaw, L., Lithgow, J.K., and Foster, S.J. (2002). sigmaB modulates virulence determinant expression and stress resistance: characterization of a functional rsbU strain derived from Staphylococcus aureus 8325–4. J. Bacteriol. *184*, 5457–5467. https://doi.org/10.1128/JB.184.19.5457-5467.2002.
51. O'Reilly, M., de Azavedo, J.C.S., Kennedy, S., and Foster, T.J. (1986). Inactivation of the alpha-haemolysin gene of Staphylococcus aureus 8325–4 by site-directed mutagenesis and studies on the expression of its haemolysins. Microb. Pathog. *1*, 125–138. https://doi.org/10.1016/0882-4010(86)90015-X.
52. Rosenblum, E.D., and Tyrone, S. (1964). Serology, density, and morphology of Staphylococcal phages. J. Bacteriol. *88*, 1737–1742. https://doi.org/10.1128/jb.88.6.1737-1742.1964.
53. Delaglio, F., Grzesiek, S., Vuister, G.W., Zhu, G., Pfeifer, J., and Bax, A. (1995). NMRPipe: a multidimensional spectral processing system based on UNIX pipes. J. Biomol. NMR *6*, 277–293. https://doi.org/10.1007/BF00197809.
54. Vranken, W.F., Boucher, W., Stevens, T.J., Fogh, R.H., Pajon, A., Llinas, M., Ulrich, E.L., Markley, J.L., Ionides, J., and Laue, E.D. (2005). The CCPN data model for NMR spectroscopy: development of a software pipeline. Proteins *59*, 687–696. https://doi.org/10.1002/prot.20449.
55. Salzmann, M., Pervushin, K., Wider, G., Senn, H., and Wüthrich, K. (1998). TROSY in triple-resonance experiments: new perspectives for sequential NMR assignment of large proteins. Proc. Natl. Acad. Sci. USA *95*, 13585–13590. https://doi.org/10.1073/pnas.95.23.13585.
56. Becher, I., Werner, T., Doce, C., Zaal, E.A., Tögel, I., Khan, C.A., Rueger, A., Muelbaier, M., Salzer, E., Berkers, C.R., et al. (2016). Thermal profiling reveals phenylalanine hydroxylase as an off-target of panobinostat. Nat. Chem. Biol. *12*, 908–910. https://doi.org/10.1038/nchembio.2185.

57. Mateus, A., Bobonis, J., Kurzawa, N., Stein, F., Helm, D., Hevler, J., Typas, A., and Savitski, M.M. (2018). Thermal proteome profiling in bacteria: probing protein state in vivo. Mol. Syst. Biol. *14*, e8242. https://doi.org/10.15252/msb.20188242.

58. Becher, I., Andrés-Pons, A., Romanov, N., Stein, F., Schramm, M., Baudin, F., Helm, D., Kurzawa, N., Mateus, A., Mackmull, M.-T., et al. (2018). Pervasive Protein Thermal Stability Variation during the Cell Cycle. Cell *173*, 1495–1507.e18. https://doi.org/10.1016/j.cell.2018.03.053.

59. Kong, A.T., Leprevost, F.V., Avtonomov, D.M., Mellacheruvu, D., and Nesvizhskii, A.I. (2017). MSFragger: ultrafast and comprehensive peptide identification in mass spectrometry–based proteomics. Nat. Methods *14*, 513–520. https://doi.org/10.1038/nmeth.4256.

60. Kurzawa, N., Becher, I., Sridharan, S., Franken, H., Mateus, A., Anders, S., Bantscheff, M., Huber, W., and Savitski, M.M. (2020). A computational method for detection of ligand-binding proteins from dose range thermal proteome profiles. Nat. Commun. *11*, 5783. https://doi.org/10.1038/s41467-020-19529-8.

61. Ghai, I., Bajaj, H., Arun Bafna, J., El Damrany Hussein, H.A., Winterhalter, M., and Wagner, R. (2018). Ampicillin permeation across OmpF, the major outer-membrane channel in Escherichia coli. J. Biol. Chem. *293*, 7030–7037. https://doi.org/10.1074/jbc.RA117.000705.

62. Ghai, I., Winterhalter, M., and Wagner, R. (2017). Probing transport of charged beta-lactamase inhibitors through OmpC, a membrane channel from E. coli. Biochem. Biophys. Res. Commun. *484*, 51–55. https://doi.org/10.1016/j.bbrc.2017.01.076.

63. Studier, F.W. (2005). Protein production by auto-induction in high density shaking cultures. Protein Expr. Purif. *41*, 207–234. https://doi.org/10.1016/j.pep.2005.01.016.

64. Niesen, F.H., Berglund, H., and Vedadi, M. (2007). The use of differential scanning fluorimetry to detect ligand interactions that promote protein stability. Nat. Protoc. *2*, 2212–2221. https://doi.org/10.1038/nprot.2007.321.

65. Tian, X.-C., Huang, X., Wang, D., and Gao, F. (2014). Eco-Efficient One-Pot Synthesis of Quinazoline-2,4(1H,3H)-diones at Room Temperature in Water. Chem. Pharm. Bull. *62*, 824–829. https://doi.org/10.1248/cpb.c14-00264.

66. Lee, S.H., Jang, B.B., and Kafafi, Z.H. (2005). Highly fluorescent solid-state asymmetric spirosilabifluorene derivatives. J. Am. Chem. Soc. *127*, 9071–9078. https://doi.org/10.1021/ja042762q.

67. Kuryazov, R.S., Mukhamedov, N.S., and Shakhidoyatov, K.M. (2008). Quinazolines 1. Synthesis and chemical reactions of 6-chlorosulfonyl-quinazoline-2,4-diones. Chem. Heterocycl. Compd. *44*, 324–329. https://doi.org/10.1007/s10593-008-0048-y.

68. Elsisi, D.M., Ragab, A., Elhenawy, A.A., Farag, A.A., Ali, A.M., and Ammar, Y.A. (2022). Experimental and theoretical investigation for 6-Morpholinosulfonylquinoxalin-2(1H)-one and its haydrazone derivate: synthesis, characterization, tautomerization and antimicrobial evaluation. J. Mol. Struct. *1247*, 131314. https://doi.org/10.1016/j.molstruc.2021.131314.

69. Krishnan, H.V.S., Chowdary, S.K., Dubey, P.K., Naidu, A., and Sunkara, V. (2000). A Facile Synthesis of Mono and Dialkoxyquinoxalines. Heterocycl. Commun. *6*, 333–338. https://doi.org/10.1515/HC.2000.6.4.333.

70. Loriga, M., Vitale, G., and Paglietti, G. (1998). Quinoxaline chemistry. Part 9. Quinoxaline analogues of trimetrexate (TMQ) and 10-propargyl-5,8-dideazafolic acid (CB 3717) and its precursors. Synthesis and evaluation of in vitro anticancer activity. Farmaco *53*, 139–149. https://doi.org/10.1016/S0014-827X(98)00002-0.

71. Schlosser, M. (1964). Phosphororganische Verbindungen, I. Eine Methode zur Darstellung selektiv deuterierter Verbindungen. Chem. Ber. *97*, 3219–3233. https://doi.org/10.1002/cber.19640971131.

72. Cho, I.S., Tu, C.L., and Mariano, P.S. (1990). Electron-transfer-induced photochemical reactions of (silylallyl)iminium and benzylpyrrolinium salts by dual diradical and diradical cation cyclization pathways. J. Am. Chem. Soc. *112*, 3594–3607. https://doi.org/10.1021/ja00165a052.

CellPress
OPEN ACCESS

STAR★METHODS

KEY RESOURCES TABLE

REAGENT or RESOURCE	SOURCE	IDENTIFIER
Recombinant proteins, antibodies and chemicals		
Alpha-hemolysin	IBT Bioservices	Cat# 1401-002
Alpha-hemolysin	Sigma-Aldrich	Cat# H9395
Alpha-hemolysin	This study / HZI	N/A
Mouse anti-Hla mAb	IBT Bioservices	Cat# 0210-001; RRID: AB_3677702
Rabbit anti-Hla pAb	Sigma-Aldrich	Cat# S7531; RRID: AB_261550
Histopaque®-1077	Sigma Aldrich	Cat# 10771
CD14-FITC antibodies	Miltenyi Biotec	Cat# 130-080-701; RRID: AB_244303
CD14 MicroBeads, human	Miltenyi Biotec	Cat# 130-050-201
Phorbol 12-myristate 13-acetate	Sigma-Aldrich	Cat# P1585
VE-Cadherin Antibody	Cell Signalling	Cat# 2158; RRID: AB_2077970
BiotinPEG$_4$-Azide	Jena Bioscience	Cat# CLK-1167-5
Streptavidin Sepharose	GE Healthcare	Cat# 17511301
Critical commercial assays and kits		
Fluo-4 NW Calcium assay kit	Life Technologies	Cat# F36206
MultiTox-fluor multiplex cytotoxicity assay	Promega	Cat# G9200
CellTiter-Glo luminescent viability assay	Promega	Cat# G7572
LEGENDplex mouse inflammation kit	BioLegend	Cat# 740446
CytoTox-ONE Homogenous Membrane Integrity assay	Promega	Cat# G7891
CyQUANT LDH Cytotoxicity assay	ThermoFisher Scientific	Cat# C20300
FITC Annexin V Apoptosis Detection Kit with PI	Biolegend	Cat# 640914
NK Cell Isolation Kit, human	Miltenyi Biotec	Cat# 130-092-657
LIVE/DEAD™ Fixable Blue Dead Cell Stain Kit	Life Technologies	Cat# L23105
Colorimetric Sphingomyelinase Assay Kit	Sigma-Aldrich	Cat# MAK152
Experimental models: cells and blood		
Buffy coat bags	German Red Cross, Springe	www.blutspende-nstob.de
HSAEpC	PromoCell	Cat# C-12643
HPMEC	PromoCell	Cat# C-12281
U937 cells	DSMZ	ACC5
A549 cells	DSMZ	ACC107
THP1 cells	DSMZ	ACC16
Calu-3 cells	ATCC	HTB-55; RRID: CVCL_0609
Th1 cells	CD4$^+$ T cells	Miyao et al.[49]
Rabbit blood	Fiebig	36100010
Experimental models: strains and organism		
CD-1 male mice	Charles River	N/A
C57BL/6 male mice	Charles River	N/A
S. aureus USA300 TCH1516	ATCC	BAA-1717
S. aureus USA300 0114	BEI Resources	N/A
S. aureus USA300 0114 *Δhla*	This study	Horsburgh et al.[50] and O'Reilly et al.[51]
Staphylococcus phage 80		Rosenblum and Tyrone[52]

(*Continued on next page*)

Continued

REAGENT or RESOURCE	SOURCE	IDENTIFIER
Software and Algorithms		
FlowJo 9.9.6	FlowJo LLC	https://www.flowjo.com/
GraphPadPrism 9.5.1	GraphPad	https://www.graphpad.com/
Biorender	Biorender	https://www.biorender.com/
NMR pulse program 'zgfhigqn.2' and 'stddiffgp19.3'	Bruker	https://www.bruker.com/
MS/MS analyte 1.6.2 software	Sciex	https://sciex.com/
MS file conversion MSConvert	Proteowizard	https://proteowizard.sourceforge.io/
Peaks Studio 10.6 software	Bioinformatics Solutions Inc.	https://www.bioinfor.com/
Deposited data		
2D-TPP MS proteomics mass spectrometry data	This study	PXD046735
Photoaffinity labelling mass spectrometry proteomics data	This study	PXD050156
Others		
FACSAria II	BD Bioscience	N/A
FACSAria-IIu	BD Bioscience	N/A
LSR-Fortessa	BD Bioscience	N/A
Synergy microplate reader	Biotek (Agilent)	N/A
M200 PRO microplate reader	Tecan	N/A
Microplate reader	EnVision, Perkin	N/A
500 MHz Avance III	Bruker	N/A
700 MHz Avance III HD	Bruker	N/A
QTrap 5500 hybrid triple quadrupole/linear ion trap mass spectrometer	AB Sciex	N/A
timsTOF Pro	Bruker	N/A

EXPERIMENTAL MODEL AND STUDY PARTICIPANT DETAILS

Mammalian primary cells and cell lines

Peripheral blood mononuclear cells (PBMCs) from buffy coats

Buffy coat bags (approx. 70 ml) from blood donations of healthy human volunteers were delivered from the German Red Cross, Springe (www.blutspende-nstob.de). The donations were made on the day before the experiments. Buffy coats were produced from whole blood donations on day 1 by using an extraction bag system. Peripheral blood mononuclear cells (PBMNCs) were isolated from these buffy coat products by Ficoll density gradient centrifugation (Sigma, Histopaque-1077) on day 2. PBMCs (1-2x10^8 cells) were cultured overnight in alpha MEM medium (Life Technologies) supplemented with 12.5% fetal bovine serum (FBS #10500-064, Life Technologies), 12.5% horse serum (#H1138, Sigma Aldrich), 2 mM L-glutamine, 100 units/ml penicillin and 100 μg/ml streptomycin (Millipore/Merck), 5 ng/ml IL-2 (PeproTech). Cells were incubated at 37°C in a humid 10% CO_2 atmosphere.

Human NK cells

For isolation of natural killer (NK) cells by FACS sorting, PBMCs were incubated with fluorochrome-conjugated anti-CD3 (clone HIT3a, mouse IgG2a, BioLegend) and anti-CD56 (clone B159, mouse IgG1, BD Biosciences) monoclonal antibodies for 30 min at 8 °C on day 3. $CD3^-/CD56^+$ NK cells were isolated by FACS using a FACSAria II flow cytometer (BD Bioscience). The purity and viability of the NK cells were assessed by flow cytometry. The purity of the isolated NK cells ($CD3^-/CD56^+$) was higher than 95%.

When NK cells were freshly isolated by magnetic labelling and separation from PBMCs, a biotin-antibody cocktail and paramagnetic micro-beads for magneto bead sorting were used according to the protocol. The NK (natural killer) cell isolation kit was from Miltenyi Biotec, GmbH (#130-092-657, lot 5170623328). The kit contains biotin-conjugated monoclonal anti-human antibodies against antigens not expressed by NK cells. The negative, untouched fraction was used as NK cells. The purity of these cells was confirmed by FACS analysis and was higher than 90% ($CD3^-/CD56^+$). Cells were kept in the same medium as above and used for bioassays on day 3 and 4.

Human Monocytes and Macrophages

Peripheral blood mononuclear cells were isolated as described before for the isolation of NK cells. For FACS sorting, PBMCs were incubated with fluorochrome-conjugated anti-CD14 monoclonal antibodies (cloneTÜK4, Mouse IgG2, Miltenyi Biotec) for 30 min at

CellPress
OPEN ACCESS

8 °C. CD14$^+$ monocytes were isolated by FACS using a FACSAria II flow cytometer. The purity and viability of the monocytes were assessed by flow cytometry. The purity of the isolated monocytes (CD14$^+$) was higher than 90%.

When monocytes were freshly isolated by magnetic labelling and separation from PBMCs, the CD14-antibody and paramagnetic micro-beads for magneto bead sorting were used according to the protocol (Miltenyi Biotec #130-050-201, lot 5171109233). The positive fraction was used as CD14-monocytes. The purity of these cells was confirmed by FACS analysis with CD14-FITC antibodies (Miltenyi Biotec, #130-080-701, lot 5171109352) and was found to be higher than 90%. Cells were kept in the same medium as described above and used for bioassays on day 3 and 4.

THP1 cells (DSMZ, #ACC16) were maintained in RPMI 1640 medium supplemented with 10% FBS at 30 °C and 10% CO_2. THP1 cells were differentiated at a density of 10^6 cells/ml in the presence of 200 nM phorbol 12-myristate-13-acetate (PMA) (Sigma) containing medium for 24 h. Thereafter, PMA-containing medium was removed, fresh medium was added and cells were incubated for another 24 h at 37 °C and 10% CO_2 and subsequently used in an assay.

Human Endothelial and Epithelial Cells from Lung

Primary human small airway epithelial cells (HSAEpC, c-12643) and pulmonary microvascular endothelial cells (HPMEC, c-12281) were purchased from PromoCell. These low-passage primary cells were cultured in the growth medium as recommended by the supplier of these cells. Endothelial cells were cultured in 1% gelatin-coated plastic dishes and wells. Cells were incubated at 37 °C, 10% CO_2 and passaged once a week. They were used between passage 4 and 8.

A549 epithelial cells (DSMZ, #ACC107 were maintained in DMEM supplemented with 10% FBS at 37 °C and 10% CO_2. Cells were seeded 24 hours before an assay to allow adherence before use in an assay.

Calu-3 human bronchial epithelial cells (ATCC® HTB-55, passages 50–51) were cultivated in MEM medium supplemented with 1% non-essential amino acids, 1 mM sodium pyruvate, and 10% fetal calf serum (all Gibco™, Thermo Fisher Scientific Inc.) at 37 °C and 5% CO_2. For TEER measurements, they were seeded with 100 000 cells/cm^2 on Transwell® inserts (Corning Inc. 3470, 0.33 cm^2, 0.4 μm pores).

In vitro CD4$^+$ T cell differentiation

For the *in vitro* generation of Th1 cells naïve CD4$^+$ T cells lacking Foxp3$^+$ regulatory T cells were sorted from Foxp3^{hCD2} reporter mice (B6.Foxp3$^{tm1(CD2/CD52)Shori}$) on C57BL/6 background.[49] In brief, single cell suspensions were prepared from spleen and lymph nodes and erythrocytes were lysed by incubation with ammonium chloride buffer at room temperature for 3 min. CD4$^+$ T cells were first magnetically enriched by anti-CD4 microbeads using the autoMACS® Pro (Miltenyi Biotec). Subsequently, cells were stained with fluorescently labeled antibodies (anti-hCD2-APC, RPA-2.10; anti-CD62L-BV605, MEL-14; anti-CD4-BV605, RM4-5; anti-CD8α-APC, 53-6.7; anti-CD45R-APC, RA3-6B2; anti-CD11c-APC, N418; anti-F4/80-APC, BM8; all purchased from BioLegend, eBioscience, or BD Biosciences) and naïve CD4$^+$ T cells sorted by fluorescence-activated cell sorting (FACS) as Foxp3^{hCD2-}CD62L^{high}CD4$^+$Lin$^-$ cells (Lin: CD8α, CD45R, CD11c, F4/80) on a FACSAria-IIu (BD Biosciences) or FACS Aria-II SORP (BD Biosciences). Sorted naïve CD4$^+$ T cells were stained with the proliferation dye CellTrace™ Violet (CTV, Thermo Fisher Scientific) before cultivation. Next, CTV-labeled naïve CD4$^+$ T cells were cultured in IMDM containing 10% FCS, 1 mM sodium pyruvate, 50 U/ml Penicillin and Streptomycin, 25 mM HEPES, 50 μM beta-mercaptoethanol, and non-essential amino acids (Gibco Life Technologies and Biochrom AG), and 150,000 cells per well were seeded into 96 well flat bottom plates (Thermo Fisher Scientific) previously coated with 1 μg/ml anti CD3 (17A2, BioLegend) and 1 μg/ml anti CD28 (37.51, BioLegend). For polarization into Th1 cells, IL-12 (20 ng/ml; BioLegend) and anti-IL-4 (10 ng/ml, 11B11; BioXCell) were added. Most of the cultures received recombinant Hla (1 μg/ml) and H831 was added at indicated concentrations. On day 3, cells were removed from the stimulus and transferred to uncoated plates (Sarstedt). At this step, cells were split 1:2 and received IL-2 (5 ng/ml, R&D Systems). 24h later, cells were harvested and analyzed by flow cytometry. For detection of cell survival, cells were incubated with a UV-excitable, fixable Live/Dead dye (LIVE/DEAD™ Fixable Blue Dead Cell Stain Kit, Life Technologies) for 30 min. All flow cytometry samples were acquired at LSR-Fortessa (BD Biosciences) and data were analyzed with FlowJo® 9.9.6 (FlowJo, LLC).

S. aureus USA300 and generation of S. aureus USA300 Δhla

S. aureus USA300 was cultivated by overnight in TSB medium at 37 °C and 150 rpm. Cultures were started the following day at OD_{600} 0.05 in TSB at 37 °C and 150 rpm. Bacteria was harvested for use in infection experiments at required OD_{600} by centrifugation at 4 °C. Supernatant was discarded, pellets were washed with PBS and resuspended in the respective medium or PBS for infection.

S. aureus USA300 0114 with *hla* deletion (USA300 *Δhla*) was generated by phage-mediated transduction using the SH1000 *Δhla* as the donor strain.[50,51] *S. aureus* SH1000 *Δhla* was inoculated in 20 ml LB in the presence of 5 μg/ml erythromycin and 25 μg/ml lincomycin at 37 °C and 150 rpm. On day 2, 100 μL of 1M CaCl2 was added to the culture (final concentration 5 mM) and the flask was incubated for 5-30 minutes at 37 °C and 150 rpm. *Staphylococcus aureus* phage 80 (Φ80) was diluted 10-1, 10-2, 10-3, 10-4 and undiluted in LB with 5 mM CaCl2 (phage buffer).[52] Thereafter, 300 μL of SH1000 *Δhla* culture was added in a 15 ml tube and incubated at 52 °C for 2 min. 100 μL of diluted phage lysate including a control without lysate was added to 15 ml tubes with SH1000 *Δhla* cultures and incubated at room temperature (RT) for 15 min. 4 ml of soft agar was added to the culture and spread over blood agar plates. LB soft agar consists of softening the agar by heating and adjusting to 52 °C followed by addition of 10 μL 1 mM CaCl2. Plates were incubated at 37 °C overnight with plate upside-down (agar down, lid up). The recipient strain i.e. *S. aureus* USA300 0114 was grown overnight in 20 ml LB medium at 37 °C and 150 rpm.

On day 3, the blood agar plate wherein the highest dilution of phage yielded confluent lysis (blood agar brown, soft agar transparent, surface shiny) was selected and 2 ml of LB with 5 mM CaCl2 was added and distributed evenly. The liquid was taken in a

5 ml tube and centrifuged for 10 min at 9000 rpm and RT. The supernatant was transferred to a new tube and the lysate was filtered through a 0.45 μm filter. The filtered phage lysate was stored at 4 °C 29 until use. 100 μL of 1 M CaCl2 was added to the overnight culture of the *S. aureus* USA300 and 300 μL of the culture was transferred to four 15 ml tubes and incubated at 52 °C for 2 min. Undiluted, 1:10, 1:100 and no-lysate was prepared in phage buffer. 100 μL diluted phage lysates were added to different tubes with 300 μL USA300 cultures and incubated at RT for 15 min. Thereafter, 3 ml of soft agar (adjusted to 52 °C) with 20 mM trisodium citrate were added to the tubes and spread over LBA selection plates with 5 μg/ml erythromycin and 25 μg/ml lincomycin. The plates were incubated at 37 °C. Transductants were selected after 48h and inoculated onto new LBA plates and validated by PCR.

Animal models

Pharmacokinetic studies were conducted with male, 4-weeks-old, CD-1 outbred mice (Charles River). Lung infection model for bacterial load and IL-6 determination was carried out with specific-pathogen-free 6-weeks-old C57BL/6 male mice (Charles River). Survival studies were conducted with 7-8 weeks old C57BL/6N male mice (Charles River).

Ethics statement

The animal studies were conducted in accordance with the recommendations of the European Community (Directive 2010/63/EU, 1st January 2013). All animal procedures were performed in strict accordance with the German regulations of the Society for Laboratory Animal Science (GV- SOLAS) and the European Health Law of the Federation of Laboratory Animal Science Associations (FELASA). Animals were excluded from further analysis if sacrifice was necessary according to the humane endpoints established by the ethical board. The PK studies and acute lung infection experiments with an IL-6/CFU readout performed at HZI were approved by the ethical board of the Niedersächsisches Landesamt für Verbraucherschutz und Lebensmittelsicherheit, Oldenburg, Germany. Animals were kept in individually ventilated cages with a 10h/14h dark/light cycle and had access to food and water *ad libitum*.

The animal-related infection experiments monitoring survival were performed at Fidelta Ltd. (Selvita Group) and conducted in accordance with 2010/63/EU and National legislation regulating the use of laboratory animals in scientific research and for other purposes (Official Gazette 55/13). An Institutional Committee on Animal Research Ethics (CARE-Zg) oversees that animal related procedures are not compromising the animal welfare.

METHOD DETAILS

Cytotoxicity assay and cell viability assays

For cell toxicity we used the multitox-fluor multiplex cytotoxicity assay (kit #G9200, Promega) to simultaneously measures two protease activities: one is a marker for cell viability, and the other is a marker of cytotoxicity. The live-cell protease activity is restricted to intact viable cells. To measure dead-cell protease activity, a protease which is released from cells that have lost membrane integrity is used. The live- and dead-cell proteases produce different products, AFC and R110 which have different excitation and emission spectra, allowing them to be detected simultaneously. NK cells were plated in opaque 96-well plates with an initial density of 10000 cells/well in the presence of Hla for 16-20 h at 37 °C with 10% CO_2. Likewise, HSAEpC were seeded at a density of 20000 cells/well and incubated with Hla (± QDS inhibitors). At the end of the experiment, 2-fold buffer for the cytotoxicity assay (Promega) was added according to the manufacturer's instruction. Fluorescence was measured after 30 min. in 96-well microplate fluorimeter (Tecan M200 PRO). Each experiment was done in triplicates and at least repeated two times. The fluorescence of treated cells representing cell death related to the control (untreated) were calculated and statistically analyzed.

ATP-dependent viability was determined using the CellTiter-Glo luminescent viability assay (Promega), The assay reagent was prepared by mixing the reagent buffer and substrate in a 1:1 ratio. An equal volume was added to wells of the 96-well plate at the end of the treatment/incubation period. Plates were incubated for 10 min at room temperature, protected from light and luminescence was measured using a Biotek Synergy plate reader (Agilent).

Calcium influx assay

Calcium influx was determined in NK cells (and monocytes) using the Fluo-4 NW Calcium assay kit (Life Technologies, #F36206). Briefly, 70000 cells/well in assay buffer supplied with the kit were transferred into wells of black-walled clear-bottom 96-well plates containing the Fluo-4 dye and probenecid. Cells were incubated for 30 min at 37 °C and for 30 min at room temperature. Inhibitors were added at different concentrations followed by Hla and incubated for 3 h at 37 °C with 10% CO_2. Pore formation was determined by measuring calcium influx or the change in fluorescence using a M200 PRO microplate reader (excitation wavelength of 488 nm and emission wavelength of 530 nm (Tecan). Calcium influx in HSAEpC and HPMEC was determined by seeding 30000 cells/well and plate were incubated for 24h at 37 °C. Thereafter, medium was removed and Fluo-4 dye in buffer C and probenecid was added to cells. Cells were incubated for 30 min at 37 °C and for 30 min at room temperature followed by addition of Hla or compounds and Hla.

The activity of inhibitors on Hla variants was conducted in 96-well half-area plates. U937 cells (DSMZ, #ACC5) were seeded at a density of 60000 cells/well in assay buffer containing Fluo-4 dye and probenecid. Cells were incubated as described earlier followed by the addition of Hla variants at different concentrations. Inhibitors were tested on 1 μg/ml of Hla variants. Pore formation was determined by measuring calcium influx or the change in fluorescence at 4 h incubation at room temperature using a Biotek Synergy microplate reader (Agilent) at excitation wavelength of 488 nm and emission wavelength of 528 nm.

Hemolysis assay

Erythrocytes were isolated from rabbit blood in Alsever's solution (Fiebig, #36100010). 5 ml of rabbit blood was centrifuged at 500 g for 5 min at 4 °C without brakes in a 15 mL falcon tube. The supernatant was carefully removed and discarded. PBS was added to the pellets containing erythrocytes and leucocytes and the volume increased to 10 ml and again centrifuged at 500 g for 5 min at 4 °C without brakes. The wash step with PBS was repeated 3x. After the third wash step, the pellet was considered as 100% erythrocyte solution and stored at 4 °C. To test for the activity of inhibitors, 3.1% erythrocytes diluted in PBS were seeded in wells of v-bottom 96 well plate (Greiner Bio-one, #651180) in a volume of 80 μL. Thereafter, 10 μL inhibitors were added at different concentrations followed by the addition of Hla. The final concentration of Hla was 0.8 μg/ml. Plates were shortly mixed and incubated for 30 min at 37 °C followed by centrifugation for 5 min at 500 g without brakes. 50 μL of supernantant was transferred to a new 96-well half-area flat-bottomed plate (Costar, #3697). Hemoglobin release from lysis of erythrocytes was determined by measuring the optical density at 540 nm using a Biotek microplate reader (Agilent).

VE stain

Human pulmonary microvascular endothelial cells (HPMEC) from Promocell were grown on 8-well coverslips and incubated with 1 μg/ml Hla for 30 min in the absence or presence of H831 or H052. Hla and compounds were pre-incubated for 30 min before addition to cells. Cells were fixed in MeOH/Aceton (50:50) and immunostained with VE-cadherin antibodies (Cell Signalling) and Alexa647 or Alexa594 IgG as secondary antibodies. DNA was visualized by DAPI staining.

Studies on epithelial and microvascular leakage with primary cells

Specially designed microtiter plates (E-Plate 96 #05232368001 from ACEA Bioscience, Inc.) containing interdigitated gold microelectrodes were used to monitor the monolayer integrity or leakiness of cultured, confluent primary cells in real-time using electrical impedance (as cell index CI) as the readout. Cells were seeded (25.000 cells/well) and grown over 48 h – 72 h to become a confluent endothelial monolayer. Between 48 and 49 h e-plates were removed from the incubator and Hla (± QDS inhibitors) was added to the wells, followed by a further incubation until the end of the measurements. Especially the time period of about two hours after the addition of alpha toxin and the antagonists was monitored (see figures for impedance). We indicated impedance curves as "cell index" of human primary pulmonary microvascular endothelial cells and small airway epithelial cells.

NMR experiments

^{19}F NMR spectra were recorded on a 500 MHz Avance III (UltraShield) spectrometer equipped with a 5 mm room temperature probe (BBO) by Bruker BioSpin GmbH, at 298 K. Pulse program 'zgfhigqn.2' from standard Bruker library was used with NS800 for all ^{19}F NMR experiments.

Three samples per QDS derivative were prepared. The first sample contained 100 μM QDS, dissolved in aqueous buffer (20 mM TRIS, 300 mM NaCl, pH 8.5) and was used with the addition of 10% D_2O and 5% of DMSO-d_6. Second and third sample contained in addition 50 μM Hla and 100 μM Hla in the same buffer, respectively.

STD NMR spectra were recorded on a 700 MHz Avance III HD (UltraShield) spectrometer equipped with a 5 mm, helium-cooled cryoprobe (TCI, Bruker BioSpin GmbH) at 298 K. Pulse program 'stddiffgp19.3' from the standard Bruker library was applied with SPW9 = 0.316 mW and D29 = 50 ms. Two samples per QDS derivative were prepared: 1) reference sample with QDS derivative only (500 μM) in aqueous buffer (20 mM TRIS, 300 mM NaCl, pH 8.5) with the addition of 10% D_2O and 5% of DMSO-d_6; and 2) with the addition of 10 μM Hla in the same buffer. On-resonance irradiation was set to 0.6 ppm, off resonance irradiation to 40 ppm.

Protein NMR experiments were conducted on a 700 MHz Avance III HD (UltraShield) spectrometer equipped with a 5 mm, helium-cooled cryoprobe (TCI, Bruker BioSpin GmbH) or on different Bruker Avance III spectrometers equipped each with cryogenically cooled TCI probeheads, operating at magnetic field strengths corresponding to ^{1}H Larmor frequencies of 950 and 800 MHz. The sample temperature was set at 298 K for all experiments. Experiments were performed in 25 mM phosphate buffer, 100 mM NaCl, pH 6.8, and 8% D_2O. All data were processed with NMRPipe[53] and analyzed in CCPNMR.[54] The backbone assignment of ^{15}N-^{13}C-^{2}H HLA-H61A (27-319) was performed at 180 μM using TROSY,[55] deuterium-decoupled 3D heteronuclear experiments HNCA, HN(CO)CA, HNCACB, HNCO, and HN(CA)CO. 66% (193 out of 294) of the non-proline backbone resonances were assigned, due to the lack of back-exchange at the core of the domain.Titrations were performed using ^{15}N-^{13}C-^{2}H HLA-H61A at 125 μM with small additions of H831 up to 75 μM (0.6 equivalents) from a stock solution at 10 mM in deuterated DMSO. All chemical shift perturbations were calculated as a weighted average following the equations $CSP = ((\Delta^{1}H)^2 + (\Delta^{15}N*0.15)^2)^{1/2}$.

Pharmacokinetic (PK) studies

Male, CD-1 outbred mice were administered H052 and H831 at 60 mg/kg i.p. or s.c, respectively. Moreover, H052 and H831 were administered at 100 mg/kg p.o. and at 1 mg/kg i.v., respectively. H052 and H831 were each dissolved in a formulation containing 20% DMSO, 50% PEG400 and 30% 10xPBS for i.v., p.o., and i.p. administration. For the s.c. administration, H052 and H831 were dissolved in 10% DMSO, 20% PEG400, 20% HP-β-CD, 50% water. At the time points 0.25, 0.5, 1, 2, 4, 8, and 24 h (for s.c. and i.p.) or at t = 0.5, 1, 3 and 5 h (for p.o.) or at t = 0.25, 0.5, 1, 3 and 5 h post administration, blood was withdrawn from the lateral tail vein. Terminally, mice were euthanized to collect blood from the heart as well as to perform bronchoalveolar lavage (BAL) and to remove lungs aseptically. Additionally, H052 was administered at 20 mg/kg using an Aeroneb® lab nebulizer. At the time points 0.25, 0.5, 1, 2, 4, 8, and 24 h post administration, mice were euthanized to collect blood from the heart as well as to perform BAL and to

remove lungs aseptically. Whole blood was collected into Eppendorf tubes coated with 0.5 M EDTA and immediately spun down at 13,000 rpm for 10 min at 4 °C. Then, plasma was transferred into a new Eppendorf tube and lungs were homogenized using a Polytron tissue homogenizer. BAL fluid (BALF), lung and plasma samples were stored at -80°C until analysis.

MS compound analytics

Plasma and tissue proteins were removed from the samples by precipitation using four volumes of cold acetonitrile containing an internal standard. After filtration, the samples were diluted with an equal volume of H_2O and analyzed by LC-MS/MS (ESI+). H052 and H831 concentrations in each matrix were quantified using a Shimadzu UPLC system connected to a QTrap 5500 hybrid triple quadrupole/linear ion trap mass spectrometer (AB Sciex). Test items were separated on a C18 column with an acetonitrile/water gradient containing 0.1% formic acid as mobile phase. MS/MS instrument parameters were automatically optimized for each test item using analyte 1.6.2 software. A calibration curve was obtained from the corresponding spiked blank matrix. The regression equation of the calibration curve was used to calculate plasma, lung homogenate and BALF concentrations. Pharmacokinetic parameters were calculated using the PKSolver plug-in for Excel.

Pneumonia survival model

Three groups of ten 7-8 weeks old C57BL/6N male mice (Charles River) were infected intranasally with $5x10^8$ CFU/ mouse of *Staphylococcus aureus* USA300 TCH 1516 (ATCC BAA-1717) once at d0. Animals were infected intranasally with *S. aureus* USA300 in a volume of 50 μL/mouse. Group 1 served as a vehicle control. Group 3 was administered with H052 at 60 mg/kg via intraperitoneal (IP) route and continued in BID with 10-12 hours between doses starting at d-1 to d3 (d4). The effects of different treatments were evaluated by daily assessment of body weight change, clinical signs of illness and mortality incidence up to d4 p.i. On D4, after terminal exsanguination under ketamine + xylazine anesthesia, lungs, kidneys and liver were extirpated and placed into 10% buffered formalin for histopathology evaluation by H&E staining.

For lung histopathology analysis after 24 h of intranasal infection with $5x10^7$ CFU/mouse, animals were terminally exsanguination under ketamine + xylazine anesthesia, lungs were extirpated and placed into 10% buffered formalin.

Lung infection model for bacterial load and IL-6

Specific-pathogen-free 6-weeks-old C57BL/6 male mice were injected intraperitonealy (IP) with 60 mg/kg of H052 or vehicle control every 12 h starting 24 h before infection. For intranasal (IN) infection, mice were anesthetized by IP injection with 100 mg/kg ketamine and 10 mg/kg xylazine solution and inoculated IN with app. $5x10^8$ CFU of *S. aureus* strain USA300 in 20 μl of PBS. Mice were euthanized by carbon dioxide asphyxiation at 24 h after bacterial inoculation and bacterial loads were determined in lungs by preparing homogenates in 1 ml PBS and plating 10-fold serial dilutions on blood agar plates. Colonies were counted after overnight incubation at 37 °C. The levels of IL-6 were determined in lung homogenates using LEGENDplex mouse inflammation kit (BioLegend).

Pneumonia survival model for prophylactic and therapeutic monotherapy

Six groups of ten 8-weeks old C57BL/6N male mice (Charles River) were infected intranasally (IN) after an acclimation period of 5 days, with $4x10^8$ CFU/mouse of *Staphylococcus aureus* USA300 TCH 1516 (ATCC BAA-1717) on day 0 of the study. Animals were anaesthetized intraperitoneally (IP) with a combination of ketamine hydrochloride and xylazine. For intranasal (IN) instillation mice were held in a tilted supine position with their heads elevated to between 60 and 75 degrees above their feet during and after (for approximately 1 min) instillation. Animals were infected by IN instillation of bacterial suspensions of *Staphylococcus aureus* USA300 in a volume of 50 μL/mouse. Group 1 served as a control and was treated with vehicle 20% DMSO/50% PEG400/30% 10xPBS via intraperitoneal (IP) route, starting at +1 h p.i. and continuing twice daily (BID) up to d4 post infection (p.i.). Group 2 was treated with Linezolid at 2.5 mg/kg via subcutaneous (SC) route, starting at +1 h p.i. and then BID to d1 p.i. Group 3 was administered with H052 at 60 mg/kg IP, starting at + 1h p.i. and then BID up to d4 p.i. Animals in group 4 were treated with a combination of Linezolid and H052 at the same dosing regimens as groups 2 and 3, respectively. For group 5, the prophylactic treatment with H052 at 60 mg/kg IP was initiated on d-1 and continued in BID up to d4 p.i. Group 6 served as a model control for the reference compound and received two doses of Linezolid at 100 mg/kg IP, at +6 and +24 h p.i. The effects of H052 and Linezolid were evaluated by daily assessment of body weight change, clinical signs of illness and mortality incidence up to d5 p.i.

Assay development and high throughput screening

A high throughput screen using a Ca^{2+} influx assay was established in the human U937 leukocyte cell line (DSMZ, #ACC5). The assay was adapted to a 1536-well format using the Fluo4NW Calcium assay kit (Life Technologies). U937 cells were seeded in 1536-well plates at a density of 12,000 cells/well in assay buffer (3 μL volume), followed by the addition of 3 μL Fluo-4 NW dye solution. The Fluo-4 NW dye solution was prepared as per the manufacturer's instructions. Plates were incubated for 30 min at 37 °C, followed by 30 min at RT. Thereafter, 1 μL of the compound solution was added, followed by 2 μL of alpha-hemolysin (IBT Bioservices #1401-002), followed by shaking for 1 min at 1000 rpm and incubation at RT. Fluorescence was measured after 4 h at an excitation wavelength of 485 nm and emission wavelength of 535 nm using a plate reader (EnVision, PerkinElmer). The final assay volume in the 1536-well plates was 9 μL/well with a compound concentration of 11 μM and an Hla concentration of 13 nM. The DMSO content was 0.1%. A total of 182,122 compounds from the in-house libraries of the Lead Discovery Center and the Helmholtz Centre for Infection Research were screened with a Z'-factor of 0.79. The assay was adapted from a 384-well plate (Corning) format, wherein the volume

was 14 μL/well and consisted of 5 μL U937 cells (20,000 cells/well), 5 μL of Fluo-4 NW dye solution, 1 μL compound solution and 3 μL Hla (30 nM). The activity of Hla from two other sources (Sigma-Aldrich and HZI) was also tested and found comparable. The reduction of Ca^{2+} influx was also tested using an anti-Hla monoclonal antibody from IBT Bioservices as well as an anti-hla polyclonal antibody from Sigma-Aldrich as positive controls.

Two-dimensional thermal proteome profiling (2D-TPP)

The experiments were performed as described previously.[56] Briefly, A549 cells were treated for 90 min with H052 at 10 μM, 2 μM, 0.4 μM, 0.08 μM, 0.02 μM or with DMSO as control. After cell harvest aliquots were heated to 9 different temperatures followed by cell lysis (final buffer 0.8% NP-40, 1x Roche Complete protease inhibitor, 1x PhosStop, 1.5 mM $MgCl_2$, benzonase in PBS). Heat-induced aggregates were removed by filtration and the soluble proteins were used for MS sample preparation using an adapted SP3 procedure.[57] After TMTpro (18plex) labeling samples were pooled and pre-fractionated with high pH into 12 fractions.

LC-MS measurement and data analysis

Samples were analyzed as described previously.[58] Mass spectrometry raw files were converted to mzmL format using MSConvert (Proteowizard) using peak picking from the vendor algorithm and keeping the 200 most intense peaks. Files were then searched using MSFragger v13 in Fragpipe v18 against the *Homo sapiens* proteome, downloaded from Uniprot, identifier UP000005640, including known contaminants and the reversed protein sequences. The search parameters were as follows: tryptic digestion with a maximum of 2 missed cleavages, peptide length = 7-50, peptide tolerance = 20 ppm; MS/MS tolerance = 10 ppm; topN peaks = 300; fixed modifications = carbamidomethyl on cysteine and TMT18plex on lysine; variable modifications = acetylation on protein N termini, oxidation of methionine and TMT18plex on peptide N termini. Peptide Spectrum Matches (PSMs) validation was performed by philosopher version 4.1.0 and the false discovery rate was fixed at 1% at the PSMs, peptides and proteins level. TMT quantification was performed by TMT-Integrator using default settings. The raw output files of FragPipe (protein.tsv – files)[59] were processed using the TPP2D package.[60]

Lipid bilayer experiments

Planar lipid bilayers were formed as published.[61,62] Two home-made Delrine half-cell with 2.5 ml each are separated by a 25 μm thick Teflon septum with a hole of about 70-100 μm diameter. The septum was pre-painted with 1 μl of hexadecane dissolved in n-hexane at 1-2% (v/v) and dried for 30-35 minutes. Bilayers were made with 1,2-diphytanoyl-sn-glycerophosphocholine at a concentration of 4-5 mg/ml in n-pentane, the lipid amount corresponds to an amount necessary to cover the area with a few lipid monolayers. Addition of a <1 μl droplet containing Hla stock solution at a concentration of 0.01 μg/ml on one side caused a stepwise increase of the membrane conductance after a few minutes. The steps are interpreted as single or sometimes multiple hemolysin channel insertions. To prevent too many channel insertions, we exchanged the buffer after the first insertion. All recordings were performed with a buffer containing 1 M NaCl or 200 mM NaCl specifically specified. In agreement with the literature, the single channel conductance values of Hla in 200 mM NaCl was 0.5±0.3 nS.[35] Standard Ag/AgCl electrodes were used to detect the ionic current. The cis side electrode of the cell was connected to the ground and the trans side electrode was connected to the head-stage of an axo-patch 700B amplifier that was used for the conductance measurements in the voltage clamp mode. Signals were filtered by an on-board low pass Bessel filter at 10 kHz and recorded onto a computer hard drive with a sampling frequency of 50 kHz. Analysis of the current recordings was performed using Clamp fit (Axon Instruments).[61,62] In a control experiment Hla was incubated with individual compounds for 4-5 hours before adding to the cis and trans side of the chambers.

Photoaffinity labelling for target identification

U937 cells (2.5 x 10^6) or 50 μg/ml Hla was incubated with 100 μM of the photo-probe **14** in a total volume of 300 μl PBS for 1 h at RT. Samples were irradiated with UV light (3x Nichia NCSU276A) for 1 h at 365 nm with 50% intensity. Cells or Hla was incubated with DMSO as vehicle control. Cells were lysed with 0.1% Triton-X-100 for 30 min on ice with mixing every 10 min. Thereafter, 1.8 μL 3 mM biotin azide, 6 μL 50 mM tris(2-carboxyethyl)phosphine (TCEP), 6 μl 5 mM 2-(4-((bis((1-(tert-butyl)-1H-1,2,3-triazol-4-yl)methyl)amino) methyl)-1H-1,2,3-triazol-1-yl) acetic acid (BTTA) and 6 μl 50 mM $CuSO_4$ were added to 300 μl of each sample to initiate copper-catalysed azide-alkyne cycloaddition (CuAAC) reaction for 1 h in the dark. 50 μl streptavidin bead suspension was transferred to 1.5 μl tubes and washed 3x with PBS by mixing and centrifugation for 3 min at 400 g and RT. Samples from CuAAC were transferred to tubes containing washed streptavidin beads and incubated for 1 h under continuous mixing using a KPG stirrer at the lowest speed. The beads were then washed 3x with 1 ml 0.4 % SDS in PBS followed by 2x with 1 ml 3 M urea in dH_2O and finally 3x with 1 ml PBS. Beads were washed by mixing and centrifugation for 3 min at 400 g and RT and supernatant was discarded. 50 μL 2x Laemmli loading buffer was added to beads and boiled at 95 °C for 10 min. 25 μL of the samples were subjected to 1 mm 10% SDS gel and run for 10 min. Gels contained 1% (v/v) 2,2,2 trichloroethanol for stain-free detection of proteins and were visualised using the stain-free function of a ChemiDoc Imaging System (Bio-Rad).

Photoaffinity labelling for binding site identification

The binding site identification of the quinoxalinediones at α-hemolysin was carried out according to the following protocol. Triethylammonium bicarbonate buffer (TEAB, 50 mm, pH 8.5, 79 μL) was added to 10 wells of a 96 well plate. Recombinant α-hemolysin (9.6 mg/ml in 20 mm Tris-HCl, pH 8.5, 300 mm NaCl; manufacturer: HZI) was diluted with TEAB buffer (50 mm, pH 8.5) to

500 μg/ml and 20 μL was added to the same wells from the first step. **15** (303 μm, in DMSO, 1 μL) was added to 4 wells and **16** (303 μm, in DMSO, 1 μL) was added to 4 different wells. DMSO (1 μL) was added to the last 2 wells. The plate was wrapped into aluminum foil and incubated for 10 min at 300 rpm followed by 50 min without shaking. The plate was thereafter placed on ice in an illumination box made from Styrofoam wrapped in aluminum foil. and irradiated with λ = 254 nm (UVGL-58 Handheld UV Lamp, 6 Watt, 230 V) without the lid for 15 min. Thereafter, half of the samples (2 x 15, 2 x 16 and 1 x DMSO control) were transferred to different 1.5 ml protein LoBind® tubes (Eppendorf). The remaining samples were irradiated for additional 30 min and also transferred to different 1.5 ml protein LoBind® tubes (Eppendorf).

Trypsin preparation was carried out by dissolving 20 μg sequencing grade modified trypsin by Promega (V5111) in resuspension buffer (from supplier) (100 μL), incubation for 30 min at room temperature, storage of aliquots at −20 °C. In-solution digestion was carried out by addition of tris(2-carboxyethyl)phosphine (TCEP, 50 mm in ultrapure water, 10 μL, $c_{(final)}$ ~5 mm) to all samples and incubation at 56 °C and 300 rpm for 60 min in an Eppendorf ThermoMixer C. This was followed by addition of methyl methanethiosulfonate (MMTS, 200 mm in 2-propanol, 5 μL, $c_{(final)}$ ~10 mm) to all samples and incubation at room temperature and 300 rpm for 30 min in an Eppendorf ThermoMixer C. Thereafter, trypsin (0.2 μg/ml, 5 μL from step 14) was added to all samples followed by incubation at 37 °C and 700 rpm for 18 h in an Eppendorf ThermoMixer C. The samples were dried in a rotary vacuum concentrator RVC 2-18 CDplus from Christ at 30 °C and 1000 rpm and 0.1% formic acid (30 μL) was added to all samples

For MS/MS analysis, the peptides were loaded onto Evotips as described by the supplier Evosep. Evotips were wash dried with 20 μL solvent B and centrifuge at 800 g for 60 s and soaked in 100 μL 2-propanol until all the tips were pale white. Soaked Evotips were equilibrated with 20 μL solvent A and centrifuged at 800 g for 60 s. Samples were loaded on wet tips (1 μL in 0.1% formic acid) and centrifuged for 60 s at 800 g. Tips were washed with 20 μL solvent A and centrifuged for 60 s at 800 g. Thereafter, 100 μL solvent A was transferred and tips were centrifuged for 10 s at 800 g to keep tips wet. The peptides were eluted afterwards over an HPLC (Evosep One, Bruker) connected to a quadrupole time-of-flight mass spectrometer (timsTOF Pro, Bruker).

The peptides were identified using the Peaks Studio 10.6 software with the following settings. Search parameters include, Parent Mass Error Tolerance – 20.0 ppm, Fragment Mass Error Tolerance – 0.03 Da, Precursor Mass Search Type – monoisotopic, Enzyme – Trypsin, Max Missed Cleavages – 1, Digest Mode – Specific. Fixed Modifications with Beta-methylthiolation (45.99 Da) and variable Modifications with Oxidation (15.99 Da), **15** (444.09 Da) and **16** (447.11 Da) were included in the settings.

Additional search parameters included, Max Variable PTM per Peptide – 3, Database – HaemolysinSaureus, Taxon – All, Searched Entry – 1, FDR Estimation – Enabled, De novo score (%) threshold – 15, Peptide hit threshold (-10logP) – 30.0, Peaks run ID – 3, Merge Options – merged, Precursor Options – corrected, Charge Options – [2 – 5], Filter RT – [0.0 – 21.0], Filter Charge – [2 – 5], Process – true, Associate chimera – yes. The ion source was ESI (nano-spray), fragmentation mode was CID, CAD (y and b ions), MS Scan Mode and MS/MS Scan Mode were TimsTOF.

An overall protein sequence coverage of 84% was achieved. For the identification of the binding site, the PTM profile option in the Peaks Software was used with the restriction of a minimal Ascore of 20.0. The areas under the peaks of each feature (specific m/z, RT, charge, $-10\lg P$) corresponding to a certain peptide were used for the quantitative analysis of modified and non-modified peptides. In the presence of only one equivalent photoprobe, W286 was identified as the main binding site of the quinoxalinediones. This finding was consistent for all samples and independent from the irradiation time and the usage of the deuterated (**16**) or not deuterated photoprobe (**15**). Nevertheless, a second binding site could be recognized at Y54, which was modified by the probes in six of eight samples.

The same experiment was carried out with higher amounts of the probe using 10 and 50 equivalents of **15** and **16** respectively. In contrast to the previous experiment, only one irradiation time of 15 min was used. With higher amounts of the photoprobes additional modifications occurred at K63, V64, Y94, Y174, Y217 (Figure S4). This is likely due to unspecific labeling of the probes, being present in an excess. Nevertheless, the main binding sites are again W286 and Y54, which is reflected by the relatively high amounts of the respective modified peptides in all of the eight samples. The amino acids W106 and W205 were also modified to a significant extent, that was however small in comparison to Y54 and W286. For this reason, they were assumed to be unspecifically labeled. The same applies for Y94, which was only labeled in the presence of 50 equivalents of **16** (see figures for amino acid modification after incubation with photoprobe).

LDH assay

A549 cells (DSMZ, #ACC107) were maintained in RPMI 1640 cell culture medium + glutamine (PAN Biotech GmbH; #P04-22100; P04-05500) supplemented with 10% fetal calf serum (Capricorn, #FBS-11A) and were grown at 37 °C, 5% CO_2. Compounds or DMSO were pre-diluted at different concentrations in 15 μl cell culture medium RPMI1640 + 5% FCS + 10 mM HEPES in black μclear 384 well-plates (Greiner BioOne). Shortly afterwards, 10 μl of 70 nM *S. aureus* alpha-hemolysin (IBT Bioservices, #1401-002) was added to get a final assay concentration of 20 nM. Thereafter, 10 μl of A549 cells were added (20.000 cells/well diluted in assay medium). With a final assay volume of 35 μL, assay plates were incubated for 5h at 37°C/5% CO_2 in humidified chambers. An anti-*S. aureus* Hla monoclonal antibody (IBT Bioservices, #0210-001) was used as a positive control.LDH in the culture supernatant was determined after 5 h incubation according to the manufacturer instructions of the CytoTox-ONE Homogenous Membrane Integrity assay (Promega, cat no. G7891). Shortly, 20 μl of cell culture supernatant were incubated in a separated black μclear 384 well plate at 25 °C for 20 min, mixed with 20 μl of the LDH reagent using an orbital shaker (1 min, 300 rpm) and further incubated for 5 min at 25 °C. The reaction was stopped by addition of 10 μl stop-reagent, provided with the assay kit. Shortly afterwards, the fluorescent signal was measured by a plate reader (Victor X5, Perkin Elmer) using the filters 531 nm (extinction) and 590 nm (emission).

EC_{50} values were calculated with the software Excel Fit (IDBS, Guildford, UK) from 3-fold dilution series comprising at least eight concentrations in duplicates.

MTT assay

MTT [3-(4,5-dimethylthiazol-2-yl)2,5-diphenyltetrazolium bromide] (Sigma) was used to measure the metabolic activity of cells which are capable of reducing it by dehydrogenases to a violet-coloured formazan product. First 120 μL aliquots of a cell suspension (50,000 cells/ml) were added in 96-well microplates, then 60 μL of serial dilutions of the test compounds were added. After 5 d of incubation at 37 °C and 10% CO_2, 20 μL MTT in phosphate-buffered saline (PBS) were added to a final concentration of 0.5 mg/ml. After 2 h the precipitate of formazan crystals was centrifuged and the supernatant discarded. The precipitate was washed with 100 μL PBS and dissolved in 100 μL isopropanol containing 0.4% hydrochloric acid. The resulting color was measured at 590 nm using a Tecan infinite M200 PRO plate reader. All investigations were carried out in two parallel experiments.

Whole cell infection model

A549 cells and differentiated THP1 cells (dTHP1) were seeded in 96-well plates 10^5 cells/well and infected in a total volume of 100 μl in RPMI 1640 medium. *S. aureus* USA300 WT or *Δhla* was cultivated overnight and cultures were started the following day at OD_{600} 0.05 in TSB at 37 °C and 150 rpm. 5 ml of bacterial suspensions at OD_{600} 0.5 was centrifuged at 500 rpm for 5 min at 4 °C and the supernatant was discarded. Pellets were washed with PBS and resuspended in RPMI 1640 medium. Volume was adjusted to infected cells with 10 μl bacterial suspension resulting in a multiplicity of infection (MOI) of 10 as determined by CFU enumeration. Plates were incubated at 37 °C and 10% CO_2 for 6 h. To test the activity of QDS inhibitors, 10 μL of 10-fold concentrated compounds were added to wells with cells before the addition of *S. aureus*.

LDH release in the infection model

LDH release was determined after 6 h using the CyQUANT LDH Cytotoxicity assay kit (Thermo Fischer Scientific, Germany). Plates were centrifuged at 250 g for 3 min and 50 μl of supernatant was transferred to a 96-well plate. 50 μl of LDH reaction mixture was prepared as per manufacturer's instructions and added to the wells, mixed and incubated for 30 min at RT in dark. Thereafter, 50 μl of stop solution was added, mixed and LDH release determined by measuring absorbance at 490 nm and 680 nm (background) using a microplate reader (Synergy, BioTek Instruments, Germany)

Apoptosis-necrosis staining for the infection model

The viability of infected cells was characterised by flow cytometry using the Annexin V-FITC Apoptosis Detection Kit with PI (Biolegend, USA) as per the manufacturer's instructions. A549 cells were infected at 10^6 cells/well in a 6-well plate with *S. aureus* USA300 WT or *Δhla* at an MOI of 10 and total volume of 1 ml in RPMI 1640 medium. Cells were washed 6 h post-infection with Biolegend's cell staining buffer to stop the infection. Cells were detached with 200 μl Accutase, centrifuged for 5 min at 1200 rpm and resuspended in 100 μl Annexin V binding buffer. Cells were transferred to round-bottom 5 ml tubes, 5 μl of FITC - Annexin V and 10 μl of PI solution were added, mixed gently and incubated for 15 min at RT in dark. Thereafter, 400 μl Annexin V binding buffer were added to each tube and samples were analysed by flow cytometry with the LSR II SORP (BD Bioscience, Franklin Lakes, USA) using appropriate settings. Cells were primarily gated based on size to exclude bacterial cells and debris followed by a secondary gate to exclude doublets. 10000 events, i.e. cells, were counted from each sample and analysed. The data was analysed using the FlowJo v10 software.

Western blot for Hla

1 ml of infection medium 6 h post infection or bacterial culture (control) were placed in 1.5 ml tubes and centrifuged at 9000 rpm for 5 min at 4 °C. Supernatants were transferred to 1.5 ml tubes and filtered through a 0.2 μm filter. 500 μl of the filtrate were concentrated 10-fold by centrifugation using Vivaspin 500 centrifugal concentrators (5-kDa MWCO) as per manufacturer's instructions. 20 μl of the concentrated filtrate was subjected to 10% SDS-PAGE. Gels contained 1% (v/v) 2,2,2-trichloroethanol for stain-free visualisation. PVDF membranes were activated by immersing in 100% methanol followed by dH_2O and subsequently for 5 min in transfer buffer. Proteins were blotted on activated PVDF membranes in a semi-dry blotter for 60 min at 2 mA/cm2. Membranes were blocked in PBS containing 5% (w/w) dry milk powder for 60 min at RT incubated overnight in 1 μg/ml mouse anti-Hla mAb in blocking solution at 4 °C. Membranes were washed 3x with PBS containing 0.1% Tween 20 and incubated with anti-mouse IgG HRP diluted 1:2500 in blocking solution, for 60 min at RT. Following 3x washing, HRP activity was determined using the Clarity ECL Western blotting substrate and a ChemiDoc MP for documentation. Signal intensities were analysed with the Image Lab software.

Recombinant protein production

A construct for the USA 300 wild type with C-terminal Strep-tag II was obtained in the vector pPR-IBA1 (Prof. S. Engelmann, HZI). Other variants were ordered as synthetic genes with C-terminal Strep-tag II, codon-optimized for expression in *E. coli* in the vector pET28a (GenScript). The proteins were expressed in *E. coli* BL21 (DE3) Star in auto-inducing medium[63] at 20 °C. For non-labeled protein, ZYM-5052 was used as expression medium for 20-24 hours, while expression for isotope labeling was carried out either in P-5052 minimal medium supplemented with ^{15}N ammonium sulfate or C-750501 minimal medium supplemented with ^{13}C-glycerol and optionally ^{15}N-ammonium chloride and/or D_2O. Expression cultures for isotope labeling were incubated for 72 - 96 hours. The cell

pellets were resuspended in a buffer containing 20 mM Tris/HCl pH 8.5, 300 mM NaCl, one tablet of cOmplete EDTA-free protease inhibitor cocktail (Roche) and lysed by sonication. The proteins were isolated from the supernatants after centrifugation for 1 h at 100,000 x g using a self-packed 10 ml column with Strep-Tactin Superflow High Capacity resin (IBA) and eluted from the column with a single step of 5 mM D-desthiobiotin. Gel filtrations were carried out using a HiLoad 16/600 Superdex 75 pg column (GE Healthcare) in 20 mM Tris/HCl pH 8.5, 300 mM NaCl. The peak fractions were concentrated and flash-frozen in liquid nitrogen.

For recombinant production of site-specific constructs, following changes were made to the above mentioned protocol to comply with EU guidelines for recombinant production of toxic proteins. *E. coli* KRX (Promega) was used instead of *E. coli* BL21 (DE3) Star. Cell were grown in TB medium supplemented with 2 mM $MgSO_4$ until an OD of 0.6 -1 was reached. The cultures were then cooled to 20 °C, rhamnose was added to final concentration of 0.1% (w/v) from a 20% (w/v) stock solution, and cultures were cultivated for another 20 hours at 20 °C. A StrepTactin XT 4Flow High capacity (IBA) was used for the purification. The protein was eluted with 50 mM biotin. Size exclusion chromatography (SEC) was done using a S200 26/60 column in 20 mM Tris pH 8.5, 150 mM NaCl and 5% glycerol.

Differential Scanning Floriometry

Melting temperatures of selected purified HLA Variants were determined by using a thermal shift assay.[64] The purified HLA variants were diluted to a final concentration of 10 μM in Tris Buffer (20 mM Tris pH 8.5, 150 mM NaCl) and mixed 1:1 with 10 x SYPRO Orange (Stock: 5000x, Invitrogen) in Tris Buffer on ice in a 96-well PCR Plate (Biorad). The PCR plate was then sealed and briefly centrifuged and loaded into a CFX96 Touch Real-Time PCR Detection System (Biorad). The fluorescence of the samples was monitored during a thermal denaturation with a heat gradient of 4° C/min using the "FRET Channel" for detection. Melting temperatures were determined in triplicates.

Sphingomyelinase activity assay

The activity of QDS inhibitors on neutral sphingomyelinase (SMase) was tested using the colorimetric sphingomyelinase kit (Sigma). The sphingomyelinase standard was reconstituted as per manufacturer's protocol to make a 10 U/ml solution in 20 μl PBS containing 0.1% BSA. The detection reagent was reconstituted with 100 μl DMSO resulting in a 200x stock solution. 25 μL of 10 mU/ml sphingomyelin were transferred to wells of a 96-well half area plate. 5 μl of 10x Hla-inhibitors were added to the wells with sphingomyelin, mixed and incubated for 30 min. Thereafter, 20 μL of 5 mU/ml SMase solution was added to each well, mixed and incubated for 1 h at 37 °C. Thereafter, 25 μL of sphingomyelinase assay mixture was added to each well, incubated at 37 °C for 1 h in the dark and absorbance measured at 655 nm with a microplate reader. Wells without sphingomyelin or SMase served as controls. Additionally, a SMase standard curve was generated in each plate with different concentrations of SMase.

In vitro pharmacology

QDS were tested in a binding assay for NMDA antagonism at a concentration of 10 μM. Compound binding was calculated as a % inhibition of the binding of a radioactively labeled ligand. Secondary functional assays were performed in a dose-dependent manner in agonist and antagonist format. All assays were contracted to and performed by Eurofins Discovery, France.

Starting Materials for chemical synthesis

Starting materials were purchased from commercial suppliers (Sigma-Aldrich, TCI, BLDpharm, abcr, Carbolution, Thermo Scientific, Alfa Aesar, Acros Organics) and used without further purification. NaOD in D_2O (10 ml, 40 w/w %) was purchased as a commercial solution from Sigma Aldrich or Alfa Aesar. See also Scale up synthesis for H052 and Chemical synthesis.

Accurate Mass method

High resolution masses were obtained using a Maxis II TM HD mass spectrometer (Bruker Daltonics, Bremen, Germany).

NMR methods

Proton (^1H) and carbon (^{13}C) nuclear magnetic resonance (NMR) spectra were measured with an Oxford Varian 400/54 (400 MHz) spectrometer or a Bruker Avance II (300 MHz) spectrometer, or with a Bruker Avance III (500 MHz), or a Bruker Avance III HD (700 MHz) spectrometer with residual protonated solvent ($CHCl_3$ δ 7.26; MeOH δ 3.30; DMSO δ 2.50; MeCN δ 1.94) as standard. The NMR data of the synthesized examples are in agreement with their corresponding structural assignments. See also NMR spectra.

Flash Column Chromatography

Purification on reverse phase was done with a Pure C-850 FlashPrep system (Büchi) using FlashPure EcoFlex C18 cartridges (Büchi). A gradient of water and acetonitrile was used as an eluent. Dryloads were prepared with silica gel C18, 0.035-0.07, 400-220 mesh (Carl Roth).

Normal phase purification was carried out with a Pure C-810 Flash system (Büchi) using FlashPure cartridges (Büchi). A gradient of cyclohexane and ethyl acetate or dichloromethane and methanol was used as an eluent. Dryloads were prepared with silica gel, 60 Å, 230-400 mesh, 40-63 μm (Merck).

CellPress
OPEN ACCESS

Conventional column chromatography was carried out with silica gel, 60 Å, 230-400 mesh, 40-63 μm (Merck) using the eluents described in the synthesis procedures.

High-Performance Liquid Chromatography (HPLC)

HPLC was carried out with a Dionex UltiMate 3000 system (Thermo Scientific) using a Luna® 5 μm C18(2) 100 Å, LC column 250 x 21.2 mm, AXIA™ packed (phenomenex). As an eluent, water and acetonitrile were used without or with 0.1% formic acid.

Scale up synthesis for H052

Step-1

[NOTE: The reaction was performed in 2 batches (2 x 100 g), however the work-up and purification was performed after combining the crude from the two batches.]

Chlorosulfonic acid $ClSO_3H$ (2 L) was added dropwise to compound **1** (200 g, 1.13 mol) at 0 °C. The resulting reaction mixture was stirred at 100 °C for 16 h. The reaction mixture was cooled to room temperature and slowly quenched into cold water (10 L). The precipitated solid was filtered and washed with water (3 x 500 ml) and dried to afford compound **2** (318 g, crude) as an off-white solid.

LC-MS: 68.68%, m/z = 275.35 $[M+H]^+$.

Step-2

[NOTE: The reaction was performed in 4 batches (4 x 50 g), however the work-up and purification was performed after combining the crude from all the batches.]

To a degassed solution of compound **3** (4 x 50 g, 0.97 mol), compound **4** (4 x 40.6 g, 1.16 mol) and Cs_2CO_3 (4 x 236 g, 2.91 mol) in a mixture of 1, 4-dioxane (4 x 500 ml) and water (4 x 25 ml) was added $Pd(PPh_3)_4$ (4 x 14 g, 0.04 mol) at room temperature. The resulting reaction mixtures were stirred for 16 h at 80 °C. After completion of the reactions (monitored by TLC & LC-MS), the reaction mixtures were cooled to room temperature, combined, diluted with water (1 L) and extracted with EtOAc (4 x 500 ml). The combined organic layer was washed with water (2 x 150 ml), brine (250 ml), dried over anhydrous Na_2SO_4 and concentrated under reduced pressure. The crude product was purified by flash chromatography using 100-200 g silica gel column, eluting with 20-30% EtOAc in pet-ether as an eluent to afford compound **5** (207 g, 96%) as a brown solid.

LC-MS: 68.56%, m/z = 222.15 $[M+H]^+$.

Step-3

[NOTE: The reaction was performed in 2 batches (2 x 50 g), however the work-up and purification was performed after combining the crude from the two batches.]

To a stirred solution of compound **5** (2 x50 g, 0.45 mol) in DCM (2 x 250 ml) was added pyridine (2 x 750 ml) at RT. The resulting reaction mixture was stirred for 5 min, prior to the addition of compound **2** (2 x 123 g, 0.89 mol) at 0 °C. The resulting reaction mixture was stirred for 16 h at room temperature. After completion of the reactions (monitored by TLC and LC-MS), the reaction mixtures were combined, quenched with cold water (5 L) and the precipitated solid was filtered. The solid was washed with water (3 x 500 ml), 1N HCl (2 x 500 ml), water (3 x 500 ml), diethyl ether (2 x 300 ml), hexane (2 x 300 ml) and dried to afford **H052** (140 g, 67%) as a pale brown solid.

^1H NMR (400 MHz, DMSO) δ: 12.11 (s, 1H), 11.98 (s, 1H), 10.84 (s, 1H), 7.80 (s, 1H), 7.40-7.36 (m, 2 H), 7.30-7.22 (m, 4H), 7.08 (dd, *J*= 8.4 Hz, 2.0 Hz), 7.03 (s, 1H), 2.55 (s, 3H).

HPLC: 96.95% (max plot), 97.37 % (215 nm); Mass: 460.18 $[M+H]^+$.

Chemical synthesis

7-Methylquinazoline-2,4(1H,3H)-dione was synthesized according to Tian et al.[65]

3-Bromo-4-iodoaniline was synthesized according to Lee et al.[66]

N-(4-(tert-Butyl)phenethyl)-2,3-dioxo-1,2,3,4-tetrahydroquinoxaline-6-carboxamide (2)

To a solution of 2,3-dioxo-1,2,3,4-tetrahydroquinoxaline-6-carboxylic acid (30 mg, 0.15 mmol) in a mixture of EtOAc and DMF (1 : 1, 1.5 ml) was added Et_3N (60.7 μL, 44 mg, 0.44 mmol) and 2-(4-(*tert*-butyl)phenyl)ethan-1-amine (42.1 μL, 38.7 mg, 0.22 mmol) followed by T3P (173.2 μL, 0.29 mmol, 50% solution in EtOAc). The reaction mixture was stirred at 40 °C (LC-MS control). H_2O was added and the mixture was extracted with EtOAc (3x). The combined organic phases were dried over Na_2SO_4, filtered and concentrated under reduced pressure. The residue was purified by flash chromatography (C18; MeCN : H_2O) yielding 19.3 mg (36%) of the desired product.

^1H NMR (500 MHz, DMSO-d_6): δ = 12.08 (s, 1 H), 12.05 (s, 1 H), 8.57 (t, *J* = 5.6 Hz, 1 H), 7.62 (d, *J* = 1.8 Hz, 1 H), 7.55 (dd, *J* = 8.4, 1.8 Hz, 1 H), 7.31 (d, *J* = 8.3 Hz, 2 H), 7.16 (d, *J* = 8.3 Hz, 2 H), 7.12 (d, *J* = 8.4 Hz, 1 H), 3.48 – 3.40 (m, 2 H), 2.79 (t, *J* = 7.3 Hz, 2 H), 1.25 (s, 9 H) ppm.

^{13}C NMR (125 MHz, DMSO-d_6): δ = 165.37, 155.25, 155.15, 148.34, 136.47, 129.40, 128.32, 127.90, 125.52, 125.12, 121.51, 114.82, 114.58, 41.06, 34.64, 34.11, 31.22 ppm.

HRMS (ESI) calcd. for $C_{21}H_{24}N_3O_3$ $[M+H]^+$: *m/z* = 366.1818, found: 366.1821.

N-(4-Isopropylphenyl)-2,3-dioxo-1,2,3,4-tetrahydroquinoxaline-6-carboxamide (8)

2,3-Dioxo-1,2,3,4-tetrahydroquinoxaline-6-carboxylic acid (30 mg, 0.15 mmol), EDC•HCl (33.5 mg, 0.17 mmol) and HOBt•H_2O (26.7 mg, 0.17 mmol) were dissolved in DMF (2 ml). This mixture was stirred for several minutes at r. t. 4-Isopropylaniline (21.6 mg, 0.16 mmol) was added. The reaction mixture was stirred for 16 h at 50 °C, cooled down to r. t., diluted with H_2O and

extracted with EtOAc (2x). The combined organic phases were washed with H_2O and concentrated under reduced pressure. H_2O was added to the residue and the formed precipitate was filtered and dried under vacuum. Yield: 36.9 mg (78%).

^{1}H NMR (500 MHz, DMSO-d_6): δ = 12.14 (s, 1 H), 12.07 (s, 1 H), 10.18 (s, 1 H), 7.73 – 7.68 (m, 2 H), 7.67 – 7.62 (m, 2 H), 7.24 – 7.17 (m, 3 H), 2.86 (septet, *J* = 6.9 Hz, 1 H), 1.19 (d, *J* = 6.9 Hz, 6 H) ppm.

^{13}C NMR (125 MHz, DMSO-d_6): δ = 164.54, 155.28, 155.11, 143.74, 136.89, 129.66, 128.27, 126.34, 125.60, 122.19, 120.46, 115.14, 114.63, 32.93, 24.00 ppm.

HRMS (ESI) calcd. for $C_{18}H_{18}N_3O_3$ $[M+H]^+$: *m/z* = 324.1348, found: 324.1346.

3-(4-(tert-Butyl)phenyl)-N-(1,4-dimethyl-2,3-dioxo-1,2,3,4-tetrahydroquinoxalin-6-yl)propanamide (S16)

3-(4-(*tert*-Butyl)phenyl)propanoic acid (60.3 mg, 0.29 mmol), EDC•HCl (70.2 mg, 0.37 mmol) and HOBt (49.3 mg, 0.37 mmol) were dissolved in DMF (4 ml). This mixture was stirred for several minutes at r. t. 6-Amino-1,4-dimethyl-1,4-dihydroquinoxaline-2,3-dione (50 mg, 0.24 mmol) and Et_3N (50.83 µL, 36.9 mg, 0.37 mmol) were added. The reaction mixture was stirred for 1 h and then for further 2 h at 40 °C, cooled down to r. t., diluted with EtOAc and washed with sat. aq. $NaHCO_3$ (2x) and H_2O. MeOH was added to the organic phase and the organic phase was dried over $MgSO_4$, filtered and concentrated under reduced pressure. The residue was purified by flash chromatography (C18; MeCN : H_2O) yielding 51.2 mg (54%) of the desired product.

^{1}H NMR (500 MHz, DMSO-d_6): δ = 10.12 (s, 1 H), 7.76 (d, *J* = 2.0 Hz, 1 H), 7.45 (dd, *J* = 8.9, 2.0 Hz, 1 H), 7.36 (d, *J* = 8.9 Hz, 1 H), 7.30 (d, *J* = 8.2 Hz, 2 H), 7.17 (d, *J* = 8.2 Hz, 2 H), 3.51 (s, 3 H), 3.49 (s, 3 H), 2.89 (t, *J* = 7.7 Hz, 2 H), 2.63 (t, *J* = 7.7 Hz, 2 H), 1.25 (s, 9 H) ppm.

^{13}C NMR (125 MHz, DMSO-d_6): δ = 170.63, 154.03, 153.35, 148.23, 138.04, 135.54, 127.89, 127.36, 125.09, 122.81, 115.45, 114.36, 105.41, 37.97, 34.09, 31.21, 30.20, 29.81, 29.73 ppm.

HRMS (ESI) calcd. for $C_{23}H_{28}N_3O_3$ $[M+H]^+$: *m/z* = 394.2131, found: 394.2126.

2-(4-(tert-Butyl)phenyl)-N-(2,3-dioxo-1,2,3,4-tetrahydroquinoxalin-6-yl)ethane-1-sulfonamide (3)

To a solution of 6-amino-1,4-dihydroquinoxaline-2,3-dione (60 mg, 0.34 mmol) and pyridine (67 mg, 0.85 mmol) in DMSO (1.5 ml) was added a solution of 2-(4-(*tert*-butyl)phenyl)ethane-1-sulfonyl chloride (88 mg, 0.34 mmol) in CH_2Cl_2 (1.2 ml) at 0 °C over a period of 20 min. The reaction mixture was allowed warmed up to r. t. and stirred for 16 h at this temperature, poured into H_2O (20 ml) and the resulting mixture was stirred for 2 h. The resulting solid was filtered, washed with H_2O (3 times) and 1 N aq. HCl (5 ml) followed by H_2O (5 ml) and dried in vacuum. Yield: 38 mg (27%).

^{1}H NMR (500 MHz, DMSO-d_6): δ = 11.90 (s, 1 H), 11.88 (s, 1 H), 9.86 (s, 1 H), 7.27 (d, *J* = 8.2 Hz, 2 H), 7.13 (s, 1 H), 7.10 (d, *J* = 8.2 Hz, 2 H), 7.07 (d, *J* = 8.5 Hz, 1 H), 6.95 (d, *J* = 8.5 Hz, 1 H), 3.30 – 3.23 (m, 2 H), 2.97 – 2.90 (m, 2 H), 1.22 (s, 9 H) ppm.

^{13}C NMR (175 MHz, DMSO-d_6): δ = 155.21, 154.73, 148.89, 134.93, 133.20, 128.03, 126.23, 125.27, 122.49, 119.99, 115.80, 107.53, 51.37, 34.09, 31.10, 28.56 ppm.

HRMS (ESI) calcd. for $C_{20}H_{24}N_3O_4S$ $[M+H]^+$: *m/z* = 402.1488, found: 402.1487.

N-(2,3-Dioxo-1,2,3,4-tetrahydroquinoxalin-6-yl)-4-isopropylbenzenesulfonamide (9)

To a solution of 6-amino-1,4-dihydroquinoxaline-2,3-dione (60 mg, 0.34 mmol) and pyridine (67 mg, 0.85 mmol) in DMSO (1.5 ml) was added a solution of 4-isopropylbenzenesulfonyl chloride (74 mg, 0.34 mmol) in CH_2Cl_2 (1.2 ml) at 0 °C over a period of 20 min. The reaction mixture was allowed warmed up to r. t. and stirred for 16 h at this temperature, poured into H_2O (20 ml) and the resulting mixture was stirred for 2 h. The resulting solid was filtered, washed with H_2O (3 times) and 1 N aq. HCl (5 ml) followed by H_2O (5 ml) and dried in vacuum. Yield: 52 mg (43%).

^{1}H NMR (500 MHz, DMSO-d_6): δ = 11.84 (s, 1 H), 11.80 (s, 1 H), 10.24 (s, 1 H), 7.67 (d, *J* = 8.4 Hz, 2 H), 7.42 (d, *J* = 8.4 Hz, 2 H), 7.02 (d, *J* = 2.2 Hz, 1 H), 6.95 (d, *J* = 8.6 Hz, 1 H), 6.79 (dd, *J* = 8.6, 2.2 Hz, 1 H), 2.93 (sept, *J* = 6.9 Hz, 1 H), 1.17 (d, *J* = 6.9 Hz, 6 H) ppm.

^{13}C NMR (125 MHz, DMSO-d_6): δ = 155.19, 154.69, 153.64, 136.99, 132.97, 127.21, 126.85, 126.07, 122.27, 115.66, 115.43, 106.92, 33.32, 23.40 ppm.

HRMS (ESI) calcd. for $C_{17}H_{18}N_3O_4S$ $[M+H]^+$: *m/z* = 360.1018, found: 360.1016.

5-Bromo-6-methylisobenzofuran-1,3-dione (S19)

To 4-bromo-5-methylphthalic acid (5 g, 19.45 mmol) was added acetic anhydride (12.5 ml) at 0 °C. The resulting reaction mixture was refluxed for 4 h. After completion of reaction (monitored by LC-MS), the reaction mixture was concentrated under reduced pressure, quenched with water and extracted with EtOAc. The combined organic layer was dried over Na_2SO_4 and concentrated under reduced pressure. This crude was purified by column chromatography (silica gel, 90-100% EtOAc in PE as eluent) to afford 1.5 g (32%) of 5-bromo-6-methylisobenzofuran-1, 3-dione (**1**) as an off-white solid.

TLC system: Rf: 0.1 (EtOAc/pet-ether 2/8)

6-Bromo-7-methyl-2, 3-dihydrophthalazine-1, 4-dione (S20)

To a stirred solution of 5-bromo-6-methylisobenzofuran-1, 3-dione (**S19**) (500 mg, 2.10 mmol) in acetic acid (4 ml) was added hydrazine hydrate (167 mg, 5.23 mmol) at 0 °C. The resulting reaction mixture was stirred for 16 h at 70 °C. After completion of reaction (monitored by LC-MS), the reaction mixture was quenched with cold water (10 ml) and extracted with EtOAc (3 × 15 ml). The combined organic layer was dried over Na_2SO_4 and concentrated under reduced pressure to afford 500 mg of 6-bromo-7-methyl-2, 3-dihydrophthalazine-1,4-dione (**S20**) as a white solid.

TLC: R_f: 0.2 (EtOAc/PE 2/8)

MS (ESI) calcd. for $C_9H_8BrN_2O_2$ $[M+H]^+$: *m/z* 255/257, found: 255/257.

6-(Benzylthio)-7-methyl-2,3-dihydrophthalazine-1,4-dione (S21)

To a stirred solution of 6-bromo-7-methyl-2,3-dihydrophthalazine-1,4-dione (**S20**) (500 mg, 1.98 mmol) in 1,4-dioxane (5 ml) were added DIPEA (667 mg, 3.95 mmol), XanthPhos (114 mg, 0.20 mmol), Pd_2dba_3 (90 mg, 0.10 mmol), phenylmethanethiol (294 mg,

2.37 mmol) and degassed with argon for 5 min. The reaction mixture was stirred for 3 h at 150 °C under microwave irradiation. After completion of reaction (monitored by LC-MS), the reaction mixture was concentrated under reduced pressure, quenched with water (15 ml) and extracted with EtOAc (3 × 15 ml). The combined organic layer was dried over Na_2SO_4 and concentrated under reduced pressure. This crude product was purified by column chromatography (silica gel 100-200 mesh, 70-80% EtOAc in PE as eluent) to afford 200 mg (34%) of 6-(benzylthio)-7-methyl-2,3-dihydrophthalazine-1,4-dione (**S21**) as an off-white solid.

TLC: R_f (EtOAc/PE 2/8): 0.2

MS (ESI) calcd. for $C_{16}H_{15}N_2O_2S$ $[M+H]^+$: *m/z* 299, found: 299.

7-Methyl-1,4-dioxo-1,2,3,4-tetrahydrophthalazine-6-sulfonyl chloride (S22)

To a stirred solution of 6-(benzylthio)-7-methyl-2,3-dihydrophthalazine-1,4-dione (**S21**) (200 mg, 2.09 mmol) in acetic acid (4 ml), water (2 ml) was added *N*-chlorosuccinimide (38.90 mg, 0.67 mmol) at 0 °C. The resulting reaction mixture was stirred for 16 h at r. t. After completion of reaction (monitored by LC-MS), the reaction mixture was quenched with cold water (30 ml) and extracted with EtOAc (3 × 30 ml). The combined organic layer was dried over Na_2SO_4 and concentrated under reduced pressure to afford 150 mg of 7-methyl-1,4-dioxo-1,2,3,4-tetrahydrophthalazine-6-sulfonyl chloride (**S22**) as an off-white solid. The crude product was directly used for next step without any further purification.

TLC: Rf: 0.1 (EtOAc/PE 2 : 8).

7-Methyl-1,4-dioxo-N-(4-(trifluoromethoxy)phenyl)-1,2,3,4-tetrahydrophthalazine-6-sulfonamide (13)

To a stirred solution of 7-methyl-1,4-dioxo-1,2,3,4-tetrahydrophthalazine-6-sulfonyl chloride **(S22)** (120 mg, 0.43 mmol) in pyridine (1 ml) was added 4-(trifluoromethoxy)aniline (77.5 mg, 0.43 mmol) at 0 °C. The resulting reaction mixture was stirred for 16 h at r. t. After completion of reaction (monitored by LC-MS), the reaction mixture was quenched with cold water (5 ml) and extracted with EtOAc (3 × 15 ml). The combined organic layer was dried over Na_2SO_4 and concentrated under reduced pressure. This crude product was purified by prep-(C18; H_2O: MeCN + NH_4HCO_3) as an eluent. The compound containing fractions were evaporated and dried to get 7-methyl-1,4-dioxo-*N*-(4-(trifluoromethoxy)phenyl)-1,2,3,4-tetrahydrophthalazine-6-sulfonamide (10 mg, 6%) as a white solid.

^{1}H NMR (500 MHz, DMSO-d_6): δ = 12.07 – 10.72 (br. s, 2 H), 8.52 (s, 1 H), 8.00 (s, 1 H), 7.22 (d, *J* = 8.9 Hz, 2 H), 7.11 (d, *J* = 8.9 Hz, 2 H), 2.76 (s, 3 H) ppm.

^{13}C NMR (125 MHz, DMSO-d_6): δ = 169.11, 143.74, 141.21, 139.63, 128.28, 127.27, 126.74, 122.17, 121.05, 120.95, 119.02, 20.17 ppm.

HRMS (ESI) calcd. for $C_{32}H_{25}F_6N_6O_{10}S_2$ $[2M+H]^+$: *m/z* = 831.0978, found: 831.0974.

Mixture of 7-methylquinoxalin-2(1H)-one (S23) and 6-methylquinoxalin-2(1H)-one (S24)

Ethyl 2-oxoacetate (1.2 g, 12 mmol, 50% in toluene) was added to a suspension of 4-methylbenzene-1,2-diamine (1.2 g, 10 mmol) in EtOH (10 ml). The reaction mixture was stirred at reflux in an oil bath for 1 h, then at r. t. for 3 h. The precipitate was filtered, washed with EtOH and dried under reduced pressure yielding 1.3 g (81%) of a mixture of unseparable regioisomers **S23** and **S24** (ratio *ca.* 57 : 43).

^{1}H NMR (500 MHz, DMSO-d_6): δ = 12.35 (s, 1 H), 8.14 (s, 0.57 H), 8.09 (s, 0.43 H), 7.65 (d, *J* = 8.2 Hz, 0.43 H), 7.58 (s, 0.57 H), 7.38 (dd, *J* = 8.2, 1.9 Hz, 0.57 H), 7.21 (d, *J* = 8.2 Hz, 0.57 H), 7.12 (dd, *J* = 8.2, 1.9 Hz, 0.43 H), 7.08 (s, 0.43 H), 2.40 (s, 1.3 H), 2.38 (s, 1.7 H) ppm.

Mixture of 7-methyl-2-oxo-1,2-dihydroquinoxaline-6-sulfonyl chloride (S25) and 6-methylquinoxalin-2(1H)-one (S24)

The mixture of 7-methylquinoxalin-2(1H)-one (**S23**) and 6-methylquinoxalin-2(1H)-one (**S24**) (1.3 g, 8 mmol) was added in portions to chlorosulfonic acid (7 ml, 12.3 g, 106 mmol), after which the mixture was heated (under reflux) at 110 °C for 4 h. The reaction mixture was cooled to r. t. and poured into crushed ice. The resulting solid was filtered, washed with cold water and dried under reduced pressure and used for the next step without further purification. Analysis of the crude product mixture showed that 6-methylquinoxalin-2(1H)-one (**S24**) did not react under these conditions and only 7-methyl-2-oxo-1,2-dihydroquinoxaline-6-sulfonyl chloride (**S25**) was formed.

7-Methyl-2-oxo-N-(4-(trifluoromethoxy)phenyl)-1,2-dihydroquinoxaline-6-sulfonamide (S11)

The mixture of 7-methyl-2-oxo-1,2-dihydroquinoxaline-6-sulfonyl chloride (**S25**) and 6-methylquinoxalin-2(1H)-one (**S24**) obtained from the previous reaction was added to a stirred solution of 4-(trifluoromethoxy)aniline (1.6 g, 9 mmol) in pyridine (10 ml). The reaction mixture was stirred for 18 h at r.t. and poured into 2 N HCl. The product was filtered and purified by column chromatography RP (C18; H_2O: MeCN) yielding 340 mg (11% over two steps) of the crude product. 50 mg of the crude product was purified by HPLC (C18; H_2O: MeCN + 0.1% HCOOH). Yield: 35 mg.

^{1}H NMR (500 MHz, DMSO-d_6): δ = 12.65 (s, 1 H), 12.33 (s, 1 H), 8.21 (s, 1 H), 8.18 (s, 1 H), 7.26 (d, *J* = 8.4 Hz, 2 H), 7.21 – 7.15 (m, 3 H), 2.64 (s, 3 H) ppm.

^{13}C NMR (125 MHz, DMSO-d_6): δ = 154.97, 152.88, 144.06, 139.07, 136.67, 135.19, 132.04, 130.27, 129.25, 122.26, 120.19, 118.94, 19.94 ppm.

HRMS (ESI) calcd. for $C_{16}H_{13}F_3N_3O_4S$ $[M+H]^+$: *m/z* = 400.0579, found: 400.0570.

N-(2-Chloro-4′-fluoro-[1,1′-biphenyl]-4-yl)-7-methyl-2-oxo-1,2-dihydroquinoxaline-6-sulfonamide (S12)

To a stirred solution of 2-chloro-4′-fluoro-[1,1′-biphenyl]-4-amine (859 mg, 3.89 mmol) in pyridine (20 ml) was added a mixture of 7-methyl-2-oxo-1,2-dihydroquinoxaline-6-sulfonyl chloride (**S25**) and 6-methylquinoxalin-2(1H)-one (**S24**) obtained from the sulfochlorination reaction (1.0 g) at 0 °C. The resulting reaction mixture was stirred for 16 h at r. t. poured into cold water and extracted

with EtOAc. The combined organic layer was dried over Na_2SO_4 and concentrated under reduced pressure. This crude product was purified by HPLC (C18; H_2O: MeCN + 0.1% NH_4HCO_3). The compound containing fractions were evaporated and dried to get the desired product (150 mg, 9%) as an off-white solid.

^{1}H NMR (500 MHz, DMSO-d_6): δ = 12.69 (s, 1 H), 10.98 (s, 1 H), 8.26 (s, 1 H), 8.20 (s, 1 H), 7.39 – 7.34 (m, 2 H), 7.23 (d, *J* = 8.4 Hz, 1 H), 7.26 – 7.19 (m, 4 H), 7.15 (dd, *J* = 8.5, 2.2 Hz, 1 H), 2.68 (s, 3 H) ppm.

^{13}C NMR (125 MHz, DMSO-d_6): δ = 162.62, 160.68, 155.01, 153.02, 139.13, 138.12, 135.35, 134.28, 133.57, 132.36, 131.96, 131.70, 131.36, 131.29, 130.29, 129.29, 119.10, 118.78, 117.01, 115.16, 114.99, 19.97 ppm.

N-*(4-Ethylphenyl)-2-oxo-1,2-dihydroquinoxaline-6-sulfonamide (S6)*

To a stirred solution of 4-ethylaniline (19.3 mg, 0.16 mmol) in pyridine (0.6 ml) was added 2-oxo-1,2-dihydroquinoxaline-6-sulfonyl chloride (30 mg, 0.12 mmol) at r. t.. The resulting reaction mixture was stirred for 16 h at r. t. and concentrated under reduced pressure. The residue was purified by flash chromatography (C18; MeCN: H_2O) yielding 29.2 mg (56%) of the desired product.

^{1}H NMR (500 MHz, DMSO-d_6): δ = 12.71 (s, 1 H), 10.24 (s, 1 H), 8.23 (s, 1 H), 8.05 (d, *J* = 2.1 Hz, 1 H), 7.84 (dd, *J* = 8.7, 2.1 Hz, 1 H), 7.38 (d, *J* = 8.7 Hz, 1 H), 7.06 (d, *J* = 8.6 Hz, 2 H), 7.01 (d, *J* = 8.6 Hz, 2 H), 2.47 (q, *J* = 7.6 Hz, 2 H), 1.08 (t, *J* = 7.6 Hz, 3 H) ppm.

^{13}C NMR (125 MHz, DMSO-d_6): δ = 154.83, 153.79, 139.81, 135.13, 135.05, 133.91, 130.99, 128.49, 128.39, 127.53, 120.60, 116.74, 27.39, 15.44 ppm.

HRMS (ESI) calcd. for $C_{32}H_{31}N_6O_6S_2$ $[2M+H]^+$: *m/z* = 659.1746, found: 659.1743.

N-*(4-Isopropylphenyl)-2-oxo-1,2-dihydroquinoxaline-6-sulfonamide (S7)*

To a stirred solution of 4-isopropylaniline (21.5 mg, 0.16 mmol) in pyridine (0.6 ml) was added 2-oxo-1,2-dihydroquinoxaline-6-sulfonyl chloride (30 mg, 0.12 mmol) at r. t.. The resulting reaction mixture was stirred for 16 h at r. t. and concentrated under reduced pressure. The residue was purified by flash chromatography (C18; MeCN : H_2O) yielding 31.2 mg (57%) of the desired product.

^{1}H NMR (500 MHz, DMSO-d_6): δ = 12.72 (s, 1 H), 10.26 (s, 1 H), 8.24 (s, 1 H), 8.07 (d, *J* = 2.1 Hz, 1 H), 7.86 (dd, *J* = 8.7, 2.1 Hz, 1 H), 7.39 (d, *J* = 8.7 Hz, 1 H), 7.10 (d, *J* = 8.4 Hz, 2 H), 7.01 (d, *J* = 8.4 Hz, 2 H), 2.76 (septet, *J* = 6.9 Hz, 1 H), 1.10 (d, *J* = 6.9 Hz, 6 H) ppm.

^{13}C NMR (125 MHz, DMSO-d_6): δ = 154.84, 153.80, 144.36, 135.15, 135.11, 134.04, 131.01, 128.38, 127.51, 127.04, 120.44, 116.77, 32.69, 23.80 ppm.

HRMS (ESI) calcd. for $C_{34}H_{35}N_6O_6S_2$ $[2M+H]^+$: *m/z* = 687.2059, found: 687.2054.

N-*(4-bromo-3-methylphenyl)-2-oxo-1,2-dihydroquinoxaline-6-sulfonamide (S8)*

To a stirred solution of 4-bromo-3-methylaniline (29.2 mg, 0.16 mmol) in pyridine (0.6 ml) was added 2-oxo-1,2-dihydroquinoxaline-6-sulfonyl chloride (30 mg, 0.12 mmol) at r. t. The resulting reaction mixture was stirred for 16 h at r. t. and concentrated under reduced pressure. The residue was purified by flash chromatography (C18; MeCN : H_2O) yielding 33.9 mg (54%) of the desired product.

^{1}H NMR (500 MHz, DMSO-d_6): δ = 12.75 (s, 1 H), 10.51 (s, 1 H), 8.24 (s, 1 H), 8.08 (d, *J* = 2.1 Hz, 1 H), 7.87 (dd, *J* = 8.6, 2.1 Hz, 1 H), 7.42 (d, *J* = 8.6 Hz, 1 H), 7.40 (d, *J* = 8.6 Hz, 1 H), 7.08 (dd, *J* = 2.6, 0.4 Hz, 1 H), 6.89 (ddd, 8.6, 2.6, 0.4 Hz, 1 H), 2.22 (s, 3 H) ppm.

^{13}C NMR (125 MHz, DMSO-d_6): δ = 154.84, 153.88, 138.19, 137.16, 135.35, 133.51, 132.81, 131.02, 128.37, 127.56, 122.19, 119.14, 118.88, 116.89, 22.59 ppm.

HRMS (ESI) calcd. for $C_{30}H_{25}Br_2N_6O_6S_2$ $[2M+H]^+$: *m/z* = 788.9623, found: 788.9613.

N-*(4-(tert-Butyl)phenyl)-2-oxo-1,2-dihydroquinoxaline-6-sulfonamide (S9)*

To a stirred solution of 4-(*tert*-butyl)aniline (23.6 mg, 0.16 mmol) in pyridine (0.6 ml) was added 2-oxo-1,2-dihydroquinoxaline-6-sulfonyl chloride (30 mg, 0.12 mmol) at r. t.. The resulting reaction mixture was stirred for 16 h at r. t. and concentrated under reduced pressure. The residue was purified by flash chromatography (C18; MeCN : H_2O) yielding 34.2 mg (60%) of the desired product.

^{1}H NMR (500 MHz, DMSO-d_6): δ = 8.23 (s, 1 H), 8.08 (d, *J* = 2.1 Hz, 1 H), 7.87 (dd, *J* = 8.6, 2.1 Hz, 1 H), 7.39 (d, *J* = 8.6 Hz, 1 H), 7.24 (d, *J* = 8.9 Hz, 2 H), 7.02 (d, *J* = 8.9 Hz, 2 H), 1.18 (s, 9 H) ppm.

^{13}C NMR (125 MHz, DMSO-d_6): δ = 154.94, 153.76, 146.52, 135.27, 134.87, 134.11, 131.05, 128.34, 127.48, 125.97, 119.93, 116.86, 33.98, 31.08 ppm.

HRMS (ESI) calcd. for $C_{36}H_{39}N_6O_6S_2$ $[2M+H]^+$: *m/z* = 715.2372, found: 715.2367.

N-*(4-chlorophenyl)-2-oxo-1,2-dihydroquinoxaline-6-sulfonamide (S15)*

To a stirred solution of 4-chloroaniline (20.3 mg, 0.16 mmol) in pyridine (0.6 ml) was added 2-oxo-1,2-dihydroquinoxaline-6-sulfonyl chloride (30 mg, 0.12 mmol) at r. t.. The resulting reaction mixture was stirred for 16 h at r. t. and concentrated under reduced pressure. The residue was purified by flash chromatography (C18; MeCN : H_2O) yielding 34.0 mg (64%) of the desired product.

^{1}H NMR (500 MHz, DMSO-d_6): δ = 13.10 – 12.01 (br. s, 1 H), 11.00 – 10.06 (br. s, 1 H), 8.24 (s, 1 H), 8.07 (d, *J* = 2.1 Hz, 1 H), 7.85 (dd, *J* = 8.6, 2.1 Hz, 1 H), 7.39 (d, *J* = 8.6 Hz, 1 H), 7.30 (d, *J* = 9.0 Hz, 2 H), 7.12 (d, *J* = 9.0 Hz, 2 H) ppm.

^{13}C NMR (125 MHz, DMSO-d_6): δ = 154.84, 153.89, 136.62, 135.36, 133.43, 131.01, 129.26, 128.34, 128.26, 127.57, 121.67, 116.89 ppm.

HRMS (ESI) calcd. for $C_{28}H_{21}Cl_2N_6O_6S_2$ $[2M+H]^+$: *m/z* = 671.0341, found: 671.0341.

7-Methyl-1,5-dihydro-2H-benzo[b][1,4]diazepine-2,4(3H)-dione (S26)

4-Methylbenzene-1,2-diamine (2.5 g, 20 mmol) was added to a mixture of malonic acid (1 g, 10 mmol) and aq. HCl (10 ml, 4 n, 40 mmol). The reaction mixture was stirred for 3 h at 125-130 °C (oil bath temperature), cooled down to r. t. and filtered. The product was dried in vacuo yielding 790 mg (42%) of the desired product (**S26**).

^{1}H NMR (500 MHz, DMSO-d_6): δ = 10.32 (s, 1 H), 10.28 (s, 1 H), 7.03 – 6.95 (m, 2 H), 6.91 (s, 1 H), 3.14 (s, 2 H), 2.26 (s, 3 H) ppm.

8-Methyl-2,4-dioxo-2,3,4,5-tetrahydro-1H-benzo[b][1,4]diazepine-7-sulfonyl chloride (S27)

A mixture of 7-methyl-1,5-dihydro-2H-benzo[*b*][1,4]diazepine-2,4(3*H*)-dione (**S26**) (790 mg, 4.2 mmol) and chlorosulfonic acid (5 ml) was stirred for 3 h at 110 °C. Then it was poured onto ice and the product was filtrated and dried under reduced pressure. The product was used without further characterization. Yield: 380 mg (31%).

7-Methyl-2,4-dioxo-1,2,3,4-tetrahydroquinazoline-6-sulfonyl chloride (S28)

7-Methyl-2,4-dioxo-1,2,3,4-tetrahydroquinazoline-6-sulfonyl chloride (**S28**) was synthesized according to Kuryazov et al.[67] 7-Methylquinazoline-2,4(1*H*,3*H*)-dione (1 g, 5.7 mmol) was added portion wise with stirring to chlorosulfonic acid (5 ml) cooled to 5-10 °C at such a rate that the reaction temperature did not exceed 15 °C. The reaction mixture was heated to 60 °C, held at this temperature for 6 h, and poured into crushed ice. The precipitate formed was filtered off, washed with water, and dried under reduced pressure. Yield: 920 mg (59%).

^{1}H NMR (500 MHz, DMSO-d_6): δ = 11.19 (s, 1 H), 11.11 (s, 1 H), 8.23 (s, 1 H), 6.90 (s, 1 H), 2.56 (s, 3 H) ppm.

General Procedure 1 (GP1) for Sulfochlorination of Substituted 1,4-Dihydro-quinoxaline-2,3-diones

Chlorosulfonic acid (13 ml, 23.2 g, 200 mmol) was added to the substituted 1,4-dihydro-quinoxaline-2,3-dione (20 mmol) and the reaction mixture was stirred at 115 °C for 3 h, cooled to r. t. and poured onto ice. The precipitate was filtered and washed with ice water. The product was dried in vacuo to yield the desired product that was used for the next step without further purification.

2,3-Dioxo-1,2,3,4-tetrahydroquinoxaline-6-sulfonyl chloride (S29)

2,3-Dioxo-1,2,3,4-tetrahydroquinoxaline-6-sulfonyl chloride (**S29**) was synthesized according to GP1 starting from chlorosulfonic acid (13 ml, 23.2 g, 200 mmol) and 1,4-dihydroquinoxaline-2,3-dione (3.2 g, 20 mmol). Yield: 4.5 g (87%). The ^{1}H NMR spectrum of this compound is in accordance with the published data.[68]

7-Methyl-2,3-dioxo-1,2,3,4-tetrahydroquinoxaline-6-sulfonyl chloride (S30)

7-Methyl-2,3-dioxo-1,2,3,4-tetrahydroquinoxaline-6-sulfonyl chloride (**S30**) was synthesized according to GP1 starting from chlorosulfonic acid (10 ml, 17.5 g, 150 mmol) and 6-methyl-1,4-dihydro-quinoxaline-2,3-dione (2 g, 11 mmol). Yield: 2.8 g (90%).

^{1}H NMR (500 MHz, DMSO-d_6): δ = 11.87 (s, 1 H), 11.81 (s, 1 H), 7.61 (s, 1H), 6.85 (s, 1 H), 2.46 (s, 3 H) ppm.

General Procedure 2 (GP2) for Synthesis of Substituted Sulfonamides

Substituted sulfonyl chloride (3.6 mmol) was added to a solution of aniline (4.0 mmol) in pyridine (5 ml) at r. t. The reaction mixture was stirred for 2.5 h at r. t. and concentrated under reduced pressure. The residue was purified by column chromatography (first column: normal phase silica, CH_2Cl_2 : MeOH = 97 : 3 to 91 : 9, second column: C18 silica, MeCN : H_2O) yielding the desired product.

8-Methyl-2,4-dioxo-N-(4-(trifluoromethoxy)phenyl)-2,3,4,5-tetrahydro-1H-benzo[b][1,4]diazepine-7-sulfonamide (S17)

8-methyl-2,4-dioxo-*N*-(4-(trifluoromethoxy)phenyl)-2,3,4,5-tetrahydro-1*H*-benzo[*b*][1,4]diazepine-7-sulfonamide was obtained according to GP2 from 8-methyl-2,4-dioxo-2,3,4,5-tetrahydro-1*H*-benzo[*b*][1,4]diazepine-7-sulfonyl chloride (**S27**) (370 mg, 1.3 mmol) and 4-(trifluoromethoxy)aniline (227 mg, 1.3 mmol) in pyridine (5 ml). The product was purified by column chromatography (normal phase, CH_2Cl_2 : MeOH = 97: 3 to 91 : 9) and then RP (C18 : H_2O: MeCN). Yield: 139 mg (25%).

^{1}H NMR (500 MHz, DMSO-d_6): δ = 10.71 (s, 1 H), 10.65 (s, 1 H), 10.52 (s, 1 H), 7.76 (s, 1 H), 7.24 (d, *J* = 9.1 Hz, 2 H), 7.14 (d, *J* = 9.1 Hz, 2 H), 7.05 (s, 1 H), 3.22 (s, 2 H), 2.51 (s, 3 H) ppm.

^{13}C NMR (125 MHz, DMSO-d_6): δ = 165.59, 165.45, 143.94, 136.67, 133.20, 133.18, 132.71, 127.09, 125.35, 124.06, 122.14, 120.04, 120.02 (q, $J_{C\text{-}F}$ = 256 Hz), 45.25, 18.97 ppm.

^{19}F NMR (470 MHz, DMSO-d_6): δ = −57.16 ppm.

HRMS (ESI) calcd. for $C_{17}H_{15}F_3N_3O_5S$ $[M+H]^+$: *m/z* = 430.0685, found: 430.0679.

7-Methyl-2,4-dioxo-N-(4-(trifluoromethoxy)phenyl)-1,2,3,4-tetrahydroquinazoline-6-sulfonamide (7)

7-Methyl-2,4-dioxo-*N*-(4-(trifluoromethoxy)phenyl)-1,2,3,4-tetrahydroquinazoline-6-sulfonamide was obtained according to GP2 from 7-methyl-2,4-dioxo-1,2,3,4-tetrahydroquinazoline-6-sulfonyl chloride (**S28**) (275 mg, 1.0 mmol) and 4-(trifluoromethoxy) aniline (177 mg, 1.0 mmol) in pyridine (5 ml). The product was purified by column chromatography (first column: normal phase, CH_2Cl_2 : MeOH = 97: 3 to 91 : 9, second column: C18 silica, H_2O: MeCN). Yield: 233 mg (56%).

^{1}H NMR (500 MHz, DMSO-d_6): δ = 11.49 (s, 1 H), 11.45 (s, 1 H), 10.71 (s, 1 H), 8.34 (s, 1 H), 7.26 (d, *J* = 9.1 Hz, 2 H), 7.15 (d, *J* = 9.1 Hz, 2 H), 7.04 (s, 1 H), 2.60 (s, 3 H) ppm.

^{13}C NMR (125 MHz, DMSO-d_6): δ = 161.80, 150.20, 144.19, 143.96, 143.79, 136.58, 131.39, 129.23, 122.26, 120.45, 119.83 (q, $J_{C\text{-}F}$ = 255 Hz), 118.64, 112.11, 20.19 ppm.

^{19}F NMR (470 MHz, DMSO-d_6): δ = −57.16 ppm.

HRMS (ESI) calcd. for $C_{16}H_{13}F_3N_3O_5S$ $[M+H]^+$: *m/z* = 416.0528, found: 416.0523.

N-(4-(tert-Butyl)phenethyl)quinoxaline-6-sulfonamide (S13)

N-(4-(*tert*-Butyl)phenethyl)quinoxaline-6-sulfonamide was obtained according to GP2 from quinoxaline-6-sulfonyl chloride (20 mg, 0.09 mmol) and 2-(4-(*tert*-butyl)phenyl)ethan-1-amine (17 mg, 0.1 mmol) in pyridine (2 ml) for 30 min at r. t. H_2O was added and the mixture was extracted with EtOAc. The organic phase was washed with 2 N HCl, dried over $MgSO_4$, filtered and concentrated. A mixture of MeOH and H_2O (ca. 1 : 10) was added. The product was filtered and dried *in vacuo* yielding 14 mg (44%) of the desired product.

^{1}H NMR (500 MHz, DMSO-d_6): δ = 9.11 – 9.09 (m, 2 H), 8.45 (d, *J* = 2.0 Hz, 1 H), 8.29 (d, *J* = 8.8 Hz, 1 H), 8.13 (dd, *J* = 8.8, 2.0 Hz, 1 H), 8.09 (t, *J* = 5.7 Hz, 1 H), 7.22 (d, *J* = 8.3 Hz, 2 H), 7.05 (d, *J* = 8.3 Hz, 2 H), 3.07 – 3.00 (m, 2 H), 2.65 (t, *J* = 7.3 Hz, 2 H), 1.21 (s, 9 H) ppm.

^{13}C NMR (125 MHz, DMSO-d_6): δ = 148.49, 147.99, 147.48, 143.40, 141.47, 141.23, 135.42, 130.98, 128.33, 128.10, 126.68, 125.02, 44.09, 34.77, 34.06, 31.14 ppm.

HRMS (ESI) calcd. for $C_{20}H_{24}N_3O_2S$ $[M+H]^+$: *m/z* = 370.1589, found: 370.1583.

N-*(4-(tert-Butyl)phenethyl)-2-oxo-2,3-dihydro-1H-benzo[d]imidazole-5-sulfonamide (S14)*

N-(4-(*tert*-Butyl)phenethyl)-2-oxo-2,3-dihydro-1*H*-benzo[*d*]imidazole-5-sulfonamide was obtained according to GP2 from 2-oxo-2,3-dihydro-1*H*-benzo[*d*]imidazole-5-sulfonyl chloride (50 mg, 0.22 mmol) and 2-(4-(*tert*-butyl)phenyl)ethan-1-amine (46 mg, 0.26 mmol) in pyridine (3 ml) for 16 h at r. t. H_2O was added and the precipitate was filtered. The precipitate was washed with CH_2Cl_2 and dried *in vacuo* yielding 33.1 mg (41%) of the desired product.

^{1}H NMR (500 MHz, DMSO-d_6): δ = 11.10 (s, 1 H), 11.00 (s, 1 H), 7.52 (t, *J* = 5.8 Hz, 1 H), 7.39 (dd, *J* = 8.1, 1.7 Hz, 1 H), 7.30 (s, 1 H), 7.26 (d, *J* = 8.3 Hz, 2 H), 7.08 – 7.02 (m, 3 H), 2.90 – 2.83 (m, 2 H), 2.61 (t, *J* = 7.5 Hz, 2 H), 1.24 (s, 9 H) ppm.

^{13}C NMR (125 MHz, DMSO-d_6): δ = 155.35, 148.47, 135.68, 132.92, 132.01, 129.68, 128.29, 125.06, 120.03, 108.19, 106.65, 44.22, 34.66, 34.08, 31.17 ppm.

HRMS (ESI) calcd. for $C_{38}H_{47}N_6O_6S_2$ $[2M+H]^+$: *m/z* = 747.2998, found: 747.2996.

2,3-Dioxo-N-(4-(trifluoromethoxy)phenyl)-1,2,3,4-tetrahydroquinoxaline-6-sulfonamide (S2)

2,3-Dioxo-*N*-(4-(trifluoromethoxy)phenyl)-1,2,3,4-tetrahydroquinoxaline-6-sulfonamide was obtained according to GP2 from 2,3-dioxo-1,2,3,4-tetrahydroquinoxaline-6-sulfonyl chloride (**S29**) (100 mg, 0.4 mmol) and 4-(trifluoromethoxy)aniline (75 mg, 0.4 mmol) in pyridine for 18 h at r. t. The reaction mixture was dissolved in MeOH, and HCl (2 M) was added. MeOH was evaporated under reduced pressure. The formed precipitate was filtered and the filter cake was washed with H_2O (2x), and cyclohexane. The product was dried under *in vacuo* yielding 36.4 mg (24%) of the desired product.

^{1}H NMR (500 MHz, DMSO-d_6): δ = 12.17 (s, 1 H), 12.09 (s, 1 H), 10.58 (s, 1 H), 7.52 (d, *J* = 2.0 Hz, 1 H), 7.45 (dd, *J* = 8.4, 2.0 Hz, 1 H), 7.26 (d, *J* = 8.5 Hz, 2 H), 7.19 (d, *J* = 8.4 Hz, 1 H), 7.16 (d, *J* = 8.5 Hz, 2 H) ppm.

^{13}C NMR (125 MHz, DMSO-d_6): δ = 155.18, 154.93, 144.32, 129.50, 125.97, 122.15, 121.47, 121.23, 121.05, 119.01, 115.55, 113.60 ppm.

HRMS (ESI) calcd. for $C_{15}H_{10}F_3N_3NaO_5S$ $[M+Na]^+$: *m/z* = 424.0191, found: 424.0195.

2,3-Dioxo-N-(4-propylphenyl)-1,2,3,4-tetrahydroquinoxaline-6-sulfonamide (S1)

2,3-Dioxo-*N*-(4-propylphenyl)-1,2,3,4-tetrahydroquinoxaline-6-sulfonamide was obtained according to GP2 from 2,3-dioxo-1,2,3,4-tetrahydroquinoxaline-6-sulfonyl chloride (**S29**) (20 mg, 0.077 mmol) and 4-propylaniline (11 mg, 0.084 mmol) in pyridine (300 μL) for 2 h at r. t. The reaction mixture was diluted with H_2O and extracted with EtOAc (3x). The combined organic phases were dried over Na_2SO_4, filtered and concentrated under reduced pressure. The crude product was purified by column chromatography (C18; MeCN : H_2O + 0.05% HCOOH). The product containing fractions were lyophilized yielding 10.8 mg (39%) of the desired product.

^{1}H NMR (500 MHz, DMSO-d_6): δ = 12.59 – 9.93 (br m, 3 H), 7.51 (d, *J* = 1.9 Hz, 1 H), 7.41 (dd, *J* = 8.4, 1.9 Hz, 1 H), 7.17 (d, *J* = 8.4 Hz, 1 H), 7.03 (d, *J* = 8.4 Hz, 2 H), 6.96 (d, *J* = 8.4 Hz, 2 H), 2.42 (t, *J* = 7.4 Hz, 2 H) 1.49 (sextet, *J* = 7.4 Hz, 2 H), 0.82 (t, *J* = 7.4 Hz, 3 H) ppm.

^{13}C NMR (125 MHz, DMSO-d_6): δ = 155.38, 155.11, 137.80, 135.50, 133.76, 129.40, 128.94, 125.92, 121.42, 120.40, 115.55, 113.81, 36.52, 24.02, 13.62 ppm.

N-*(4-(tert-Butyl)phenethyl)-2,3-dioxo-1,2,3,4-tetrahydroquinoxaline-6-sulfonamide (4)*

N-(4-(*tert*-Butyl)phenethyl)-2,3-dioxo-1,2,3,4-tetrahydroquinoxaline-6-sulfonamide was obtained according to GP2 from 2,3-dioxo-1,2,3,4-tetrahydroquinoxaline-6-sulfonyl chloride (**S29**) (30 mg, 0.12 mmol) and 2-(4-(*tert*-butyl)phenyl)ethan-1-amine (23 mg, 0.13 mmol) in pyridine (600 μL) for 30 min at r. t. Some drops of H_2O were added and volatiles were removed under reduced pressure. The residue was purified by flash chromatography (silica; CH_2Cl_2 : MeOH = 100 : 0 to 90 : 10) yielding 20.6 mg (43%) of the desired product as a white powder.

^{1}H NMR (500 MHz, DMSO-d_6): δ = 12.19 (s, 1 H), 12.09 (s, 1 H), 7.72 (t, *J* = 5.8 Hz, 1 H), 7.54 (d, *J* = 2.0 Hz, 1 H), 7.47 (dd, *J* = 8.4, 2.0 Hz, 1 H), 7.27 (d, *J* = 8.3 Hz, 2 H), 7.23 (d, *J* = 8.4 Hz, 1 H), 7.07 (d, *J* = 8.3 Hz, 2 H), 2.95 – 2.88 (m, 2 H), 2.63 (t, *J* = 7.6 Hz, 2 H), 1.24 (s, 9 H) ppm.

^{13}C NMR (125 MHz, DMSO-d_6): δ = 155.23, 155.01, 148.53, 135.58, 134.35, 128.89, 128.32, 125.82, 125.07, 121.34, 115.52, 113.63, 44.20, 34.71, 34.09, 31.17 ppm.

N-*(4-Isopropylphenyl)-2,3-dioxo-1,2,3,4-tetrahydroquinoxaline-6-sulfonamide (10)*

N-(4-Isopropylphenyl)-2,3-dioxo-1,2,3,4-tetrahydroquinoxaline-6-sulfonamide was obtained according to GP2 from 2,3-dioxo-1,2,3,4-tetrahydroquinoxaline-6-sulfonyl chloride (**S29**) (30 mg, 0.12 mmol) and 4-isopropylaniline (17 mg, 0.13 mmol) in pyridine (600 μL) for 30 min at r. t. Some drops of H_2O were added and volatiles were removed under reduced pressure. The residue was purified by flash chromatography (silica; CH_2Cl_2 : MeOH = 100 : 0 to 90 : 10) yielding 19.6 mg (45%).

^{1}H NMR (500 MHz, DMSO-d_6): δ = 12.28 – 11.95 (br. s, 2 H), 10.37 – 10.04 (br. s, 1 H), 7.52 (d, *J* = 2.0 Hz, 1 H), 7.44 (dd, *J* = 8.5, 2.0 Hz, 1 H), 7.19 (d, *J* = 8.5 Hz, 1 H), 7.09 (d, *J* = 8.5 Hz, 2 H), 6.97 (d, *J* = 8.5 Hz, 2 H), 2.77 (sept, *J* = 6.9 Hz, 1 H), 1.11 (d, *J* = 6.9 Hz, 6 H) ppm.

^{13}C NMR (125 MHz, DMSO-d_6): δ = 155.19, 154.95, 144.12, 135.23, 133.75, 129.25, 126.96, 125.84, 121.48, 120.28, 115.50, 113.70, 32.70, 23.82 ppm.

N-*(4-(tert-Butyl)phenyl)-2,3-dioxo-1,2,3,4-tetrahydroquinoxaline-6-sulfonamide (5)*

N-(4-(*tert*-Butyl)phenyl)-2,3-dioxo-1,2,3,4-tetrahydroquinoxaline-6-sulfonamide was obtained according to GP2 from 2,3-dioxo-1,2,3,4-tetrahydroquinoxaline-6-sulfonyl chloride (**S29**) (30 mg, 0.12 mmol) and 4-(*tert*-butyl)aniline (19 mg, 0.13 mmol) in pyridine

(600 μL) for 30 min at r. t. Some drops of H_2O were added and volatiles were removed under reduced pressure. The residue was purified by flash chromatography (silica; CH_2Cl_2 : MeOH = 100 : 0 to 90 : 10) yielding 27.5 mg (64%).

^{1}H NMR (500 MHz, DMSO-d_6): δ = 12.20 – 12.03 (br. s, 2 H), 10.30 – 10.16 (br. s, 1 H), 7.54 (d, J = 2.0 Hz, 1 H), 7.46 (dd, J = 8.5, 2.0 Hz, 1 H), 7.24 (d, J = 8.9 Hz, 2 H), 7.19 (d, J = 8.5 Hz, 1 H), 6.99 (d, J = 8.9 Hz, 2 H), 1.19 (s, 9 H) ppm.

^{13}C NMR (125 MHz, DMSO-d_6): δ = 155.19, 154.95, 146.32, 134.94, 133.84, 129.26, 125.89, 125.86, 121.47, 119.78, 115.52, 113.68, 33.98, 31.10 ppm.

N-*(4-(tert-Butyl)benzyl)-2,3-dioxo-1,2,3,4-tetrahydroquinoxaline-6-sulfonamide (17)*

N-(4-(*tert*-Butyl)benzyl)-2,3-dioxo-1,2,3,4-tetrahydroquinoxaline-6-sulfonamide was obtained according to GP2 from 2,3-dioxo-1,2,3,4-tetrahydroquinoxaline-6-sulfonyl chloride (**S29**) (30 mg, 0.12 mmol) and (4-(*tert*-butyl)phenyl)methanamine (20.7 mg, 0.13 mmol) in pyridine (600 μL) for 1.5 h at r. t. Volatiles were removed under reduced pressure. The residue was purified by flash chromatography (C18; MeCN : H_2O). The product containing fractions were lyophilized yielding 19.1 mg (43%).

^{1}H NMR (500 MHz, DMSO-d_6): δ = 12.08 (s, 2 H), 8.13 (s, 1 H), 7.49 (d, J = 2.0 Hz, 1 H), 7.44 (dd, J = 8.4, 2.0 Hz, 1 H), 7.24 (d, J = 8.4 Hz, 2 H), 7.18 (d, J = 8.4 Hz, 1 H), 7.10 (d, J = 8.4 Hz, 2 H), 3.93 (d, J = 4.2 Hz, 2 H), 1.21 (s, 9 H) ppm.

^{13}C NMR (125 MHz, DMSO-d_6): δ = 155.21, 154.98, 149.53, 134.87, 134.27, 128.68, 127.45, 125.58, 124.84, 121.34, 115.42, 113.79, 45.92, 34.14, 31.10 ppm.

HRMS (ESI) calcd. for $C_{19}H_{21}N_3NaO_4S$ $[M+Na]^+$: m/z = 410.1150, found: 410.1145.

N-*(4-Isopropylphenyl)*-N,*7-dimethyl-2,3-dioxo-1,2,3,4-tetrahydroquinoxaline-6-sulfonamide (6)

N-(4-Isopropylphenyl)-*N*,7-dimethyl-2,3-dioxo-1,2,3,4-tetrahydroquinoxaline-6-sulfonamide was obtained according to GP2 from 7-methyl-2,3-dioxo-1,2,3,4-tetrahydroquinoxaline-6-sulfonyl chloride (**S30**) (30 mg, 0.11 mmol) and 4-isopropyl-*N*-methylaniline hydrochloride (20.7 mg, 0.11 mmol) in pyridine (0.5 ml) for 10 min at r. t. H_2O was added, and the mixture was extracted with EtOAc. The combined organic phases were dried over Na_2SO_4, filtered and concentrated under reduced pressure. The residue was purified by flash chromatography (C18; MeCN : H_2O). The product containing fractions were lyophilized yielding 20.5 mg (47%).

^{1}H NMR (500 MHz, DMSO-d_6): δ = 12.22 – 11.86 (br. s, 2 H), 7.61 (s, 1 H), 7.22 (d, J = 8.4 Hz, 2 H), 7.09 (d, J = 8.4 Hz, 2 H), 6.98 (s, 1 H), 3.12 (s, 3 H), 2.87 (sept, J = 6.9 Hz, 1 H), 2.07 (s, 3 H), 1.17 (d, J = 6.9 Hz, 6 H) ppm.

^{13}C NMR (125 MHz, DMSO-d_6): δ = 155.45, 154.74, 147.62, 138.58, 132.04, 129.36, 129.28, 126.85, 126.45, 123.66, 118.20, 117.01, 38.15, 32.98, 23.81, 19.50 ppm.

HRMS (ESI) calcd. for $C_{19}H_{21}N_3NaO_4S$ $[M+Na]^+$: m/z = 410.1150, found: 410.1155.

N-*(4-(tert-Butyl)phenyl)-7-methyl-2,3-dioxo-1,2,3,4-tetrahydroquinoxaline-6-sulfonamide (11)*

N-(4-(*tert*-Butyl)phenyl)-7-methyl-2,3-dioxo-1,2,3,4-tetrahydroquinoxaline-6-sulfonamide was obtained according to GP2 from 7-methyl-2,3-dioxo-1,2,3,4-tetrahydroquinoxaline-6-sulfonyl chloride (**S30**) (275 mg, 1 mmol) and 4-(*tert*-butyl)aniline (223 mg, 1.5 mmol) in pyridine (5 ml). The reaction mixture was stirred for 4 h at r. t. 2 N HCl was added and the formed precipitate was filtered, washed with H_2O (3 times) and dried *in vacuo* yielding 174 mg (45%). An analytical sample of the product was additionally purified by HPLC (C18; H_2O : MeCN + 0.1% HCOOH).

^{1}H NMR (500 MHz, DMSO-d_6): δ = 12.09 (s, 1 H), 11.94 (s, 1 H), 10.31 (s, 1 H), 7.73 (s, 1 H), 7.23 (d, J = 8.9 Hz, 2 H), 6.99 (s, 1 H), 6.97 (d, J = 8.9 Hz, 2 H), 2.51 (s, 3 H), 1.18 (s, 9 H) ppm.

^{13}C NMR (125 MHz, DMSO-d_6): δ = 155.41, 154.79, 145.94, 134.79, 132.00, 131.23, 129.12, 125.91, 123.47, 118.88, 118.13, 116.72, 33.95, 31.09, 19.26 ppm.

HRMS (ESI) calcd. for $C_{19}H_{22}N_3O_4S$ $[M+H]^+$: m/z = 388.1331, found: 388.1326.

7-Methyl-2,3-dioxo*-N-*(4-(trifluoromethoxy)phenyl)-1,2,3,4-tetrahydroquinoxaline-6-sulfonamide (H831)

7-Methyl-2,3-dioxo-*N*-(4-(trifluoromethoxy)phenyl)-1,2,3,4-tetrahydroquinoxaline-6-sulfonamide was obtained according to GP2 from 7-methyl-2,3-dioxo-1,2,3,4-tetrahydroquinoxaline-6-sulfonyl chloride (**S30**) (1 g, 3.6 mmol) and 4-(trifluoromethoxy)aniline (0.7 g, 4.0 mmol) in pyridine (5 ml). Column chromatography (first column: normal phase silica, CH_2Cl_2 : MeOH = 97 : 3 to 91 : 9, second column: C18 silica, MeCN : H_2O) yielded 620 mg (41%) of the desired product. R_f = 0.40 (CH_2Cl_2 : MeOH = 10 : 1).

^{1}H NMR (500 MHz, DMSO-d_6): δ = 12.08 (s, 1 H), 11.92 (s, 1 H), 10.62 (s, 1 H), 7.73 (s, 1 H), 7.25 (d, J = 9.1 Hz, 2 H), 7.14 (d, J = 9.1 Hz, 2 H), 7.02 (s, 1 H), 2.51 (s, 3 H) ppm.

^{13}C NMR (125 MHz, DMSO-d_6): δ = 155.31, 154.68, 144.02, 136.75, 131.45, 131.18, 129.26, 123.50, 122.09, 122.02 (q, J_{C-F} = 256 Hz), 120.34, 118.18, 116.60, 19.18 ppm.

^{19}F NMR (470 MHz, DMSO-d_6): δ = −57.09 ppm.

HRMS (ESI) calcd. for $C_{16}H_{13}F_3N_3O_5S$ $[M+H]^+$: m/z = 416.0528, found: 416.0523.

N-*(2-chloro-4′-fluoro-[1,1′-biphenyl]-4-yl)-7-methyl-2,3-dioxo-1,2,3,4-tetrahydroquinoxaline-6-sulfonamide (H052)*

N-(2-chloro-4′-fluoro-[1,1′-biphenyl]-4-yl)-7-methyl-2,3-dioxo-1,2,3,4-tetrahydroquinoxaline-6-sulfonamide was obtained according to GP2 from 2-chloro-4′-fluoro-[1,1′-biphenyl]-4-amine (230 mg, 1.04 mmol) and 7-methyl-2,3-dioxo-1,2,3,4-tetrahydroquinoxaline-6-sulfonyl chloride (**S30**) (411 mg, 1.5 mmol) in pyridine (5 ml). The product was purified by column chromatography (C18 silica, MeCN : H_2O). Yield: 185 mg (39%).

^{1}H NMR (500 MHz, DMSO-d_6): δ = 12.11 (s, 1 H), 11.98 (s, 1 H), 10.84 (s, 1 H), 7.80 (s, 1 H), 7.38 (dd, J = 8.9, 5.5 Hz, 2 H), 7.29 (d, J = 8.5 Hz, 1 H), 7.26 – 7.22 (m, 3 H), 7.09 (dd, J = 8.4, 2.2 Hz, 1 H), 7.03 (s, 1 H), 2.55 (s, 3 H) ppm.

^{13}C NMR (125 MHz, DMSO-d_6): δ = 162.31, 160.92, 155.37, 154.73, 134.33, 133.42, 132.18, 131.65, 131.31, 131.26, 131.25, 129.45, 123.58, 118.79, 118.31, 117.11, 116.66, 115.04 (d, J_{C-F} = 23 Hz), 19.24 ppm.

HRMS (ESI) calcd. for $C_{21}H_{16}ClFN_3O_4S$ $[M+H]^+$: m/z = 460.0534, found: 460.0539.

2,3-Dimethoxy-6-methylquinoxaline (S31)

2,3-Dimethoxy-6-methylquinoxaline (**S31**) was obtained according to Krishnan et al.[69] A mixture of 2,3-dichloro-6-methylquinoxaline (3 g, 14 mmol), K_2CO_3 (3.9 g, 28 mmol) and benzyltriethylammoniumchloride (413 mg, 1.8 mmol) in methanol (30 ml) was heated under reflux for 4 h. The solvent was removed under reduced pressure, and the residue was stirred with water. The precipitate was filtrated, dried under reduced pressure. Yield: 2.8 g (98%).

^{1}H NMR (700 MHz, $CDCl_3$): δ = 7.66 (d, J = 8.3 Hz, 1 H), 7.57 (s, 1 H), 7.32 (dd, J = 8.3, 2.0 Hz, 1 H), 4.15 (s, 3 H), 4.14 (s, 3 H), 2.50 (s, 3 H) ppm.

6-(Bromomethyl)-2,3-dimethoxyquinoxaline (S32)

6-(Bromomethyl)-2,3-dimethoxyquinoxaline (**S32**) was obtained in close analogy to Loriga et al.[70] A mixture of 2,3-dimethoxy-6-methylquinoxaline (2.8 g, 13.7 mmol), *N*-bromosuccinimide (2.7 g, 15.1 mmol) and benzoyl peroxide (350 mg, with 25% H_2O) in absolute $CHCl_3$ without stabilizer (90 ml) was heated under reflux for 16 h. On cooling, volatiles were removed under reduced pressure and the residue was purified by column chromatography (petroleum ether: ethyl acetate = 97: 3 to 50: 50). Yield: 2.78 g (72%).

^{1}H NMR (700 MHz, $CDCl_3$): δ = 7.80 (d, J = 2.0 Hz, 1 H), 7.75 (d, J = 8.4 Hz, 1 H), 7.52 (dd, J = 8.4, 2.0 Hz, 1 H), 4.65 (s, 2 H), 4.16 (s, 3 H), 4.15 (s, 3 H) ppm.

((2,3-Dimethoxyquinoxalin-6-yl)methyl)triphenylphosphonium bromide (S33)

A mixture of 6-(bromomethyl)-2,3-dimethoxyquinoxaline (**S32**) (2.8 g, 9.8 mmol) and triphenyl phosphine (2.6 g, 9.8 mmol) in toluene (20 ml) was heated at reflux for 4 h. After cooling, the solid was collected by filtration, washed with toluene and dried under vacuum at 50 °C to give the desired compound. Yield: 4.1 g.

^{1}H NMR (700 MHz, DMSO-d_6): δ = 7.93 – 7.89 (m, 3 H), 7.77 – 7.68 (m, 12 H), 7.58 (d, J = 8.4 Hz, 1 H), 7.43 (t, J = 2.0 Hz, 1 H), 7.05 (dt, J = 8.4, 2.0 Hz, 1 H), 5.35 (d, $J_{P\text{-}H}$ = 15.6 Hz, 2 H), 4.01 (s, 3 H), 3.96 (s, 3 H) ppm.

2,3-Dimethoxy-6-(methyl-d_3)quinoxaline (S34)

2,3-Dimethoxy-6-(methyl-d_3)quinoxaline (**S34**) was obtained using a modified procedure by Schlosser.[71,72] To a solution of ((2,3-dimethoxyquinoxalin-6-yl)methyl)triphenylphosphonium bromide (**S33**) (4.1 g, 7.5 mmol) in THF (20 ml) was added a solution of NaOD in D_2O (10 ml, 40 w/w %). The reaction mixture was stirred at 25 °C for 18 h. EtOAc and water were added to the reaction mixture. The EtOAc layer was separated, dried over Na_2SO_4 and concentrated under reduced pressure. The residue was separated by column chromatography (PE: EtOAc = 100: 0 to 97: 3). Yield: 1.08 g (69%).

^{1}H NMR (700 MHz, $CDCl_3$): δ = 7.67 (d, J = 8.3 Hz, 1 H), 7.58 (d, J = 2.0 Hz, 1 H), 7.32 (dd, J = 8.3, 2.0 Hz, 1 H), 4.15 (s, 3 H), 4.14 (s, 3 H) ppm.

^{13}C NMR (175 MHz, $CDCl_3$): δ = 149.93, 149.45, 137.12, 136.61, 135.19, 128.39, 125.96, 54.10, 54.09, 20.57 (h, $J_{C\text{-}D}$ = 18 Hz) ppm.

MS (ESI) calcd. for $C_{11}H_{10}D_3N_2O_2$ $[M+H]^+$: m/z = 208, found: 208.

6-(Methyl-d_3)-1,4-dihydroquinoxaline-2,3-dione (S35)

To a solution of 2,3-dimethoxy-6-(methyl-d_3)quinoxaline (**S34**) (1.08 g, 5.2 mmol) in dioxane (15 ml) was added 2 m HCl (15 ml), and the reaction mixture was heated at 80 °C for 16 h. The reaction mixture was allowed to cool down to r. t. and dioxane was evaporated under reduced pressure. The formed precipitate was filtered off, washed with water and dried in vacuo. Yield: 847 mg (90%).

^{1}H NMR (700 MHz, DMSO-d_6): δ = 11.85 (s, 1 H), 11.83 (s, 1 H), 7.00 (d, J = 8.5 Hz, 1 H), 6.91 (s, 1 H), 6.89 (d, J = 8.5 Hz, 1 H).

^{13}C NMR (175 MHz, DMSO-d_6): δ = 155.29, 154.98, 132.16, 125.45, 123.77, 123.30, 115.14, 114.97, 19.71 (h, $J_{C\text{-}D}$ = 18 Hz) ppm.

MS (ESI) calcd. for $C_9H_6D_3N_2O_2$ $[M+H]^+$: m/z = 180, found: 180.

7-(Methyl-d_3)-2,3-dioxo-1,2,3,4-tetrahydroquinoxaline-6-sulfonyl chloride (S36)

7-(Methyl-d_3)-2,3-dioxo-1,2,3,4-tetrahydroquinoxaline-6-sulfonyl chloride (**S36**) was synthesized according to GP1 starting from 6-(methyl-d_3)-1,4-dihydroquinoxaline-2,3-dione (**S35**) (840 mg, 4.69 mmol) in HSO_3Cl (5 ml). Yield: 1 g (77%). The compound was used for the next step without further characterization.

7-(Methyl-d_3)-2,3-dioxo-N-(4-(trifluoromethoxy)phenyl)-1,2,3,4-tetrahydroquinoxaline-6-sulfonamide (S4)

7-(Methyl-d_3)-2,3-dioxo-*N*-(4-(trifluoromethoxy)phenyl)-1,2,3,4-tetrahydroquinoxaline-6-sulfonamide was obtained according to GP2 from 7-(methyl-d_3)-2,3-dioxo-1,2,3,4-tetrahydroquinoxaline-6-sulfonyl chloride (**S36**) (100 mg, 0.36 mmol) and 4-(trifluoromethoxy) aniline (50 mg, 0.28 mmol) in pyridine (5 ml). The crude product was purified by column chromatography (C18; H_2O : MeCN) and then HPLC (H_2O : MeCN + 0.1% HCOOH)). Yield: 30 mg (26%) of the desired product.

^{1}H NMR (500 MHz, DMSO-d_6): δ = 12.12 (s, 1 H), 11.95 (s, 1 H), 10.68 (s, 1 H), 7.73 (s, 1 H), 7.26 (d, J = 9.1 Hz, 2 H), 7.13 (d, J = 9.1 Hz, 2 H), 7.00 (s, 1 H) ppm.

^{13}C NMR (175 MHz, DMSO-d_6): δ = 155.35, 154.72, 144.03, 136.72, 131.45, 131.08, 129.32, 123.54, 122.18, 120.28, 122.00 (q, $J_{C\text{-}F}$ = 258 Hz), 118.20, 116.61, 18.84 – 18.02 (m) ppm.

^{19}F NMR (470 MHz, DMSO-d_6): δ = −57.08 ppm.

HRMS (ESI) calcd. for $C_{16}H_{10}D_3F_3N_3O_5S$ $[M+H]^+$: m/z = 419.0716, found: 419.0711.

N-(2-chloro-4′-fluoro-[1,1′-biphenyl]-4-yl)-7-(methyl-d_3)-2,3-dioxo-1,2,3,4-tetrahydroquinoxaline-6-sulfonamide (S5)

N-(2-chloro-4′-fluoro-[1,1′-biphenyl]-4-yl)-7-(methyl-d_3)-2,3-dioxo-1,2,3,4-tetrahydroquinoxaline-6-sulfonamide was obtained according to GP2 from 2-chloro-4′-fluoro-[1,1′-biphenyl]-4-amine (50 mg, 0.23 mmol) and 7-(methyl-d_3)-2,3-dioxo-1,2,3,4-tetrahydroquinoxaline-6-sulfonyl chloride (**S36**) (100 mg, 0.36 mmol) in pyridine (5 mL). The crude product was purified by column chromatography (C18; H_2O : MeCN) and then HPLC (H_2O : MeCN + 0.1% HCOOH)). Yield: 27 mg (27%).

^{1}H NMR (700 MHz, DMSO-d_6): δ = 12.12 (s, 1 H), 11.98 (s, 1 H), 10.84 (s, 1 H), 7.80 (s, 1 H), 7.38 (dd, J = 9.0, 5.5 Hz, 2 H), 7.29 (d, J = 8.4 Hz, 1 H), 7.26 – 7.22 (m, 3 H), 7.09 (dd, J = 8.4, 2.3 Hz, 1 H), 7.03 (s, 1 H) ppm.

^{13}C NMR (175 MHz, DMSO-d_6): δ = 162.32, 160.93, 155.38, 154.74, 138.16, 134.33 (d, $J_{c\text{-}F}$ = 3 Hz), 133.47, 132.17, 131.66, 131.31, 131.27, 131.15, 129.46, 123.60, 118.80, 118.32, 117.10, 116.65, 115.05, (d, $J_{c\text{-}F}$ = 20 Hz), 18.84 – 18.02 (m) ppm.

^{19}F NMR (470 MHz, DMSO-d_6): δ = −114.55 ppm.

HRMS (ESI) calcd. for $C_{21}H_{13}D_3ClFN_3O_4S$ $[M+H]^+$: m/z = 463.0722, found: 463.0718.

Tert-butyl (4′-amino-2′-bromo-[1,1′-biphenyl]-4-yl)carbamate (S37)

3-Bromo-4-iodoaniline (801 mg, 2.69 mmol), (4-((*tert*-butoxycarbonyl)-amino)phenyl)-boronic acid (702 mg, 2.96 mmol) and tetrakis (triphenylphosphine)palladium(0) (311 mg, 269 μmol) were dissolved in toluene (10 mL) and ethanol (5 mL) under argon atmosphere. Sodium carbonate solution (5 mL, 1 m, 5 mmol) was added and the mixture was stirred for 13 h at 110 °C. The reaction mixture was cooled down to room temperature and deionized water (50 mL) was added. The mixture was extracted with ethyl acetate (3 x 120 mL). The combined organic layers were dried over sodium sulfate, filtrated and volatiles were removed under reduced pressure. The crude product was purified by flash chromatography (petroleum ether/acetone, 90:10 to 80:20). The product was obtained as a colorless solid (726 mg, 2.00 mmol, 74%).

^{1}H NMR (700 MHz, DMSO-d_6): δ = 9.36 (s, 1 H), 7.44 (d, ^3J = 8.6 Hz, 2 H), 7.19 (m_c, 2 H), 6.98 (d, ^3J = 8.3 Hz, 1 H), 6.87 (d, ^4J = 2.3 Hz, 1 H), 6.59 (dd, ^3J = 8.3 Hz, ^4J = 2.3 Hz, 1 H), 5.40 (br. s, 2 H), 1.48 (s, 9 H) ppm.

^{13}C NMR (175 MHz, measured as DEPTQ, DMSO-d_6): δ = 152.8, 149.2, 138.1, 134.7, 131.6, 129.6, 128.4, 122.0, 117.6, 117.2, 113.4, 79.0, 28.2 ppm.

HRMS (ESI) calcd. for $C_{17}H_20BrN_2O_2$ $[M+H]^+$: m/z = 363.0703, found:363.0704.

Tert-butyl (4′-amino-2′-((trimethylsilyl)ethynyl)-[1,1′-biphenyl]-4-yl)carbamate (S38)

Under argon atmosphere *tert*-butyl (4′-amino-2′-bromo-[1,1′-biphenyl]-4-yl)carbamate (**S37**) (408 mg, 1.12 mmol), sodium tetrachloropalladate (61.0 mg, 207 μmol), *tert*-butyldicyclohexylphosphonium tetrafluoroborate (140 mg, 409 μmol) and copper (I) iodide (39.8 mg, 209 μmol) were dissolved in dry diisopropylamine (10 mL). Trimethylsilyacetylene (1.10 g, 1.60 mL, 11.2 mmol) was added and the reaction mixture was stirred for 24 h at 80 °C. Volatiles were removed under reduce pressure. The crude was purified by column chromatography (petroleum ether/methyl tert-butyl ether, 80:20 to 70:30). The product was obtained as a brown solid (330 mg, 867 μmol, 77%).

^{1}H NMR (700 MHz, DMSO-d_6): δ = 9.33 (br. s, 1 H), 7.45-7.39 (m, 4 H), 7.07 (d, ^3J = 8.4 Hz, 1 H), 6.72 (d, ^4J = 2.4 Hz, 1 H), 6.64 (dd, ^3J = 8.4 Hz, ^4J = 2.4 Hz, 1 H), 5.26 (br. s, 2 H), 1.48 (s, 9 H), 0.13 (s, 9 H) ppm.

^{13}C NMR (175 MHz, DMSO-d_6): δ = 152.8, 147.5, 137.9, 133.7, 130.6, 129.9, 128.8, 120.1, 117.7, 117.3, 115.5, 106.3, 95.4, 79.0, 28.2, −0.22 ppm.

HRMS (ESI) calcd. for $C_{22}H_{29}N_2O_2Si$ $[M+H]^+$: m/z = 381.1993, found: 381.1993.

Tert-butyl (4′-((7-methyl-2,3-dioxo-1,2,3,4-tetrahydroquinoxaline)-6-sulfonamido)-2′-((trimethylsilyl)ethynyl)-[1,1′-biphenyl]-4-yl)carbamate (S39)

Under argon atmosphere *tert*-butyl (4′-amino-2′-((trimethylsilyl)ethynyl)-[1,1′-biphenyl]-4-yl)carbamate (**S38**) (250 mg, 657 μmol), 7-methyl-2,3-dioxo-1,2,3,4-tetrahydro-quinoxaline-6-sulfonyl chloride (**S30**) (203 mg, 739 μmol) and 4-dimethylaminopyridine (20.2 mg, 165 μmol) were dissolved in dry pyridine (5 mL). The reaction solution was stirred for 4 h at room temperature, additional 7-methyl-2,3-dioxo-1,2,3,4-tetrahydro-quinoxaline-6-sulfonyl chloride (**S30**) (220 mg, 801 μmol) was added to the reaction and stirred for 13 h at room temperature. To the reaction solution, deionized water (10 mL) was added and the pH value of the aqueous phase was adjusted to 5 with 1 m hydrochloric acid. It was extracted with ethyl acetate (3 x 80 mL), dried over sodium sulfate, filtrated and volatiles removed under reduced pressure. The crude product was purified by flash chromatography (acetonitrile/water) to obtain the product as a colorless solid (377 mg, 609 μmol, 93%).

^{1}H NMR (500 MHz, DMSO-d_6): δ = 12.10 (s, 1 H), 11.95 (s, 1 H), 10.60 (s, 1 H), 9.41 (s, 1 H), 7.76 (s, 1 H), 7.46 (d, ^3J = 8.6 Hz, 2 H), 7.40 (d, ^3J = 8.6 Hz, 2 H), 7.28 (d, ^3J = 8.2 Hz, 1 H), 7.18-7.11 (m, 2 H), 7.01 (s, 1 H), 2.54 (s, 3 H), 1.47 (s, 9 H), 0.12 (s, 9 H) ppm.

^{1}H NMR (500 MHz, MeCN-d_3): δ = 7.75 (s, 1 H), 7.45 (d, ^3J = 8.7 Hz, 2 H), 7.41 (d, ^3J = 8.7 Hz, 2 H), 7.25 (d, ^3J = 8.5 Hz, 1 H), 7.18 (d, ^4J = 2.3 Hz, 1 H), 7.14 (dd, ^3J = 8.5 Hz, ^4J = 2.3 Hz, 1 H), 7.04 (s, 1 H), 2.59 (s, 3 H), 1.48 (s, 9 H), 0.12 (s, 9 H) ppm.

^{13}C NMR (125 MHz, measured as DEPTQ, MeCN-d_3): δ = 156.2, 155.6, 154.0, 140.7, 139.9, 137.1, 134.2, 133.5, 133.0, 131.4, 130.6, 130.3, 125.1, 124.5, 122.5, 121.9, 119.5, 118.7, 118.1, 105.0, 99.1, 80.7, 28.6, 20.1, −0.3 ppm.

HRMS (ESI) calcd. for $C_{31}H_{35}N_4O_6SSi$ $[M+H]^+$: m/z = 619.2041, found: 619.2041.

N-(4′-amino-2-ethynyl-[1,1′-biphenyl]-4-yl)-7-methyl-2,3-dioxo-1,2,3,4-tetrahydroquinoxaline-6-sulfonamide hydrochloride (S40)

Tert-butyl (4′-((7-methyl-2,3-dioxo-1,2,3,4-tetrahydroquinoxaline)-6-sulfon-amido)-2′-((trimethylsilyl)-ethynyl)-[1,1′-biphenyl]-4-yl) carbamate (**S39**) (363 mg, 587 μmol) was dissolved in tetrahydrofuran (3 mL) and tetrabutylammonium fluoride solution in tetrahydrofuran (0.60 mL, 1 m, 600 μmol) was added. Excess tetrabutylammonium fluoride was removed by filtration through silica using a mixture of petroleum ether and acetone as eluent. The beige desilylated product (273 mg) was used in the next step by suspending it in a 4 m hydrochloric acid solution in dioxane (8 mL) and stirring for 2 h at room temperature. The solvent was removed under reduced pressure to yield the crude beige hydrochloride product (269 mg) which was used without any further purification.

MS (ESI) calcd. for $C_{23}H_{19}N_4O_4S$ $[M+H]^+$: m/z = 447, found: 447.

N-(4′-azido-2-ethynyl-[1,1′-biphenyl]-4-yl)-7-methyl-2,3-dioxo-1,2,3,4-tetrahydroquinoxaline-6-sulfonamide (15)

N-(4′-amino-2-ethynyl-[1,1′-biphenyl]-4-yl)-7-methyl-2,3-dioxo-1,2,3,4-tetra-hydroquin-oxaline-6-sulfonamide hydrochloride (**S40**) (115 mg, ca. 238 μmol) from the previous step was dissolved in acetic acid (4 mL, 90%) and cooled down to 0 °C. Sodium nitrite (88.4 mg, 1.28 mmol) was added portion wise and the mixture was stirred for 25 min at 0 °C. Sodium azide (78.7 mg, 1.21 mmol)

was added and the solution was stirred for 1 h at 0 °C. The solvent was removed under reduced pressure and the crude product was purified by flash chromatography (acetonitrile/water). The product was obtained as a colorless solid (86.2 mg, 182 μmol, 76%).

^{1}H NMR (700 MHz, DMSO-d_6): δ = 12.10 (s, 1 H), 11.97 (s, 1 H), 10.73 (s, 1 H), 7.79 (s, 1 H), 7.51 (m_c, 2 H), 7.31-7.24 (m, 2 H), 7.19-7.13 (m, 3 H), 7.02 (s, 1 H), 4.18 (s, 1 H), 2.55 (s, 3 H) ppm.

^{13}C NMR (175 MHz, DMSO-d_6): δ = 155.4, 154.7, 138.7, 137.4, 137.1, 135.7, 131.5, 131.2, 130.5, 130.4, 129.3, 123.5, 122.8, 120.4, 119.4, 118.8, 118.2, 116.6, 84.0, 82.4, 19.3 ppm.

HRMS (ESI) calcd. for $C_{23}H_{16}N_6NaO_4S$ $[M+Na]^+$: m/z = 495.0846, found: 495.0846.

Tert-butyl (4′-((7-(methyl-d$_3$)-2,3-dioxo-1,2,3,4-tetrahydroquinoxaline)-6-sulfonamido)-2′-((trimethylsilyl)ethynyl)-[1,1′-biphenyl]-4-yl)carbamate (S41)

7-(Methyl-d_3)-2,3-dioxo-1,2,3,4-tetrahydroquinoxaline-6-sulfonyl chloride (**S36**) (138 mg, 363 μmol), *tert*-butyl (4′-amino-2′-((trimethylsilyl)ethynyl)-[1,1′-biphenyl]-4-yl)carb-amate (**S38**) (155 mg, 558 μmol) and 4-dimethylaminopyridine (7.5 mg, 61.4 μmol) were dissolved in dry pyridine (3 mL). The reaction was stirred for 3.5 h at room temperature. The solvent was removed under reduced pressure and the crude purified by column chromatography (CH_2Cl_2/MeOH, 98:2). The product was yielded as an off-white solid (168 mg, 270 μmol, 74%).

^{1}H NMR (700 MHz, DMSO-d_6): δ = 12.11 (s, 1 H), 11.96 (s, 1 H), 10.60 (s, 1 H), 9.41 (s, 1 H), 7.76 (s, 1 H), 7.46 (d, ^{3}J = 8.7 Hz, 2 H), 7.40 (d, ^{3}J = 8.7 Hz, 2 H), 7.28 (d, ^{3}J = 8.3 Hz, 1 H), 7.16-7.13 (m, 2 H), 7.02 (s, 1 H), 1.47 (s, 9 H), 0.11 (s, 9 H) ppm.

^{13}C NMR (175 MHz, measured as DEPTQ, DMSO-d_6): δ = 155.4, 154.8, 152.7, 139.0, 138.3, 136.2, 132.2, 131.5, 131.2, 130.3, 129.3, 129.2, 123.6, 122.8, 120.6, 119.8, 118.3, 117.3, 116.7, 104.5, 97.8, 79.2, 28.1, 18.5*, −0.4 ppm. * assigned via HMBC

HRMS (ESI) calcd. for $C_{31}H_{32}D_3N_4O_6SSi$ $[M+H]^+$: m/z = 622.2229, found: 622.2218.

Tert-butyl (2′-ethynyl-4′-((7-(methyl-d$_3$)-2,3-dioxo-1,2,3,4-tetrahydroquinoxaline)-6-sulfonamido)-[1,1′-biphenyl]-4-yl)carbamate (S42)

Tert-butyl (4′-((7-(methyl-d_3)-2,3-dioxo-1,2,3,4-tetrahydroquinoxaline)-6-sulfonamido-)-2′-((trimethylsilyl)ethynyl)-[1,1′-biphenyl]-4-yl)carbamate (**S41**) (152 mg, 244 μmol) was dissolved in dry tetrahydrofuran (1.5 mL). A 1 m solution of tetrabutylammonium fluoride in tetrahydrofuran was added (300 μL, 300 μmol). The solution was stirred for 4 h at room temperature. The solvent was removed under reduced pressure and the crude purified by column chromatography (CH_2Cl_2/MeOH, 95:5). The product was obtained as a colorless solid (132 mg, 240 μmol, 98%).

^{1}H NMR (700 MHz, DMSO-d_6): δ = 12.10 (s, 1 H), 11.97 (s, 1 H), 10.65 (s, 1 H), 9.42 (s, 1 H), 7.77 (s, 1 H), 7.46 (d, ^{3}J = 8.5 Hz, 2 H), 7.35 (m_c, 2 H), 7.25 (d, ^{3}J = 8.5 Hz, 1 H), 7.24 (d, ^{4}J = 2.5 Hz, 1 H), 7.14 (dd, ^{3}J = 8.5 Hz, ^{4}J = 2.5 Hz, 1 H), 7.02 (s, 1 H), 4.13 (s, 1 H), 1.47 (s, 9 H) ppm.

^{13}C NMR (175 MHz, measured as DEPTQ, DMSO-d_6): δ = 155.4, 154.8, 152.8, 139.0, 138.4, 136.4, 132.5, 132.3, 131.5, 131.2, 130.4, 129.4, 129.2, 123.6, 123.0, 120.4, 119.6, 118.3, 117.6, 116.7, 83.7, 79.2, 28.2, 18.5* ppm.

* assigned via HMBC

HRMS (ESI) calcd. for $C_{28}H_{24}D_3N_4O_6S$ $[M+H]^+$: m/z = 550.1834, found: 550.1835.

N-(4′-amino-2-ethynyl-[1,1′-biphenyl]-4-yl)-7-(methyl-d$_3$)-2,3-dioxo-1,2,3,4-tetrahydroquinoxaline-6-sulfonamide hydrogenchloride (S43)

Tert-butyl (2′-ethynyl-4′-((7-(methyl-d_3)-2,3-dioxo-1,2,3,4-tetrahydroquinoxaline)-6-sulfonamido)-[1,1′-biphenyl]-4-yl)carbamate (**S42**) (110 mg, 200 μmol) was dissolved in 4 m hydrogen chloride 1,4-dioxane solution (3.5 mL). The reaction was stirred for 3 h at room temperature. The solvent was removed under reduced pressure. The crude product was obtained as a colorless solid and used without further purification.

N-(4′-azido-2-ethynyl-[1,1′-biphenyl]-4-yl)-7-(methyl-d$_3$)-2,3-dioxo-1,2,3,4-tetrahydroquinoxaline-6-sulfonamide (16)

N-(4′-amino-2-ethynyl-[1,1′-biphenyl]-4-yl)-7-(methyl-d_3)-2,3-dioxo-1,2,3,4-tetrahydro-quinoxaline-6-sulfonamide hydrogenchloride (**S43**) (max. 200 μmol) was dissolved in 90% acetic acid (2.5 mL) and cooled to 0 °C. Sodium nitrite (71.1 mg, 1.03 mmol) was added and the reaction stirred for 20 min at 0 °C. After the addition of sodium azide (69.2 mg, 1.06 mmol) stirring was continued for 75 min at 0 °C. Afterwards, the solvent was removed under reduced pressure. After purification via reverse phase flash chromatography the product was obtained as a colorless solid (88.0 mg, 185 μmol, 93% over two steps).

^{1}H NMR (500 MHz, DMSO-d_6): δ = 12.13 (s, 1 H), 11.99 (s, 1 H), 10.76 (s, 1 H), 7.78 (s, 1 H), 7.50 (m_c, 1 H), 7.28 (d, ^{3}J = 8.5 Hz, 1 H), 7.26 (d, ^{4}J = 2.4 Hz, 1 H), 7.17-7.12 (m, 3 H), 7.01 (s, 1 H), 4.19 (s, 1 H) ppm.

^{13}C NMR (125 MHz, measured as DEPTQ, DMSO-d_6): δ = 155.5, 154.9, 138.8, 138.4, 137.5, 135.8, 131.5, 131.2, 130.6, 130.5, 129.4, 123.6, 122.8, 120.5, 119.4, 118.9, 118.4, 116.7, 84.2, 73.1, 19.7* ppm.

*assigned via HMBC

HRMS (ESI) calcd. for $C_{23}H_{13}D_3N_6NaO_4S$ $[M+Na]^+$: m/z = 498.1034, found: 498.1034.

Tert-butyl (4-(2-(3-(but-3-yn-1-yl)-3H-diazirin-3-yl)ethoxy)phenyl)carbamate (S44)

To a solution of *tert*-butyl (4-hydroxyphenyl)carbamate (251 mg, 1.2 mmol) in DMF (5 mL) was added a solution of 3-(but-3-yn-1-yl)-3-(2-iodoethyl)-3H-diazirine (143 mg, 0.58 mmol) in DMF (1 mL). Cs_2CO_3 (228 mg, 0.7 mmol) was added under Ar and the reaction mixture was stirred in the dark for 16 h at r. t. Water was added and the mixture was extracted with EtOAc (3x). Combined organic phases were dried over Na_2SO_4, filtered and concentrated under reduced pressure. Purification by column chromatography (PE : EtOAc = 20 : 1 to 5 : 1) yielded 12 mg (6%) of the desired compound.

^{1}H NMR (500 MHz, $CDCl_3$): δ = 7.28-7.23 (m, 2 H), 6.82 (d, J = 9.0 Hz, 2 H), 6.36 – 6.32 (m, 1 H), 3.79 (t, J = 6.2 Hz, 2 H), 2.06 (td, J = 7.5, 2.6 Hz, 2 H), 1.98 (t, J = 2.6 Hz, 1 H), 1.86 (t, J = 6.2 Hz, 2 H), 1.73 (t, J = 7.5 Hz, 2 H), 1.51 (s, 9 H) ppm.

^{13}C NMR (125 MHz, $CDCl_3$): δ = 154.50, 153.10, 131.83, 120.50, 115.01, 82.76, 80.31, 69.17, 62.94, 32.97, 32.67, 29.70, 28.37, 13.29 ppm.

N-(4-(2-(3-(But-3-yn-1-yl)-3H-diazirin-3-yl)ethoxy)phenyl)-7-methyl-2,3-dioxo-1,2,3,4-tetrahydroquinoxaline-6-sulfonamide (14)

tert-Butyl (4-(2-(3-(but-3-yn-1-yl)-3*H*-diazirin-3-yl)ethoxy)phenyl)carbamate (**S44**) (12 mg, 36 μmol) was dissolved in CH_2Cl_2 (2 mL) at 0 °C and TFA (1 mL) was added. The reaction mixture was stirred for 2 h at r. t. Volatiles were evaporated under reduced pressure. The residue was dissolved in pyridine (2 mL) and 7-methyl-2,4-dioxo-1,2,3,4-tetrahydroquinazoline-6-sulfonyl chloride (**S30**) (13.7 mg, 50 μmol) was added. The rection mixture was stirred for 2 h at r. t. Volatiles were removed under reduced pressure and the residue was purified by column chromatography (silica; CH_2Cl_2: MeOH = 1: 0 to 10: 1). Yield: 1.9 mg (12%). R_f = 0.32 (CH_2Cl_2: MeOH = 10: 1).

^{1}H NMR (500 MHz, CD_3OD): δ = 7.65 (s, 1 H), 7.05 (s, 1 H), 6.98 (d, J = 9.1 Hz, 2 H), 6.76 (d, J = 9.1 Hz, 2 H), 3.75 (t, J = 6.0 Hz, 2 H), 2.59 (s, 3 H), 2.22 (t, J = 2.7 Hz, 1 H), 2.02 (td, J = 7.5, 2.7 Hz, 2 H), 1.80 (t, J = 6.0 Hz, 2 H), 1.63 (t, J = 7.5 Hz, 2 H) ppm.

HRMS (ESI) calcd. for $C_{22}H_{22}N_5O_5S$ $[M+H]^+$: m/z = 468.1342, found: 468.1337.

QUANTIFICATION AND STATISTICAL ANALYSIS

For all assays, arithmetic mean and standard deviation across multiple replicates was used as a measure of center and spread. Statistical analysis was done using GraphPad Prism 9. Statistical significance for the assays with Th1 cells (Figure 3G), co-culture of A549 cells (Figures 3H, 3I, S2D, S2F, and S3D), mode of action assays (Figures 4A–4D) were determined by unpaired, two tail *t*-test. Statistical significance for experiments with TEER measurement (Figures S1G and S1H) was determined by one-way ANOVA with post-hoc Dunnett's test. Statistical analysis for in vivo survival studies (Figures 6E and 6F) was determined by the log rank test (Mantel-Cox), bacterial burden and IL-6 determination was done by unpaired, two tail *t*-test. Statistical significance for transepithelial resistance experiments were determined by one-way ANOVA with post-hoc Dunnett's test.

Flow cytometry data for co-culture experiments with A549 cells (Figures 3H and S2) were collected by recording 10,000 events for each sample and analysed using FlowJo v10. Gates used to quantify the fraction of events with Annexin V (FITC-A, apoptosis) and PI (PerCP-CY5-5-A, necrosis) labelled cells were determined from the control samples and the details have been included in the respective figure legend (Figure S2).